Physiological Chemistry and Physics and Medical NMR Volume 37, Number 1, 2005

Addresses of Chief Editor and Editorial College

Toshihiko Ubuka
Department of Clinical Nutrition
Kawasaki University of Medical Welfare
Kurashiki, Okayama, 701-0193, Japan

Denys Wheatley
Department of Cell Pathology
University of Aberdeen
Aberdeen AB24 4FA, Scotland
United Kingdom

EDITORIAL AND BUSINESS OFFICE

Physiological Chemistry and Physics
and Medical NMR
P.O. Box 1452
Melville, New York 11747

Editor In Chief, Dr. Gilbert N. Ling
Managing Editor, Margaret M. Ochsenfeld

SCOPE: PCP provides a forum for the review and publication of reports of original research in a broad range of subjects in biophysics, biochemistry and cellular physiology. Reports of direct applications of basic knowledge to human studies are invited; examples would include the measurements of relaxation times as part of NMR imaging. Single experiments, conclusions based on inadequate statistics, purely speculative papers, and clinical case reports are not accepted.

POLICY: The pages of PCP are accessible to competing viewpoints, interpretations, theories and opinions. Debate is invited via Editorial Comments and Letters to the Editor. Criteria for evaluating submissions include soundness of the study and clarity of presentation, and papers are not rejected on the basis of interpretation or theory, however controversial. PCP believes that scientific issues should be settled by investigation and open debate, not by an appeal to anonymous authority.

PCP attempts to achieve a balance between freedom of expression and constructive peer review. All papers are refereed by reviewers who may remain anonymous, but the Chief Editors make all final decisions, and will handle appeals from authors who feel their papers are unfairly reviewed.

The Editors endeavor to make decisions regarding acceptance or rejection of manuscripts quickly, and have set self-imposed deadlines for doing so. Referees also are given deadlines.

TYPES OF PAPERS: *Regular papers* may be experimental or theoretical. *Short notes, Priority notes* and *Letters* in response to published papers are invited. *Reviews* are desired, but authors are urged to contact an Editor before sending a finished review manuscript. *Symposia* may be published as regular or supplemental issues.

SUBSCRIPTIONS: Price is US$80.00 per volume in the United States and US$87.00 outside the United States. *Physiological Chemistry and Physics and Medical NMR* is published biannually, 2 issues per year, the volume numbered yearly. New subscriptions will start with the first issue of the volume in progress, unless the subscriber directs otherwise. Most back issues are available

Instructions to Authors

SUBMISSIONS: An original and two copies of all material are requested. The original must be typewritten on one side only. Papers should be sent to Dr. Gilbert N. Ling, Editor, P.O. Box 1452, Melville, New York 11747 U.S.A. Manuscripts should be submitted only to this journal and not have been published in part or whole in another publication, except as short preliminary notes, abstracts, or as unpublished work in reviews or symposia. Be sure to keep a copy of your manuscript.

NOTE: Referees will be instructed to destroy their copies of the manuscript after reviewing them. We will return only the original manuscript to you for revision or if rejected.

MANUSCRIPTS: All material should be typed double-spaced with margins at least one inch wide and pages numbered consecutively beginning with the title page. In addition to a paper copy, send an IBM- or Macintosh-compatible file on a floppy disk or CD, in Word or Wordperfect. *Title Page* should include title (of at most 100 characters and spaces), full names of authors as you wish them to be published, names and cities of institutional affiliation(s) of authors and of institution(s) where the studies were performed, and name, full address, telephone number, fax number and e-mail address of the person to whom correspondence, proofs, and reprint requests are to be sent. Four to six *key words* should be listed on the title page. These words will assist indexers. Also, at bottom of title page include a short running title of 40 characters or less.

Abstract should be concise and no longer than 225 words. *Body* may or may not be divided into Introduction, Materials and Methods, Results and Discussion, depending on the length and nature of the paper. Introductory remarks should indicate clearly the significance of the work presented. *References* may be indicated in the text and listed in the reference list in whatever style the author prefers, but we prefer that titles of articles be omitted.

TABLES: Tables should be typewritten on separate sheets and identified by roman numerals (eg. Table III) and titles. Table notes should be keyed by superscript italic lower-case letters (eg. [a]Control). The approximate locations of *tables* and *figures* should be indicated in the margins of the manuscript.

ILLUSTRATIONS: Original artwork or glossy photostatic prints, together with two photocopies (like Xerox copies) should be provided. Each illustration should be numbered on the back in pencil, along with the authors' names. It is preferred that line drawings be made on paper that is not larger than 8 1/2 by 13 inches, and that the drawing be its intended size in the printed paper. Most figures will occupy 1/2 to full column, that is 5 inches wide. Lines and lettering should be thick enough to allow reduction. A drawing of overall dimension of 8 by 10 inches that will be reduced to 1/4 of its original size should be lettered with 18-point (capitals 6 mm high, lower-case 4 mm high) or larger lettering. Glossy photostatic prints are acceptable, and should be attached firmly to a sheet of paper the same size as the manuscript. Postacceptance: If possible send figures as an image file using TIFF or JPEG formatting scanned at a resolution of 600 dpi.

PHOTOGRAPHS: High-quality black and white glossy prints should be provided in triplicate, and may be provided as one print plus two photocopies if the photocopies are sufficiently clear to portray the original to referees. Photographs should be attached firmly to a sheet of paper the same size as the manuscript. Photographs that have been scanned and stored as a TIFF file with a resolution of 300 dpi may also be submitted.

REFEREES: Two anonymous referees will be sought for each paper. Authors are encouraged to suggest names and addresses of suitable referees. Referees will be given deadlines for mailing manuscripts back or phoning reviews in, and will be invited to provide editorial statements or Letters that deal with issues raised by submitted papers.

REPRINTS: An order form is enclosed with proofs sent to authors.

PAGE CHARGES: Page charge is $20.00 per published page. It may be waived in the case of severe international exchange difficulties. An additional charge of $15.00 will be levied for photographs that require screening (eg., E.M's, chromatograms, scans).

Physiol. Chem. Phys. & Med. NMR (2005) *37*: 1–63

An Updated and Further Developed Theory and Evidence for the Close-contact, One-on-one Association of Nearly All Cell K^+ with β- and γ-Carboxyl Groups of Intracellular Proteins

Gilbert N. Ling

Damadian Foundation for Basic and Cancer Research
Tim and Kim Ling Foundation for Basic and Cancer Research
c/o Fonar Corporation, 110 Marcus Drive
Melville, NY 11747
Email: gilbertling@dobar.org

Abstract: The primary focus of this communication is to present an updated and advanced version of the theory of close-contact association of molecules and ions through the spatial fixation and aggregation of the adsorbing sites. The last sections of the text also review a collection of relevant *in vitro* and *in vivo* experimental findings gathering since seventy years ago. Though some of these findings were published before the theory, old and new, they all support the theory that close-contact association with the β-, and γ-carboxyl groups of intracellular proteins causes the selective accumulation of potassium ions (K^+) in living cells.

"POTASSIUM IS of the soil and not the sea; it is of the cell but not the sap." With this thought-provoking remark, W. O. Fenn launched his 1940 *Physiological Review* article on "The Role of Potassium in Physiological Processes" (Fenn 1940.) Six years later, I began my career as a cell physiologist at the Department of Physiology of the University of Chicago. My Ph.D. thesis was on what was then erroneously designated as the *membrane potential* (of single muscle fibers), which shows exquisite sensitivity to the concentration of the potassium ion (K^+) in the bathing medium (Ling and Gerard 1950.) Naturally, Fenn's review was a trusted source of information on what we knew up to that time.

In retrospect, I can say that that was how I thought at the time. I had no idea then that decades later I would come upon something that Fenn, in my view, should have included in his 1940 review as a matter of course but did not. This was a paper by Benjamin Moore,

Herbert Roaf and Arthur Webster in the prominent *Biochemical Journal.* First, it was published years before Fenn wrote his 1940 review (Moore *et al* 1912.); second, Moore *et al*'s paper contained what could be rephrased to read:

> Potassium is of the soil, sodium is of the sea; potassium is of the cell, sodium is of the sap.

Nor was that all that Fenn left out. For Moore and his coworkers also suggested that this selective accumulation of potassium ion (K^+) over sodium ion (Na^+) in living cells and in soil could have a common origin. That is, both could result from a preferential affinity of the solid component of each system for K^+ over Na^+(Moore *et al* 1912, pp. 112–113.) The solid component of soil includes hydrated aluminum silicates we call clay. The solid component of the living cell is the proteins.

Eventually, I discovered in a still earlier review of Fenn what could have been Fenn's reason for his later exclusion of Moore *et al*'s ideas of potassium adsorption. "Since potassium is almost the only cation inside (the cell) and since it is all (or nearly all) necessary to make the osmotic pressure equal inside and out, it is difficult to suppose that the distribution of potassium in the normal untreated cell is essentially different from the distribution of the water" (Fenn 1936.) Or put differently, no potassium could be adsorbed or otherwise bound to the solid components of the cell and thus removed from the cell water.

In fact, it was this same idea coupled with what was believed to be proof of free cell water that had enabled Nobel laureate, A.V. Hill to banish the bound water-bound potassium concept altogether (Hill 1930; Hill and Kupalov 1930; for its long term historic aftermath, see Ling 2001, pp. 38–39.) Thus, the Hungarian biophysicist, E. Ernst who was at the scene, recalled later in his 1963 book "Biophysics of Striated Muscle" what happened at this critical juncture in time (Ernst 1963, p. 112.)

For Ernst believed that it was A.V. Hill who *actually* persuaded (the same) W. O. Fenn, Rudolph Höber and other opinion-makers of the time to abandon the idea of bound K^+ (and of bound water) in favor of the living cell as a "simple osmotic system." {By a simple osmotic system, Ernst meant living cells as semipermeable-membrane-enclosed solution of free water and free solutes (e.g., potassium ions,) *added by GL.*} (Ernst 1963, p. 112.) (How and why these osmotic reasons were later disproved can be found on p. 38 and p. 100 of Ling 2001.)

However, the rejection of Moore *et al*'s bound potassium concept had the backing of other prominent scientists in addition to A.V. Hill. Nonetheless, Hill's argument might well be the shot that set off the stampede.

Danish biochemist, Karl Linderstrom-Lang considered a native protein molecule as a sphere with its net electric charges uniformly smeared over its surface. Counter-ions carrying opposite electric charges to the electric charges of the protein exist exclusively as free ions in the surrounding *ion cloud* (Linderstrom-Lang 1924; Edsall and Wyman 1958, pp. 512–522.) In other words, proteins do not bind potassium or other ions. This *ion cloud* idea was not original. It came from Peter Debye's famous Limiting Law of electrolyte solutions (Debye and Hückel 1923, 1927.) (For details, see Appendix A.)

In summary, much of what was said above apropos of Moore *et al* belongs to the limbo of forsaken ideas in the early 20th century cell physiology. During my entire tenure first as a graduate student and later as a postdoctoral student — *the only theory of the living cell known to me was the membrane theory.* That, notwithstanding I was in the (world's finest) Department of Physiology of the University of Chicago and under the guidance of the world's most open-minded and admirable supervisor and teacher, Prof. Ralph W. Gerard.

And, at the time, the membrane theory was in the struggle of half-heartedly shifting

from the original sieve membrane theory to what is later known as the membrane pump theory. The most prominent pump being considered was the sodium pump *alias* sodium-potassium-pump. To maintain the low sodium and high potassium profile, these pumps were installed in the cell membrane, pumping K^+ into the cell and Na^+ out of the cell, day and night, year after year without end.

My unescorted journey that led to where Moore et al once visited — and beyond

It was a Monday afternoon in the spring of 1948 when I gave a graduate student seminar on the sodium pump. My hope to give a comprehensive and informative report on the subject got me nowhere. I had no trouble finding rapidly gathering evidence that had disproved the sieve membrane theory. Thus, tracer studies showed again and again that (hydrated) Na^+, sucrose and other solutes supposedly too big to go through membrane pores in fact enter and leave the cell with ease (for a list of important references, see Endnote 1.) However, high and low I searched, I could not find any convincing evidence that demonstrated the existence of a sodium pump in the cell membrane of the frog muscle, the squid axon or the human red blood cell. Yet each of these extensively investigated living cells retains a concentration profile of low Na^+ but high K^+ like that illustrated in Figure 1.

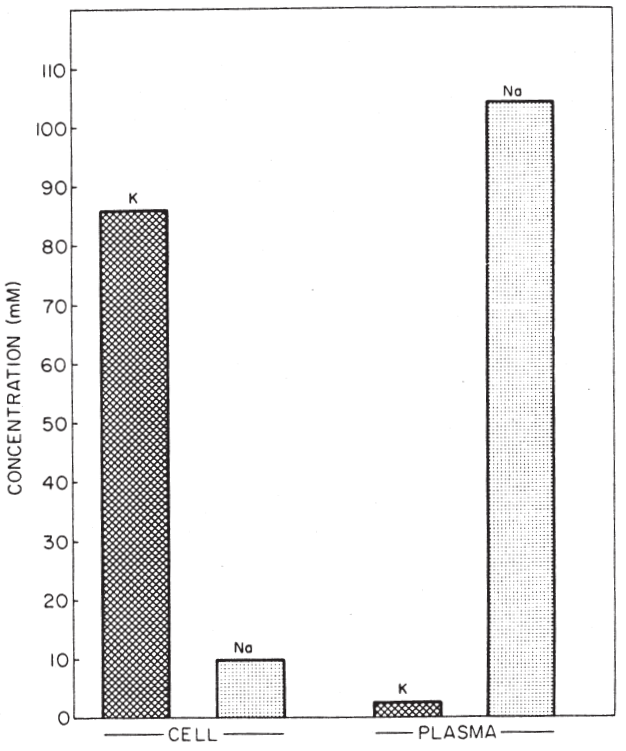

FIGURE 1. Equilibrium concentrations of K^+ and Na^+ in frog muscle cells and in frog plasma. (Ling 1984, with kind permission of Springer Science and Business Media)

Shortly afterward, I carried out some simple experiments of my own design. It did not take me long to reach a tentative conclusion. The maintenance of a high K^+ and low Na^+ content in frog muscle cells could not depend on a continual supply of metabolic energy, which is, however, indispensable for any sustained pumping activity like the membrane pump theory postulates.

Table I illustrates the kind of data that I collected at that time. (For more extensive later data, see Table 8.4 in Ling 1962 or the same table reproduced *verbatim* in Appendix 1 of Ling 1997.) It shows that the asymmetrical distribution of high K^+ and low Na^+ in a variety of frog tissues remained unchanged hours after both the oxidative and glycolytic metabolism had been put to a stop. (For a full account of the disproof of the membrane pump hypothesis, see "Debunking the Alleged Resurrection of the Sodium Pump Hypothesis," Ling 1997.)

After completing my postdoctoral studies at the University of Chicago, I obtained my first job at the famous Johns Hopkins Medical School in Baltimore. Somewhere between 1950 and 1951, while browsing around and "thinking" in the Welsh Library basement, I hit upon a new idea — an idea, which soon grew into *a set of new ideas*. In retrospect, these ideas actually marked the beginning of the *association-induction hypothesis*, the first and only surviving unifying theory of cell and sub-cellular physiology in existence up to now (Ling 1962.)

TABLE I. Effect of combined action of the poison, iodoacetate and pure nitrogen at 0°C upon the K^+ contents of frog muscle and nerves.

Frog No.	Type of Tissue	Muscle No.		Weight (gms.)	mM. K^+/l. of intracellular water
1	Sartorius	1	Control	0.0870	60.7
		2	Expt'l	0.0750	69.8
1	Semitendinosus	1	Control	0.0710	72.6
		2	Expt'l	0.0795	81.8
1	Tibialis anticus longus	1	Control	0.0938	71.1
		2	Expt'l	0.0900	79.2
2	N. ischiadicus +	1	Control	0.0300	38.1
	N. tibialis + N. peroneus	2	Expt'l	0.0260	39.5
3	Sartorius	1	Control	0.0730	73.4
		2	Expt'l	0.0700	78.0
3	Semitendinosus	1	Control	0.0660	83.0
		2	Expt'l	0.0730	77.4
3	N. ischiadicus +	1	Control	0.0260	42.8
	N. tibialis + N. peroneus	2	Expt'l	0.0242	40.0

		Muscles	Nerves
Average	Control	100.0%	100.0%
	Expt'l	105.2%	98.5%

Duration of incubation was 5 hours. Experimental solution contained 0.5 mM Na iodoacetate and pure nitrogen. Control Ringer's solution was equilibrated with air. (from Ling 1952, by permission of the Johns Hopkins University Press, Baltimore)

To understand the new ideas I introduced, we must begin with a *simple truth*. The only distinguishing features between K^+ and Na^+ are their respective *short-range* attributes; their long-range attributes as monovalent cations are identical. Among the various short-range attributes, the most outstanding are their respective Born repulsion constants (see Ling 1962, p. 65.) This difference makes K^+ larger than Na^+ in their respective bare states.

However, after encountering water, the order of their sizes is reversed. Clothed now more or less permanently in a shell of water molecules, the hydrated Na^+ becomes larger than the hydrated K^+. In fact, this difference in their respective hydrated sizes was invoked repeatedly to explain the selectivity of K^+ over Na^+ in the living cell as well as in inanimate systems. These non-living systems include nature-made aluminum silicates (soil and clay) and man-made aluminum silicates (permutits) as well as other man-made cross-linked polymers known as ion exchange resins.

Thus, for the selective accumulation of K^+ over Na^+ in living cells the sieve membrane theory mentioned in passing above offers one *size-dependent* mechanism. That is, a sieve-like cell membrane is punctured with rigid pores in the otherwise impermeable cell membrane. The rigidity and size of these uniform pores were such that they would permit the passage of ions and molecules smaller than the pores but bar the passage of the larger ones — like the hydrated Na^+ — absolutely and permanently (Boyle and Conway 1941.) However, as also mentioned above, radioactive tracer and other studies demonstrated that this theory was wrong. (Hydrated) Na^+ as well as other large solutes can traverse the cell membrane without difficulty (see Ling 1993, Table II for the permeability of the living cell membrane to very big molecules.)

Then, Gregor (1948, 1951) and Katchalsky (1954) made their respective attempts to explain the K^+ over Na^+ selectivity in *cation exchange resin* — a new industrial product that could trace its origin to the confluence of the science of soil chemistry and the permutit industry. In Gregor's and Katchalsky's respective size-dependent theories, it is the mechanical pressure generated by a stretched elastic resin matrix, which squeezes out the larger hydrated Na^+ but retains the smaller hydrated K^+ in the resin. As their figures reproduced here as Figure 2 and 3 show, neither Na^+ nor K^+ are engaged in close-contact association with the fixed anionic sites.

However, both theories were made untenable later when exchange resins carrying phosphonic and carboxyl groups made their appearance and were shown to select Na^+ over K^+ rather than the other way round as in the earlier sulfonate exchange resins (Bregman 1953.)

(This discovery also put in jeopardy Ling's Fixed Charge Hypothesis to be described in the following section. How that crisis actually turned into a blessing, stimulating the development of a more general theory of variable ionic selectivity — a key feature of the association-induction (AI) Hypothesis — can be found on pp. 136–143 of Ling 2001.)

It was thus the third attempt in history when I offered my size-dependent *quantitative mechanism* for the selective accumulation of K^+ over Na^+ in living cells. As a by-product, the theory could also explain the selective uptake of K^+ in soils as well as (early sulfonate) cation exchange resin. This, of course, is in harmony with the idea first suggested by Moore *et al* in 1912 and quoted above. Namely, living cells and soils share a similar mechanism for the selective K^+ accumulation — an idea, as pointed out earlier, I did not know until many years after 1952 (Ling 1951, 1952, pp. 772–773.)

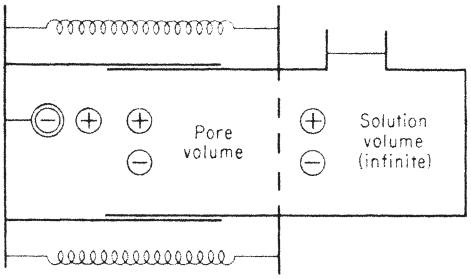

FIGURE 2. Gregor's model of ion exchange resin. The matrix is represented by elastic springs, which are stretched when the resin swells. Note that there is no close-contact one-on-one association of free positively charged ion ⊕ and fixed negative ions ⊖. (after Helfferich 1962)

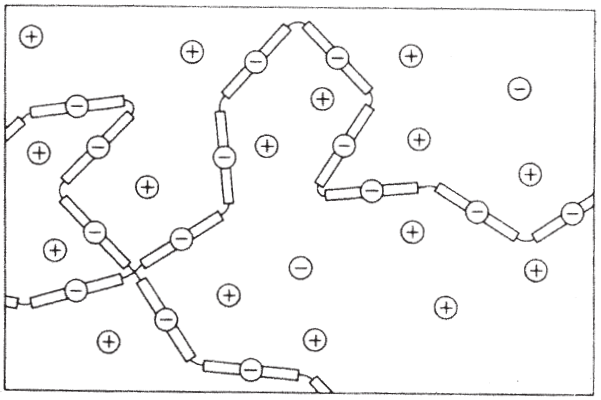

FIGURE 3. Katchalsky's model of ion exchange resin. The matrix is represented by a cross-linked network of chains. Note that there is no close-contact one-on-one association of free cations ⊕ and fixed anions ⊖. (after Hellferich 1962)

Ling's Fixed Charge Hypothesis

My 1952 theory, referred to in years following as *Ling's Fixed Charge Hypothesis* (LFCH) (Ling 2001, Chapter 10) could be divided into four parts and each will be briefly described next.

In Part I, I suggested that negatively charged β- and γ-carboxyl groups carried respectively on the *aspartic* and *glutamic residues* of cell proteins — like myosin in muscle — could be in (close-contact) association with either hydrated K^+ or hydrated Na^+. Now the electrostatic or Coulombic attraction between a positive charge and a negative charge follows the inverse square law. That is, it equals the product of the two electric charges divided by the product of the square of the distance of separation, r, and the dielectric constant, D. Owing to the *dielectric saturation* phenomena (Debye and Pauling 1925) however, the effective dielectric constant in the close vicinity of charged ions is much lower than its macroscopic value of 81 (see inset of Figure 4.) As a result, the energy of

association (ΔE) is much stronger for the smaller hydrated K^+ than for the larger hydrated Na^+ (main figure of Figure 4.) And the Boltzmann distribution law would dictate that of the trillions upon trillions of β- and γ-carboxyl groups in the cell, by far the great majority would preferentially take up the smaller hydrated K^+ over the larger hydrated Na^+. Selective K^+ accumulation over Na^+ in the cell would be thus accomplished.

At that time, the selectivity ratio I computed was about 7. It is not nearly as high as that shown in living cells like the frog muscle — at 100 or even higher, see legend of Figure 24 — the cause of this disparity will be explained below. Nonetheless, the value of 7 is considerably higher than that in most cationic ion exchange resins around 2 (see below.)

However, *the selectivity based on the difference in Coulombic attraction applies only to the fraction of K^+ (and/or Na^+) that is in close-contact association with the* β- *and* γ-*carboxyl groups.* It does not apply to ions that are not in close-contact association. Indeed, in order to achieve the selectivity observed in living cells, most of the available β- and γ-carboxyl groups must be engaged in close-contact association with either a K^+ or a Na^+.

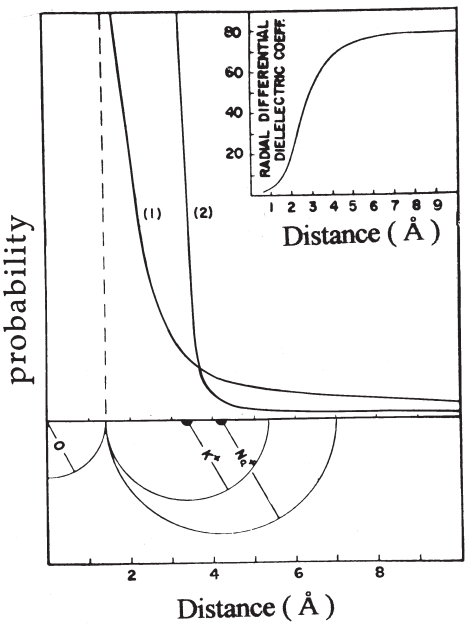

FIGURE 4. A theoretical model for the selective adsorption of K^+ over Na^+ on a fixed oxyacid site presented in 1952 as part of Ling's Fixed Charge Hypothesis (LFCH.) Computation takes into account the lowering of the dielectric constant of water (referred to in the Inset as "radial differential dielectric coefficient") when approaching an ion as illustrated in Inset. Theoretical curve (2) shows the probability of finding a monovalent cation (e.g., K^+, Na^+) associated with the fixed oxyacid anion — partially represented at extreme left of bottom section of the figure — at distance (away from the center of the oxygen atom of the oxyacid group) indicated on the abscissa in Angstrom units. Note that only the hydrated K^+ with its smaller radius shown in the bottom figure can enter the "shell of high probability of association" around the oxygen atom of the negatively-charged oxyacid group and becomes selectively adsorbed over the larger hydrated Na^+ (the center of which stays largely out of the shell of high probability) also shown in the bottom part of the figure. (Ling 1952, by permission of the Johns Hopkins University Press, Baltimore)

However, this theoretical requirement of full close-contact ionic association was in conflict with the prevailing belief of the time as discussed at some length above. That is, most workers in the protein chemistry (e.g., Linderstrom-Lang) and in the ion-exchange-resin science-technology (e.g., Gregor and Katchalsky.) insisted that all ions in the vicinity of proteins and within cation exchange resins be *fully dissociated* (see Figure 2 and 3.)

Then, *in vitro* studies of isolated proteins have shown that they do not take up K^+ over Na^+ at all (Beatley and Klotz 1951; Carr 1956, p. 177) or do so in amount and specificity far below that needed to explain selective accumulation in living cells (for list of additional older references, see Ref. 99 in Ling 2001.)

Finally, there is the challenging fact that the selective accumulation of K^+ over Na^+ in cells is lost upon cell death (see Figure 56 in Ling 2001.)

To provide reasonable answers to each of these pieces of apparently contradictory evidence, I introduced three other sets of new ideas or hypotheses, numbered respectively Part 2, Part 3 and Part 4.

Part 2 of the theoretical idea has been called the "*salt-linkage hypothesis.*" In this, I argued that proteins in living cells as a rule do not exist in the same conformation as isolated "native " proteins do *in vitro* (Ling 2001, p. 243; Ling 2005.) In isolated native proteins the β- and γ-carboxyl groups are mostly engaged in forming *salt linkages* with fixed positively charged ε-amino groups and guanidyl groups on the same or other proteins (see upper left figure in Figure 16 below.) In contrast, I suggested that many of these β- and γ-carboxyl groups in living cells are free to adsorb K^+ and/or Na^+(see lower left figure of Figure 16.) (For the history and current status of the *salt-linkage* concept, see Endnote 2.)

Part 3 refers to the control of the cell protein conformation by ATP *per se.* As a *cardinal adsorbent* occupying a controlling site called the *cardinal site*, ATP achieves its function of controlling the conformation of the protein through its adsorption as intact ATP molecules and not through its hydrolytic degradation, see Figure 23 below. Since ATP is the product of energy metabolism, Part 3 of the theory explains why the selective accumulation of K^+ over Na^+ is lost upon cell death when ATP regeneration ceases.

Part 4, the last component of Ling's Fixed Charge Hypothesis has been referred to as the *Principle of Enhanced Counter-ion Association due to Charge Fixation* (Ling 1962 p. 138; 1984, p. 95; 1992, p. 39; 2001, p. 48.) It shows that spatial fixation and congregation of anionic groups would profoundly enhance the statistical probability of the association of, for example, the fixed β- and γ-carboxyl groups with free monovalent cations like K^+ and Na^+.

Thus far, however, Part 4 of what I presented in 1952 was spelled out in no more than a few sentences. Although the importance had been reiterated repeatedly in later publications, the principle has never been elaborated in detail beyond those few sentences. ***It is the primary purpose of this communication to update and to develop the idea in full.*** In addition, I will also review the supportive evidence that have been steadily collecting in the last half century. However, before I begin, several hitherto unrecognized historical errors must be set straight first.

Correcting several historical errors of omissions

The theoretical linkage made by Moore *et al* between selective K^+ accumulation in living cells — the research subject of cell physiologists — and that in soil — the research sub-

ject of agricultural chemists was discovered by me some forty years late. Like Moore *et al*'s paper, sources of hitherto undiscovered knowledge came — by bits and pieces at long intervals — not unlike paleontologists' dinosaur bones.

Thus, until very recently I did not know that an agricultural scientist of the mid-19th century, Thomas Way had already discovered that soils can preferentially take up one kind of ion (e.g., K^+) and reject another (e.g., Cl^-) (Way 1850, see also Thompson 1850.) What underlies this kind of phenomena was later described as *ion exchange*. From this soil-science beginning, new industries have sprung up manufacturing all sorts of ion exchangers mentioned above, including water-softening permutits (see Jenny 1932), and still later the modern ion exchange resins. Along with the discoveries of existing but unrecognized knowledge also came the discoveries of errors of omission — if one could call them that. These historic errors of omission due to the segregated search for knowledge in different fields have been made by others and by myself.

(1) Discovering Swiss agricultural chemist, Prof. Georg Wiegner's work at last

What has been known as Ling's Fixed Charge Hypothesis (LFCH) was first announced in a preliminary note in 1951 (Ling 1951) and in full in 1952 (Ling 1952.) It has been my lifelong belief that LFCH is an original and quantitative theory of the cell physiology of selective ionic accumulation — as well as the theory of selective K^+ accumulation in earlier sulfonate ion exchange resin. This was true then. It is still true today but with a twist.

That is, the idea in Part 1 of Ling's Fixed Charge Hypothesis as it was extended to explain K^+ over Na^+ selectivity in soil and in permutit is in need of correction in regard to priority. For the Swiss agricultural chemist, Georg Wiegner had suggested an essentially similar mechanism for the phenomenon. That is, a mechanism for the selective accumulation of smaller hydrated K^+ over larger hydrated Na^+ in clay and permutit as a result a stronger Coulombic attraction from negative charges on the surface of the clay or permutit particles. Figure 5 reproduces an illustration published by Wiegner's coworker (student?), Hans Jenny (1927), who explicitly mentioned that the idea originated from Wiegner (Wiegner 1925.) That would place its introduction 27 years ahead of the publication of Ling's quantitative Fixed Charge Hypothesis — as it was extended to cover similar phenomena in soil and permutit.

(2) J. L. Pauley's publication on selective K^+ accumulation in ion exchage resin two years after the publication of Ling's Fixed Charge Hypothesis

In 1954 J. L. Pauley published a model of selective accumulation of alkali-metal ions in cation exchange resins (Pauley 1954.) His model is essentially similar to mine. It differs from mine in that the dielectric constant Pauley used is the macroscopic value of 78.54, while I took into account the *dielectric saturation phenomenon* as mentioned above. The K^+ to Na^+ selectivity ratio Pauley calculated was 1.61.

Pauley assumed (without providing a reason) that cations are "bound more or less firmly to the anionic groups of the resin." (p. 1423.) He made no reference to my earlier theory. (Nor did he mention Wiegner's theory on soil and permutits. However, he did cite Jenny's 1932 paper but only as a source for the values of hydrated ionic diameters.)

(3) Harris and Rice's publication four year after Ling's Fixed Charge Hypothesis

F.A. Harris and S.A. Rice published in 1956 in the Journal of Physical Chemistry a short note entitled "Model for Ion-Exchange Resins" (Harris and Rice 1956.) However,

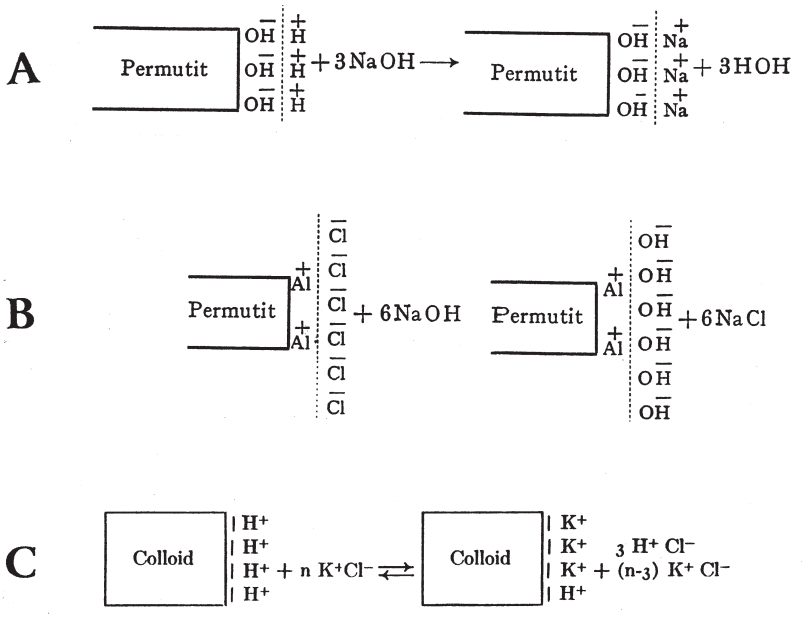

FIGURE 5. Wiegner's model of cation (A) and anion (B) exchange respectively from negatively and positively charged sites on the surface of permutits and on the negatively charged sites on the surface of colloids (C). (from Jenny 1927)

when compared with the model I presented four years earlier it was a decidedly backward step. Because theirs is not a quantitative theory, nor did they offer an explanation why ions associate with fixed anionic in view of the fact that the more visible Gregor and Katchalsky claimed the opposite. Like Pauley, Harris and Rice also did not recognize my earlier work (nor that of Wiegner on soil and permutit.)

In summary, the selective accumulation of K^+ over Na^+ in soil, various hydrated aluminum silicates (clay, permutit) and cation exchange resins all exhibit a K^+ / Na^+ selectivity ratio of around 2. The later theories of Pauley and of Harris and Rice were, in view of what would be presented below, all in the right direction. They all either assumed some degree of association or explicitly postulated association without offering a specific mechanism as Ling's Fixed Charge Hypotheis did, though only briefly at the time — but to be fully expanded below for the first time in history. And, as I had mentioned above, *without association, the proposed Coulombic mechanism could not work.*

The selectivity ratio of K^+ over Na^+ in living cells is as a rule much higher than in soil, clay, permutit or cation exchange resins. For this reason, the respective theories of Wiegner, of Pauley and of Harris & Rice each predict a selectivity ratio far too low to account for the selectivity in living cells. Nor did any one of them make the connection between selective accumulation in soil and in the living cell. That was first pointed out by Moore *et al* quoted in the opening page of this paper. Nonetheless, it was all but forgotten by then. In part at least this interference of the normal progress of science was the result of the exclusion by trusted opinion-makers in publishing reviews. Like planting false road

signs, the full impact as a rule could not be fully understood until long afterward (see Ling 2001, pp. 38–42; Ling 1997a, under "Absolute Power Corrupts Absolutely".)

The fact that so far only Ling's Fixed Charge Hypothesis could come close to producing a substantially higher selectivity ratio was for two reasons. Taking into account the *dielectric saturation* phenomenon is one. Taking into account (i.e., by proposing a new hypothesis) of the near total close-contact association between the K^+/Na^+ and the fixed anions is another.

Next, I would like to add an explanation as to why my theory could only offer a K^+ over Na^+ selectivity ratio of 7 while in living cells a selectivity ratio of 100 or even higher may be the case (see legend of Figure 24 below.) In short, it was mainly a question of choosing the right value for the dielectric constant used in the computation.

The most relevant published data on the dielectric "profile" I could find at the time was that of Graham (1950) partly reproduced as an inset in Figure 4. However, when the oxy-acid oxygen atom and the K^+ are in close contact, there are really no freely tumbling water molecules in the immediate vicinity and hence the cause for choosing a high macroscopic dielectric constant of 80. Yet the inset of Figure 4 presented in 1952 shows that the dielectric constant has reached almost to the full macroscopic value of 80 at a location only 4 Å from the center of the oxygen atom. Clearly if I had extended the region of low dielectric constant farther out to cover the entire area or at least a larger area, the calculated selectivity ratio would rise to a much higher value. That was what I did later in the more comprehensive treatment of selective ion adsorption (Ling 1962, Chapter 4.)

Finally, I want to mention something akin to, perhaps even part-and-parcel of what lay behind Fenn's exclusion from his reviews of the idea and work of Benjamin Moore, Herbert Roaf and Arthur Webster. That something is lurking in Helfferich's otherwise fine book on *Ion Exchange* (Helfferich 1962.) In essence, it was another case of abusing the position of a trusted review-writer. But instead of total omission as in the case of Fenn's review, it was in the form of an unsubstantiated sweeping attack.

The English version of Helfferich's book was published in 1962, three years after its first appearance in German. As mentioned earlier, illustrations of the theories of Gregor and reproduced as Figures 2 and 3 in this article were taken from the prominent main text of Helfferich's book on pages 97 and 99 respectively. In both illustrations, the countercations are fully dissociated despite their extremely high concentration in the resin water (reaching 3 M or even higher.) (And, despite the fact that the anionic sites are fixed in space.)

It is true that Helfferich quoted the adsorption models (of Wiegner, Jenny on soil and permutit) Pauley and Harris & Rice but not mine published before both. However, these quotes were all given in small prints, tucked away behind the statement that "Today, these approaches are of historical interest only" (p. 193.)

Hefferich gave no theoretical or experimental justifications for making such a sweeping derogatory statement. In view of what will be presented below — which completely vindicates the essential correctness of my view presented as part of LFCH (and repeated later by Pauley and by Harris & Rice.)

What this kind of unexplained putdown shows is this. The rejection of preferential adsorption as the cause of selective accumulation of K^+ in living cells (as exemplified by Fenn's exclusion of Moore *et al*'s work) was not confined to cell physiology. Rather, it was a part of a larger movement of rejecting selective adsorption as the cause of selective

accumulation of K^+ in soil, permutit and exchange resin as well. Thus, it seems that a global *culture of universal dissociation* has evolved surreptitiously; see Appendix A.

Theory of enhanced association with immobilization (and aggregations) of one kind of participating ion or molecule

As mentioned already above, in 1952 I presented very briefly at the Symposium on Phosphorus Metabolism a new theory on selective ion adsorption in living cells and in model systems including soil, permutit and ion exchange resins. One component of the theory (Part 4) deals with the question, could spatial fixation of one species of an interacting ion pair enhance strongly their association? My answer was yes with two sets of linked mechanisms. One is electrostatic and the other was described as kinetic. The following is a *verbatim* quotation of the bulk of what I wrote in 1952 (Ling 1952, p. 769.)

1) "The force of attraction between ions of opposite sign in solution is opposed by the kinetic energy of the ions themselves. If one of the ions is rigidly fixed, half of this energy is abolished, so that the ions stay on the average closer together than they would be able to do when both are free….
2) Fixation allows the close juxtaposition of a number of similarly charged ions, for the repulsive forces between them are less strong than the covalent bonds of fixation. Their individual fields thus overlap, and sum with respect to the force exerted collectively upon a free ion of opposite sign." (Ling 1952, p. 769.)

Having repeated what I expressed more than fifty years ago, I reiterate here once more what I already said above. On this, what I believe to be a critically important issue, close-contact association in consequence of site fixation, neither Weigner nor Jenny before me, nor Pauley, nor Harris & Rice after me made any comment whatsoever. They assumed full or partial *association* just as others assumed full *dissociation*. With only one lone exception, myself, neither side gave a reason why its side is correct while the other side in incorrect. However, for me to expect scientists in a different field to know what I wrote in a 135-word passage in a Symposium Volume on a highly specific biochemical problem (Phosphorus Metabolism) would be unrealistic. All these point to the urgent need to make this present paper easily accessible.

In what follows, both the kinetic mechanism and electrostatic mechanisms will be discussed but under different headings: kinetic and thermodynamic respectively. However, though both valid, the thermodynamic approach is in my view more rigorous and simpler. For this reason, I shall present the kinetic analysis as an appendix (Appendix B.) The thermodynamic analysis will be the main thesis to develop next.

A thermodynamic analysis of the cause of enhanced close-contact, one-on-one association of K^+ and other charged or uncharged particles

The primary subject of this communication is *association* between a pair of small particles or molecules, A and B, and it is described by the following equation:

$$A + B \rightleftarrows AB \, . \tag{1}$$

However, the conventional approach of a physical chemist to this problem is from the opposite direction. It is *dissociation* — represented by the same Equation 1 but read backward. As such, it is also described by an equation of the *dissociation constant*, K_{AB}, as follows:

$$K_{AB} = \frac{n_A n_B}{n_{AB}} = \frac{c_A c_B}{c_{AB}} \tag{2}$$

$$= \frac{1000}{L} \cdot \frac{(p.f.)_A (p.f.)_B}{v(p.f.)_{AB}} \cdot \exp\left(-\frac{\chi}{kT}\right), \tag{3}$$

where n_A, n_B and n_{AB} are respectively the number of A, B and AB in the vessel, c_A, c_B and c_{AB} are their respective molar concentrations. L is the Avogadro number. $(p.f.)_A$ $(p.f.)_B$ and $(p.f.)_{AB}$ are the statistical mechanical parameters called *partition functions* of A, B and AB respectively. v is the volume of the container. k is the Boltzmann constant, T the absolute temperature and χ is the dissociation energy, equal to the work needed to separate the associated ion pair AB at rest and at its lowest vibrational-rotational state to A and B each at rest and at its lowest internal energy states in a vacuum.

The partition function, represented here as (p.f.) is a theoretical parameter of central importance in the science of statistical mechanics. A partition function is the sum of $1 + \exp(\varepsilon_1/kT) + \exp(\varepsilon_2/kT) + \exp(\varepsilon_3/kT) + \cdots\cdots\exp(\varepsilon_r/kT)$, where ε_1, $\varepsilon_2 + \varepsilon_3 \cdots\cdots\varepsilon_r$ are the quantum mechanical allowed energy levels of the particles involved (Gurney 1949.)

Note that in general, $(p.f.)_A$ and $(p.f.)_B$ are positive numbers and that each causes the increase of the degree of *dissociation* and hence rise of the dissociation constant $K_{AB.}$ In contrast, $(p.f.)_{AB,}$ the partition function for the associated AB pair as well as the dissociation energy, $(-\chi)$ favors *association*. The larger the value of $(p.f.)_{AB}$ and $-\chi$, the greater the degree of association and hence the smaller the dissociation constant K_{AB}. Please keep these simple relationships in mind; they will come in handy later to understand a key point of this communication.

In theory, each of these partition functions could consist of one or the product of more than one partition function. To all intents and purposes, a mono-atomic particle in vacuum has only one partition function, namely the translational partition function, which describes the kinetic energy of the particle. A diatomic or multi-atomic particle also has a translational partition function. In addition, they also possess internal energies expressed by their respective rotational and vibrational partition functions.

In their classic treatise, *Statistical Thermodynamics,* Fowler and Guggenheim (1960 p. 377) calculated the association energy, χ, of Na^+ and Cl^- (in air), to equal 8.63×10^{-12} ergs per particle or 124 Kcal/mole. Because of such an intense attraction between them, Na^+ and Cl^- are fully associated in vacuum or air. Fowler and Guggenheim then went on to examine Na^+ and Cl^- in water. Dividing the value of χ just cited by 80, the macroscopic dielectric constant of water, they derived a dissociation constant K_{NaCl} of 7.

This, they pointed out is still too high. That is, it is not in keeping with what they believed to be near-complete dissociation even in a moderately concentrated solution of strong electrolytes like NaCl (see quote from them on page 16 of the present document.) Worse, they further pointed out that to assign a dielectric constant of 80 ignored the phenomenon of *dielectric saturation* (as I mentioned earlier.) That is, at close range, electric polarization drastically reduces the dielectric constant to a much lower value. (See inset

of Figure 4.) In that case, χ/D would become even larger and the predicted degree of dissociation would be even smaller. In the end, Fowler and Guggenheim pointed out that the unresolved problem could originate from the hydration of the ions, a subject I have referred to repeatedly above and will elaborate a bit further next.

Whereas a bare Na^+ or bare Cl^- is a spherical entity with no internal energies, hydration makes both *de facto* multi-atomic and as such they now possess rotational and vibrational energies as well. Particularly noteworthy is the emergence of rotational partition functions, which increase in magnitude sharply with increase in size and mass. In consequence, the products of the translational, rotational and vibrational partition functions of both (hydrated) Na^+ and (hydrated) Cl^- become much larger. It is true that the partition function of the associated ion pair, Na^+Cl^- would also be increased by hydration. But that increase of a single entity (the hydrated associated ion pair) would be much smaller than the increase of the products of two increased entities, the dissociated hydrated Na^+ and dissociated hydrated Cl^-. Thus hydration of the ions would definitely bring about greater dissociation of Na^+ and Cl^- in water despite the intense attraction between the oppositely charged ions.

Our next task is to return to our central subject of this communication: how, from a thermodynamic viewpoint, the *spatial fixation and aggregation of one of the interacting species,* A, affects the degree of its association with the other species, B, thus forming an one-on-one, close-contact associated pair AB like that mentioned above in Equation 1.

To begin, let us return to our simple pair of interacting gas molecules A and B in air or vacuum each at a moderate concentration. There is some weak attraction between them but largely they remain dissociated. Now with a wave of a magic wand, all the A's are joined into a large network and thus become immobilized and fixed in space. What would this magic act of immobilization do to the degree of association of B with A? The answer is to produce a dramatic increase of association.

However, to make it easier to tell how and why, we need to review some basic thermodynamics first. The Helmholtz's free energy, F, is equal to the sum of the energy of the system, E, minus the product, TS where T is the absolute temperature and S the entropy of the system. Entropy S, in turn, is equal to k ln W, where k is the Boltzmann constant and W is the number of *a priori* equally probable microscopic states of the system. W can be separated into two kinds. One kind is related to what one may call *thermal entropy*; it is the number of ways the shared amount of energy E is distributed among the quantum-mechanically allowed energy levels; and we represent it as ln W_{th}. The other kind is called *configurational entropy*, k ln W_{cf}, where W_{cf} refers to the number of ways the particles can be found occupying different positions or fixed sites.

ln W_{th} is additive. Thus, the ln W_{th} of a solution is the sum of the ln W_{th}'s of its different component particles. ln W_{cf}, on the other hand, is communal and cannot be split into different components.

With all these in hand, we can look into what would happen when all the A's are rigidly fixed in space and made into a network of fixed A's. First, by rigidly fixing and arresting all the A's motional freedom, their W_{th}^A becomes (or approaches) unity and ln W_{th}^A becomes zero (or a very small number.) Second, a new configurational entropy is created corresponding to what we shall designate as W_{cf}. Meanwhile, the B's would have the choice of either remaining free or engaging in one-on-one, close-contact association with the individual fixed A sites. The overall impact of the magic transformation or fixation is that the total ln W of the assembly will change from

$$\ln W_{th}^{A(free)} + \ln W_{th}^{B(free)} + \ln W_{th}^{AB} \tag{4}$$

to

$$\ln W_{th}^{B(assoc)} + \ln W_{th}^{B(free)} + \ln W_{cf} \, . \tag{5}$$

The disappearance of $\ln W_{th}^{A(free)}$ produces a reduction in the trend toward the *dissociated* state. The *de novo* creation of the configurational entropy term means an entropy gain of, and hence increase in the trend toward, the *associated* state. Together, immobilization of what was once free A into a network of fixed A, has generated two different but mutually complimentary entropic causes for the *enhancement of association* of A and B.

Note also that this twofold entropic mechanism for enhanced close-contact association applies to molecules carrying no net electric charges as well as to molecules or ions carrying net electric charges.

In the preliminary version of the manuscript I put together, my next step involved the presentation of a standard statistical mechanical treatment of the problem to reach a rigorous result. The treatment I chose was essentially that of Fowler and Guggenheim and as such contains nothing new beyond what they did. So on further consideration, I decided to move this derivation part to the end of the document under the designation, Appendix C.

With the derivation part out of the way, I proceed here straight to the result. However, to do that I must first define a symbol, θ, as the fraction of fixed A sites that is occupied by B and another symbol, $1-\theta$, representing the fraction of A sites unoccupied. Then the derivation given in full in Appendix C would produce the following formula:

$$\frac{\theta}{1-\theta} = \frac{p}{p^o} \, , \tag{16}$$

where p is the existing vapor pressure of the gas B and p^o is a function of the temperature T and the partition function ratio of free and adsorbed B given as Equation 17 in Appendix C. Equation 16 can be written in a different form:

$$\theta = \frac{p}{p^o + p} \, . \tag{18}$$

Formula 18 is, of course, the equivalent of an equation Irvin Langmuir introduced in 1918 for the adsorption of gas molecules on solid surfaces *via* a kinetic approach, — but traditionally given in the following form:

$$\frac{x}{m} = \frac{k_1 k_2 p}{1 + k_1 p} \, , \tag{19}$$

where x represents the amount of gas adsorbed on a given mass, m, of the adsorbent; k_1 and k_2 are constants for a given gas (Langmuir 1918.) Boundary condition considerations, however, offer us insights into the meanings of these constants.

At very high pressure, p, $k_1p >> 1$; x/m then equals k_2. In other words, k_2 is equal to the maximum number of adsorption sites per unit weight of the adsorbent; as such, it can then be represented by the symbol, [f].

At very low pressure, $k_1p << 1$. x/m then approaches k_1k_2 p and is thus linearly related to p. A reasonable interpretation is that k_1 measures the affinity of the molecule B for the adsorption site. In other words, it is the adsorption constant (or association constant) of B on the fixed site A. The reciprocal of this adsorption constant is of course the dissociation constant, K_{AB} of Equation 2 — before the magic wand has joined the free A's into a network of fixed A's now called A sites.

In summary, in the above I have imported information from two separate Chapters of Fowler and Guggenheim's classic treatise, *Statistical Thermodynamics*.

From Chapter IX on Solutions of Electrolytes, the section on Strong Electrolytes was selected. From Chapter 10 on Surface Layers, the section on Ideal Localized Monolayers was selected. One is on electrolyte solutions and the others is on adsorption of gas molecules on solid surfaces. Beside fundamental physics, there are no specific links between these Chapters. Indeed, the overall direction or orientation may even be seen as heading toward opposite directions.

Thus, the Chapter of Solutions of Electrolytes is toward dissociation. In the words of Fowler and Guggenheim, it says that: "at least in dilute and moderately concentrated solutions (of strong electrolytes) there are at most very few NaCl molecules, and in many cases the properties of the solution can be accurately accounted for on the assumption that no undissociated molecules at all are present." (Fowler and Guggenheim 1960, p. 377.)

In contrast, the Chapter on Surface Layers refers to layers of gas molecules adsorbed. Despite the fact that gas molecules like nitrogen and argon do not carry net electrical charges — the source of intense attraction between ions like Na^+ and Cl^- — they do associate with sites on solid surfaces especially at low temperature (McBain 1932.) At low or moderate concentration in free space, they behave like an ideal gas. As such, they do not associate to a significant degree.

Yet with our magic wand, a bridge between these two diverging chapters are joined together through the spatial fixation of one species of the interacting atoms. By using a thermodynamic approach, we have shown that the observed association of gas molecules on solid surfaces lies really in the spatial fixation of one of the interacting molecules we call A. This spatial fixation was unnoticed or ignored in the past because it was buried and thus hidden in the concept and word of a *solid* surface.

Thus far, I have shown that the two-fold entropic causes for increased association apply to molecules bearing net electric charges as well as to molecules bearing no electric charges. In the next section, I shall demonstrate how in the case of molecules or ions bearing net electric charges (like K^+ and Cl^-) there are additional causes for enhanced association through the spatial fixation of one of the interacting species.

The electrostatic contributions that further enhance the close-contact association of electrically charged molecules or ions due to the spatial fixation and aggregation of one interacting species

Oxalic acid, HOOC-COOH, has two carboxyl groups, which are indistinguishable. Yet, the acid dissociation constants or pK_a of the same pair of carboxyl groups are in fact quan-

titatively different. In 1923 Bjerrum offered an explanation for this seeming paradox (Bjerrum 1923.) The first dissociation from HOOC-COOH could be from either one of the two COOH groups and accordingly, there are two choices. In consequence, the first dissociation is favored by a statistical factor equal to the natural logarithm of 2 or ln 2. In the opposite direction, the first association of -OOC-COO- also has two choices. Therefore, the first association is also favored by a factor of ln 2. Taken together, the first dissociation constant differs from the second by ln 2 + ln 2 = ln 4. The reader might recognize that in this case, the number 4 is what we have referred to categorically as W_{cf}. It is the contribution from the configurational entropy, k lnW_{cf}.

The configurational entropy contribution is not the only reason for the difference in the two real-world acid dissociation constants, which are respectively 1.23, and 4.19. The difference between these two values is 2.96, which exceeds ln 4 (= 1.39) by 1.57. Bjerrum attributed this additonal difference of 1.57 to an *electrostatic effect*. That is, the dissociation of the second proton would be not only against the attraction of that (second dissociated) carboxyl group but also that of the first dissociated carboxyl group.

Of course, oxalic acid has only two similar electrically charged groups. In living systems, and model systems, there might be many similar electrically charged groups congregating together. As we move from the microscopic oxalic acid system to the system containing more and more similar electrically charged groups, we are entering into the realm where the Law of ***Macroscopic*** Electric Neutrality holds sway as I mentioned in 1952.

In fact, on this subject, Guggenheim offered a numerical example worth repeating (Guggenheim 1950, p. 330.) Consider a sphere with a radius of 1 cm. Give it an excess of one kind of electrically-charged particles or ions equal in amount to 10^{-10} gram-ions. This amount of electric charges would create an electrostatic potential of 0.95 x 10^7 volts — a voltage so enormous that you can find them only in high voltage laboratories or during thunderstorms. Yet, 10^{-10} gram-ion is such a minute number of (electrically-charged) ions, it is not detectable by any known chemical methods.

What this example tells us is that in this and other macroscopic bodies the total number of free positive charges must be "exactly" equal to the number of free negative charges — a rule known as the *Law of Macroscopic Electric Neutrality*. Protein and nucleic acid molecules in living cells are nowhere nearly as large as Guggenheim's sphere but still vastly larger than an oxalic acid molecule. Both proteins and nucleic acids possess fixed charges like the carboxyl groups of oxalic acid but in great abundance. The aggregate impact is that the value of the energy of association or adsorption, represented as $-\chi$ in Equation 3, is further enhanced. That enhancement further reduces the probability of the dissociation of the counter-cation like H^+. But, that is not all.

For the ions that do manage to dissociate will suffer further restriction also because they cannot leave the immediate vicinity without violating the law of macroscopic electric neutrality. This reduces the translational partition function of the dissociated ion and further enhances association of counter-cations like K^+. Thus, by joining and fixing into a network one species of the interacting electrically-charged molecules or ions, the additional impact of immobilizing them is also twofold.

In summary, for molecules that do not carry net electric charges, fixation of one of the interacting species in space enhances their close-contact associaiton by two entropic mechanisms, one thermal and the other configurational. For molecules and ions that do carry net electric charges like K^+ and Cl^-, these two-fold entropic mechanisms operate

fully. But their close-contact association is further increased by an electrostatic energy mechanism and by an additional entropic mechanism of reduced translational entropy.

Thus for ions and charged molcules like K^+ and Cl^-, there are all-told three independent entropic mechanisms and one energetic mechanism for enhanced close-contact ssociation. Together, this thermodynamic treatment — in harmony with a parallel kinetic analysis described under Appendix A — would predict extensive association of ions like K^+ with available β-, and γ-carboxyl groups of cell proteins as well as with negative charged groups on soil and permutit and ion exchange resin. So far, this is theory.

As pointed out earlier, our next task is to test, and if possible verify the fully-expanded version of LFCH. To do so rigorously, we need to put the theory derived into forms that are more exact. That will be the main task of the next section.

Extensions of the Langmuir adsorption isotherm

As pointed out above, Equation 16 and 18 are the equivalents of an equation Irvin Langmuir first introduced in 1918 but more commonly given in the following form

$$\frac{x}{m} = \frac{k_1 k_2 p}{1 + k_1 p}, \tag{19}$$

where x represents the amount of gas adsorbed on a given mass, m, of the adsorbent; k_1 and k_2 are constants for a given gas (Langmuir 1918.)

At some intermediate pressure, $x/m = kp^{1/n}$ with n in the range between 0 and 1 may hold. This formula, of course, takes on a form of the classical adsorption isotherm sometimes referred to as the Freundlich isotherm.

The Langmuir adsorption isotherm itself can be extended to adsorption of dissolved molecules in an aqueous solution. Thus, according to Henry's Law, the amount of a gas dissolved in a unit volume of a solvent is proportional to the gas pressure at the same temperature. The proportionality constant is the solubility of the gas and we will represent it as q_i. Representing the concentration of the gas in solution as $[p_i]$, we can substitute the gas pressure p's in Equation 19 with its concentration $[p_i]_{free}$ since q_i will cancel out. Substituting k_1 and k_2 with K_i and [f] respectively, we have

$$[p_i]_{ad} = \frac{[f]K_i[p_i]_{free}}{1 + K_i[p_i]_{free}}. \tag{20}$$

If each of the fixed sites carry a single negative charge and the dissolved molecule are of two kinds, mono-valent cations, K^+ and Na^+, we will have

$$[K^+]_{ad} = \frac{[f^-]K_K[K^+]_{free}}{1 + K_K[K^+]_{free} + K_{Na}[Na^+]_{free}} \tag{21}$$

where $[K^+]_{ad}$, the concentration of adsorbed K^+, and $[f^-]$, the concentration of fixed anions are both in moles per kilogram. K_K and K_{Na} are the respective adsorption constants of K^+ and Na^+ in $(moles/liter)^{-1}$. $[K^+]_{free}$ and $[Na^+]_{free}$ are the respective concentration of free K^+ and free Na^+. In cases, where there are more than one competing species, we have

$$[K^+]_{ad} = \frac{[f^-]K_K[K^+]_{free}}{1 + K_K[K^+]_{free} + \Sigma_i K_i[p_i]_{free}}. \quad (22)$$

Equation 20 can be also written in a generalized but reciprocal form:

$$\frac{1}{[p_i]_{ad}} = \frac{K_i}{[f]}\left(1 + \frac{[p_j]_{free}}{K_j}\right)\frac{1}{[p_i]_{free}} + \frac{1}{[f]}. \quad (23)$$

A plot of $1/[p_i]_{ad}$ as ordinate against different values of $1/[p_i]_{free}$ at zero or a constant $[p_i]_{free}$ would yield a straight line. The slopes of these straight lines would vary with the value of $[p_i]_{free}$. The quantitative values of $[f]$, K_i and K_j can be determined from the ordinate intercept, the slopes etc. in these multiple reciprocal plots (for example, see Figure 30 below.)

This then marks the formal part of the theoretical section intended to update and fully develop what was introduced in Ling's Fixed Charge Hypothesis (LFCH) over fifty years ago. However, as briefly mentioned above, the LFCH in time became the embryonic version of the unifying theory called the association-induction (AI) hypothesis. Indeed, what I have done so far in this article is further to advance the association aspect of the association-induction hypothesis. Association brings together the physical ingredients of protoplasm; induction makes them alive.

One expression of this inductive component is the nearest neighbor interaction energy ($-\gamma/2$) of Equation 31 in Appendix D as demonstrated among the fixed sites engaged in close-contact adsorption of ions like K^+, gas molecules like oxygen and polar molecules like H_2O. A recent theoretical breakthrough in the basic theory of long-range polarization-orientation of water in living cells and model systems received dramatic confirmation from the demonstration of the exclusion of microspheres from water 100 or even more μm away from a polarizing NP- (or NO-) surface of polyvinyl alcohol by Zheng and Pollack (2003.)

However, long before, there was experimental confirmation of interaction between nearest neighboring heme sites in hemoglobin (Ling 1965) and between β-, and γ-carboxyl groups of cell proteins, that quantitatively obey the prediction of the cooperative adsorption isotherm introduced by Yang and Ling in 1964. This isotherm and its variations and two illustrations (Figure D1 and D2) are presented in Appendix D. They will be cited from time to time in the next section summarizing the experimental confirmation of close-contact association of K^+ and other ions on isolated proteins and other model systems.

Experimental evidence supporting the theory of enhanced close-contact association of K^+ and other ions with spatially fixed ions bearing the opposite electric charges

Since my brief presentation in 1952 of what has been known as the *principle of enhanced ionic association with site fixation (and aggregation) of the oppositely charged ions*, supportive evidence have come from two sources: from other laboratories in work published before my theory was introduced; from my own laboratory, specifically designed and carried out to test the theory. All these studies confirm the essence of the theory; none to my

best knowledge contradicts it without being reversed. However, space limitation does not permit inclusion of all the confirmatory evidence. (See, for example, Ling 2001, p. 27, pp. 56–62, pp. 187–190.) In the following, I shall present those evidence that can be presented without an extensive background introduction. And I shall present these evidence under two headings: studies on inanimate models; studies on the living cell.

1. Studies on inanimate models

1.1 Enhanced counter-ion association with the (micellar) fixation and aggregation of long-chain electrolytes

Solutions of electrolytes conduct electricity according to Ohm's law. That is, the electric current generated is directly proportional to the applied electromotive force or EMF and inversely proportional to the resistance of the solution. The reciprocal of the resistance is known as the conductance (in units of reciprocal ohms, ohm^{-1}). Placed between two large parallel-plate electrodes 1 cm apart, the conductance of 1 gram equivalent of an electrolyte is called its *equivalence conductance*, λ. To measure the λ of an electrolyte of different concentration, the area of the parallel plate electrodes must vary accordingly.

Figure 6 shows the data of Hartley *et al* (1936) on the equivalent conductance (λ) of increasing concentration of cetyltrimethylammonium bromide and that of its component ions, cetyltrimethylammonium cation and bromide anion separately. Note that the concentration shown on the abscissa is given in the square root of gram equivalent per liter so that a wide range of concentration can be compressed to fit a limited space.

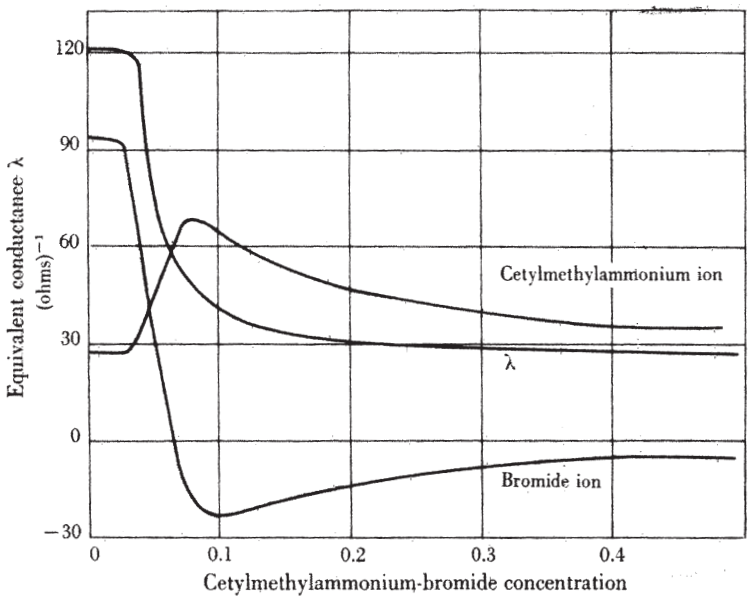

FIGURE 6. The equivalence conductance of cetyltrimethylammonium bromide and its component ions, cetyltrimethylammonium cation and bromide anion at different concentrations, c. Note that the concentrations are given as the square root of concentration, $c^{1/2}$, on the abscissa to conserve space. (figure drawn after Hartley *et al*. from Ling 1962)

Note also that at the concentration of about 0.001 gram-equivalent per liter, λ of the cetyltrimethylammonium bromide solution as a whole begins to fall sharply. It is at this concentration that the long-chain anions begin to assemble into *micelles* with expected loss of motional freedom and gain in the degree of spatial fixity. Concomitant with this change, the equivalent conductance of the long chain cation began to rise and the equivalence conductance of the bromide anion began to fall. Note also that the fall of bromide conductance did not stop at zero. It went negative. That is to say, the negatively charged bromide ion, instead of moving toward the positively charged anode, was moving toward the negatively charged cathode. This apparently anomalous behavior of the bromide ions shows that they were no longer the independent anions any more but were associated with the fixed cations of the micelles and together they continued to move toward the cathode.

I conclude this section with a word of caution. The fact that we witness the migration of the negatively charged bromide ion toward the negative cathode offers a strong argument that the bromide ion is associated with, and thus became an appendage to the positively charged micelles. Nonetheless, by itself, this fact cannot be construed as conclusive evidence for close-contact, one-on-one adsorption between bromide and micellar cationic sites. The phenomenon observed could also be explained if the Br^- ions merely follow the micelles as part of a diffuse ion cloud. We need more discriminating studies that could give us the right answer.

1.2 Demonstration of "inactivation" of free and "visible" Na^+ when sodium iso-butyrate molecules, $(CH_3 - \underset{\displaystyle COO^- Na^+}{\underset{|}{CH}} - CH_3)$ polymerize into

long chains of sodium polyacrylate $(-\underset{\displaystyle COO^-Na^+}{\underset{|}{CH}} - CH_2 -\underset{\displaystyle COO^-Na^+}{\underset{|}{CH}} - CH_2 - \underset{\displaystyle COO^-Na^+}{\underset{|}{CH}} - CH_2 -)_n$

With a Na^+-specific, sodium amalgam electrode, Kern (1948) measured the activity of Na^+ in solutions of sodium isobutyrate at concentrations ranging from 0.0125 M to 0.2 M. Table II shows that the activity coefficients, f, obtained by dividing the Na^+ *activity* measured with the Na^+-specific electrode by the total Na^+ concentration, were all close to unity. In contrast, the activity coefficient of Na^+ in solutions of polyacrylate carrying carboxyl groups at similar concentrations were much lower, ranging from 0.30 to 0.168.

The primary difference between these two sets of solutions lies in the immobilization and aggregation of the carboxyl-groups in one set and absence of such immobilization and aggregation in the other. Thus, Kern's data again confirm the theory of enhancement of counterion association with site fixation. Kern's data also corroborate Hartley's evidence of counterion association — following the immobilization and fixation of long-chain electrolytes though micellar aggregation. One may add that the main conclusions of Hartley *et al* and of Kern stated above has been confirmed by Bradley and Sulley (1948) and by Huizenga *et al* (1950.)

While Kern was of the opinion that by joining the monomers into a fixed network inactivated the Na^+, that *inactivation* also cannot be equated with close-contact one-on-one association or adsorption. Conceivably, this too can be achieved by the Na^+ hovering around anionic polyacrylate as part of a diffuse ion cloud. Once more, a discriminatory test would be needed to establish unequivocally one or the other alternative. Such a discriminatory test will be introduced in the next section.

TABLE II. Electrometric measurements of Na^+ activity of an aqueous solution of Na^+ isobutyrate and that of Na^+ polyacrylate.

Concentration of Na^+ (M)	Activity of Na^+ (M)	Activity coefficient
	Isobutyric acid, $CH_3CHCOOH\ CH_3$	
0.2	0.186	0.93
0.1	0.090	0.90
0.05	0.049	0.98
0.025	0.025	1.00
0.0125	0.0122	0.98
	Polyacrylic acid, $(\text{-}CH_2CHCOOHCH_2\text{-})_n$	
0.2	0.060	0.30
0.1	0.0315	0.315
0.05	0.0146	0.292
0.025	0.0058	0.232
0.0125	0.0021	0.168

(data from Kern 1948, table from Ling 1984 by permission of Springer-Verlag GmbH/Plenum Publishers)

1.3 Experimental proof of one-on-one, close-contact association of Na^+ with anionic sulfonate groups on linear chains of polystyrene sulfonate

Ling and Zhang repeated what Kern had done before (Ling and Zhang 1983.) But instead of polyacrylate, Ling and Zhang used sodium polystyrene sulfonate (NaPSS), which is a close model of commercial cation exchange resins; NaPSS is, in fact, a sulfonate cation exchange resin with zero percent cross-linking. Thus, if we can prove that counter-cation Na^+ is engaged in close-contact, one-on-one association with the fixed sulfonate groups in the NaPSS model, it would firmly and unequivocally establish that in the conventional cross-linked ions exchange resin the counter-cations are fully associated in a similar manner — since incorporating a cross-linking agent would further immobilize the polymer and, accordingly, further promote close contact association as made clear in the theoretical section above.

Figure 7 shows that the concentration of total Na^+ (measured by chemical analysis) and free Na^+ (measured with the Na^+-selective glass electrode) are different in solutions containing increasing concentration of the polymer, NaPSS. That only a fraction of the Na^+ present is visible to the Na-sensitive electrode confirms in essence what Kern reported earlier. If we tentatively call the invisible fraction as bound (and provide proof for this assumption later), we obtain the data presented in Figure 8.

Note that in Figure 8, the percentage of invisible Na^+ starts out at a very low value. At about 5% NaPSS concentration, the percentage of invisible Na^+ begins to rise steeply until it reaches a plateau of about 80%. This suggests an *autocooperative* aggregation (see Appendix D) similar to what is known as micellar aggregation discussed in Section 1.1.

Now, we move on to a new approach or tactic. This new tactic was designed specifically to verify the postulate of close-contact, one-on-one association of the "invisible" Na^+ (or moving-in-the wrong-direction Br^-). Before presenting the result, we need to refresh our memory on long-range attributes versus short-range attributes as we discussed earlier.

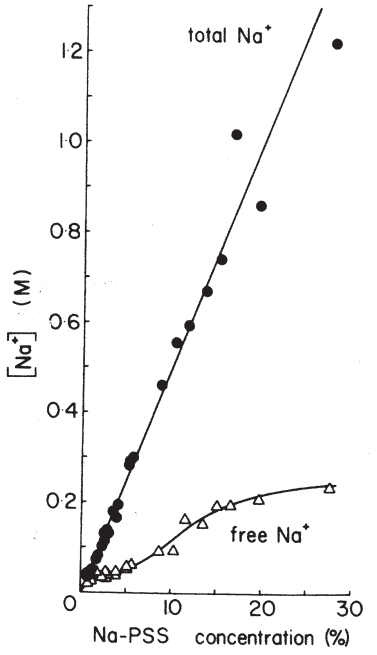

FIGURE 7. The concentration of total Na^+ and free Na^+ in increasing concentration of Na^+ polystyrene sulfonate (NaPSSP.) The abscissa represents concentration of NaPSS as percentage of solution (weight in g. /volume in ml.) Free Na^+ was detected by a Na^+-selective glass electrode. (from Ling and Zhang 1983)

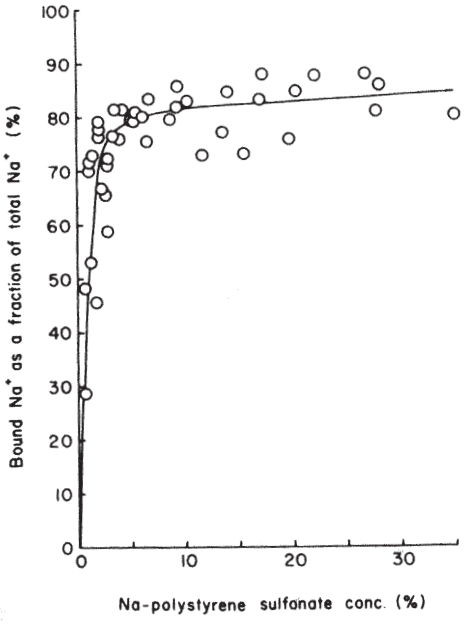

FIGURE 8. The fraction of Na^+ that exists in a form that is not detected by the Na^+-selective glass electrode in increasing concentration of NaPSS. (from Ling and Zhang 1983)

If the invisible Na^+ ions exist exclusively as part of a hovering ion cloud, they would be displaced and made visible by any other free cation. This follows because as part of a diffuse ion cloud, the total impact of any monovalent cation is that of the long-range attribute of positive electric charges. And, that long range attribute is shared by all cations, be it inorganic K^+, Rb^+, or organic cations carrying a single positive net charge like choline, guanidine, lysine or arginine (as well as multivalent cations.).

On the other hand, if that invisible Na^+ were in fact engaged in a close contact, one-on-one association, the respective impact of competing cations could be quite different. That follows because the association energies of the competing cations on the fixed anion depend on the short-range attributes like polarizability, dipole moment, Born repulsion constant etc. Since these short-range attributes of the different competing ions are as a rule different, the effectiveness of each in displacing the close-contact, one-on-one associated Na^+ would be different. This is, of course, theory. Let us now see what the actual experimental results tell us.

The experiments shown in Figure 9 confirm this general rule. To wit, the effectiveness of each (monovalent) ion in displacing the invisible Na^+ and making it visible to the Na^+-sensitive electrode varies widely. One may argue that the more powerful impact exercised by guanidine and choline over lysine might be somewhat related to the possession of α-amino and α-carboxyl groups in lysine but absent in guanidine and choline. But, that is not the right answer. Arginine, which also possess an α-amino and an α-carboxyl group is as effective or even more effective than guanidine and choline in displacing and making visible the invisible Na^+.

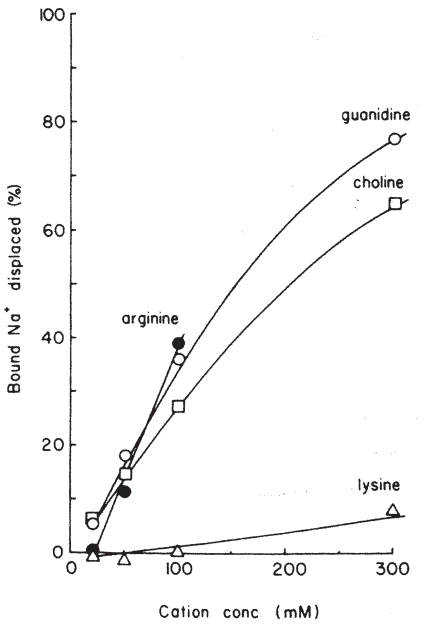

FIGURE 9 Respective fractional displacement of "invisible" Na^+ (ordinate) in 5% NaPSS solution and made visible to Na^+ selective glass electrode by increasing concentrations of competing positively-charged solutes: arginine, choline, guanidine and lysine. (from Ling and Zhang 1983)

In conclusion, this set of data has established the true significance of the invisibility of Na^+ to the Na^+ selective glass electrode. It shows that this invisibility is because these Na^+ ions are engaged in close-contact, one-on-one association with the fixed sulfonate groups. By analogy, Kern's Na^+ made invisible by the fixation and aggregation of monomeric isobutyric acid into poly-acrylic acid are similarly engaged in close-contact association. So is the Br^- moving in the wrong direction when the long-chain anions assemble into micelles.

There should be no difficulty now in believing that counter-ions in ion exchange resins are not in the form of free fully-dissociated ions as envisaged in the theories of Gregor and Katchalsky. Rather, that they are in close-contact association with fixed anionic groups as I first suggested as part of Ling's Fixed Charge Hypothesis in 1952 but presented here as an updated and fully-developed theory on pages above.

In the next study, Ling and Zhang (1984) addressed the question whether or not K^+ and other alkali metal ions also engaged in close-contact one-on-one adsorption on β- and γ-carboxyl groups of proteins when these carboxyl groups are liberated from the grip of salt-linkages.

1.4 Step by step neutralization of the fixed cationic ε-amino groups and guanidyl groups of bovine hemoglobin with NaOH produces a stoichiometric one-on-one close-contact adsorption of Na^+ on every one of the liberated β- and γ-carboxyl groups of the protein

Using essentially the same measuring technique described in the preceding section, Ling and Zhang (1984) continued their study of alkali-metal ion adsorption on the solid component of living cells, the intra-cellular protein, hemoglobin. This specific (oxygen-transporting) protein makes up 97% of the intracellular proteins of mammalian red blood cells (Ling *et al*, 1984, p. 389.) Unlike polystyrene sulfonate, hemoglobin is endowed with about an equal number of fixed cationic sites and fixed anionic sites. Apparently, most if not all of these fixed anions and fixed cations are engaged in forming *salt-linkages* (for a brief review on this subject, its controversy and its eventual resolution, see Endnote 2.)

First, we studied the adsorption of Na^+ on five native proteins — should be better called "native proteins" — in a neutral 200 mM NaCl solution. The protein concentrations studied were between 10% and 15% in concentration after the protein solution had been exhaustively dialyzed to remove contaminating ions. The contents of the dialysis sacs were then analyzed respectively with atomic absorption spectroscopy for its total Na^+ concentration and with the Na^+ selective glass electrode for its free Na^+ concentration. By difference, the concentrations of adsorbed Na^+ shown in Table III were obtained.

These data in Table III show that while native hemoglobin adsorbs no or very little Na^+, other proteins do adsorb Na^+ but to varying degrees. Thus, nearly 15% of the Na^+ in the egg albumin solution was invisible to the Na^+ selective glass electrode and from what was described in Section 1.3 above, adsorbed. In contrast, Table IV shows that the adsorption of Na^+ of all five proteins rose to 40% to 50%, when they were incubated in 200 mM NaOH instead of 200 mM NaCl. Thus, high pH dramatically increases Na^+ adsorption in all native proteins. Taken together, the data of Table III and Table IV have falsified the not uncommon belief: proteins do not adsorb alkali metal ions — a misconception that had played a key role in the ill-fated adoption of the membrane pump theory long ago (Lillie 1923.)

In agreement, Figure 10 shows that if intead of NaCl, NaOH in increasing amount it added to a hemoglobin solution, only a fraction of the Na^+ added is visible to the

TABLE III. Na^+ binding on five native globular proteins at neutral pH.

Protein					$[Na^+]_{bound}$	
Name	Concentration (%)	pH	$[Na^+]_{total}$ (mM)	$[Na^+]_{free}$ (mM)	%	μmoles/100 g. dry protein
Bovine serum	15.6	5.06	209	201	3.83	5.13
	15.4	5.06	215	201	6.73	9.41
	14.1	5.14	219	208	4.85	7.50
	14.2	5.14	215	205	4.78	7.27
	(14.8±.39)	(5.10±0.02)	(214±2.0)	(204±1.7)	(5.05±0.61)	(7.33±.87)
Egg albumin	13.4	8.43	228	188	17.5	29.7
	13.5	8.47	233	193	17.2	29.5
	11.9	7.99	227	199	12.3	23.5
	12.0	7.99	227	199	12.4	23.5
	(12.7±0.43)	(8.22±0.13)	(229±1.4)	(195±2.6)	(14.85±1.44)	(26.35±1.76)
γ-globulin	18.9	6.61	217	196	9.76	11.22
	19.0	6.62	208	200	3.94	2.07
	15.6	6.64	215	205	4.55	6.27
	15.8	6.64	206	205	5.82	3.67
	(17.3±0.94)	(6.63±0.01)	(211±2.6)	(201±2.2)	(6.02±1.3)	(5.81±2.00)
Hemoglobin	16.6	7.47	203	198	2.60	3.18
	16.6	7.47	203	200	1.67	2.04
	13.1	7.44	200	200	0.00	0.00
	13.2	7.45	205	205	0.00	0.00
	(14.9±0.99)	(7.46±0.01)	(203±1.0)	(201±1.5)	(1.07±0.64)	(1.30±0.79)
Myoglobin	13.8	7.49	209	194	7.44	11.27
	13.8	7.51	210	197	6.23	9.46
	11.0	7.41	208	198	5.02	9.50
	11.4	7.43	209	197	5.97	10.96
	(12.5±0.75)	(746±0.02)	(205±0.41)	(197±0.86)	(6.16±1.24)	(10.30±0.48)

All proteins were dissolved in 200 mM NaCl at a protein concentration of 20% (w/v) and then dialyzed against 200 mM NaCl at 4° C for 1 to 4 days. (from Ling and Zhang 1984)

TABLE IV. Percentage of bound Na^+ in NaOH-treated globular proteins.

	Bound Na^+ (% of total Na^+)		
Proteins	1	2	3
Hemoglobin	53.7, 40.7, 50.4		
Bovine serum albumin	43.5, 36.8, 49.0	52.4	56.0
Egg albumin	40.4 57.8	45.0	34.0
γ-globulin	41.3 48.7	36.0	41.0
Myoglobin	46.2		

1. 20% protein in 200 mM NaOH solution kept at room temperature overnight. 2. 10% protein in 200 mM NaOH kept at room temperarture and then dialyzed against 10 mM NaOH. 3. 10% protein in 400 mM NaOH kept at room temperature overnight and then dialyzed in 10 mM NaOH. (from Ling and Zhang 1984)

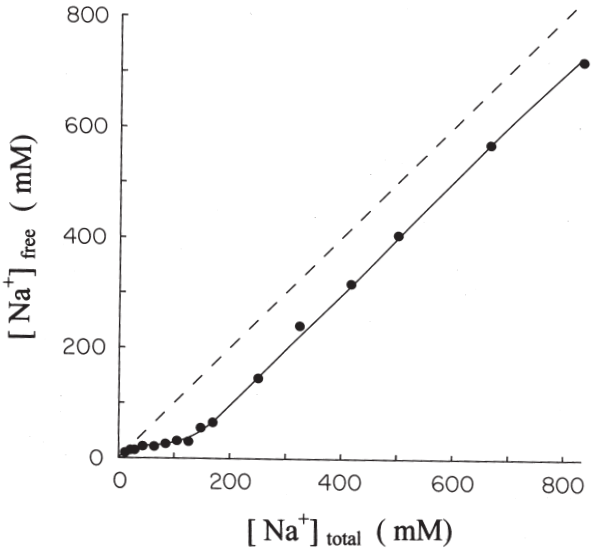

FIGURE 10. The relation between total Na^+ concentration and free Na^+ concentration detected and measured with a Na^+ selective glass electrode in a 10% hemoglobin solution containing increasing amount of NaOH. Dashed line indicates total Na^+ concentration. (from Ling and Zhang 1984)

Na-sensitive electrode, suggesting that by neutralizing the fixed cationic amino groups, the NaOH destroys the salt linkages thereby making the masked β-, and γ-carboxyl groups available.

Figures 11 and 12 show respectively how variation of free Na^+ (as NaOH) on a 10% hemoglobin solution and how variation of the concentration of hemoglobin in a fixed concentration of NaOH (125 mM, A; 250 mM, B) affect the adsorption of Na^+. Both curves show a steep initial rise before reaching a more or less flat plateau. In this general pattern, the adsorption of Na^+ on proteins resembles ion adsorption as in all the three other systems presented earlier above. Apparently, only when both the NaOH and protein have reached a certain level can full uptake of Na^+ be achieved.

However, it is the data presented in Figure 13 that is truly dramatic; it affirms what I referred to earlier in this paper as Part II of LFCH (or the salt-linkage hypothesis) (Ling 1952.) For what it shows is that the same curve that describes *the step by step neutralization of the (non-histidine) fixed* ***cationic*** *groups matches exactly the step by step stoichiometric adsorption of the* ***cation,*** *Na^+.*

What this exact matching shows is diagrammatically illustrated in Figure 14. A carboxyl group either forms a salt linkage with a fixed cation, or it adsorbs a monovalent cation. None is left free — fully and completely contradicting the Linderstrom-Lang model of proteins, in which all fixed charged groups are left free as mentioned at the early part of this communication.

Only the diagram does even more. It also shows how the titration of hemoglobin with NaOH also causes the full-scale polarization and orientation of the bulk-phase water near and farther away from the protein NHCO groups — that is, however, discussed in detail elsewhere (Ling and Hu 1988) and not further pursued here.

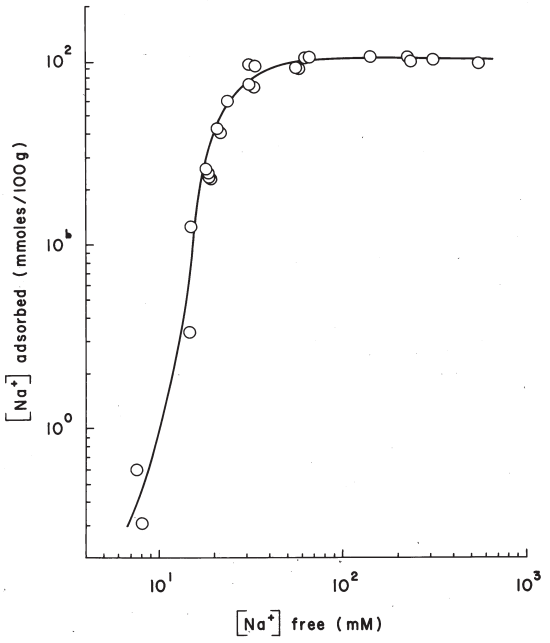

FIGURE 11. Double log plot of the concentration of "invisible" (adsorbed) Na^+ on a 10% hemoglobin solution against the "visible" (free) Na^+ concentration in the media. (from Ling and Zhang 1984)

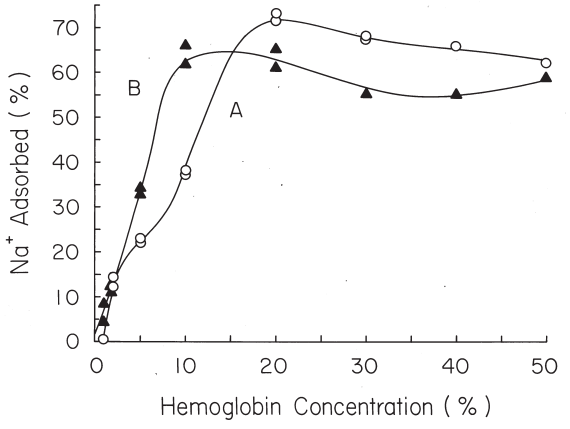

FIGURE 12. Concentration of "invisible" (adsorbed) Na^+ as a percentage of total Na^+ in a 125 mM (A) and 250 mM (B) NaOH solution, containing increasing concentration of hemoglobin. (from Ling and Zhang 1984)

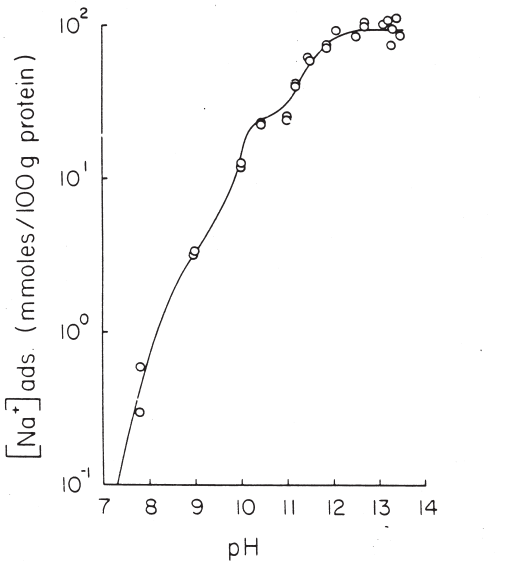

FIGURE 13. The quantitative relation between fixed cations of hemoglobin neutralized and Na^+ adsorbed. Points are experimentally measured concentrations of "invisible" Na^+ in a 10% hemoglobin solution at different pH's. The solid line going through or near most of the experimental points is the theoretically calculated composite titration curves of all the α-amino groups, ε-amino groups and guanidyl groups in 100 g. of hemoglobin. (from Ling and Zhang 1984)

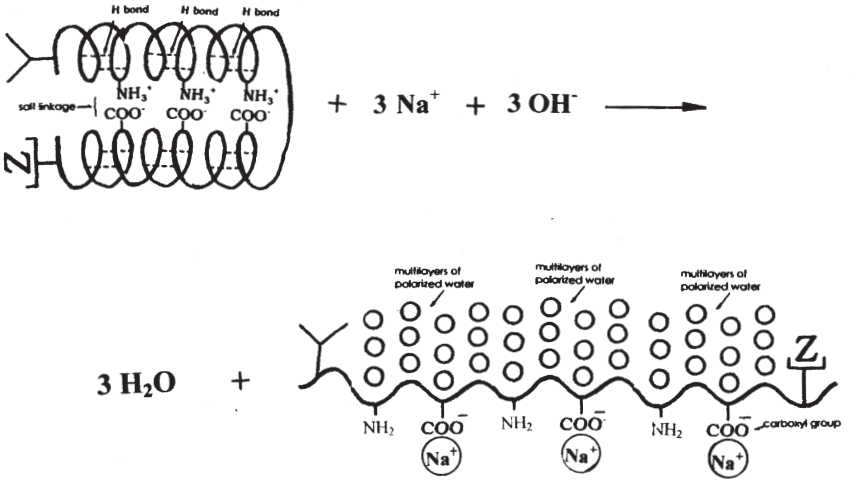

FIGURE 14. Diagrammatic illustration of the interaction of NaOH and folded native hemoglobin leading to the dissociation of the salt-linkages by the neutralization of the fixed cationic ε- amino and guanidyl groups shown as NH_3^+ and the liberation of all the β-, and γ-carboxyl groups. Each of these liberated β-, and γ-carboxyl groups then adsorbs one-on-one a Na^+. The backbone NHCO groups also liberated from their former α-helical engagement now adsorb and orient multilayers of water molecules. The stoichiometric relationship predicted between the molarity of the fixed cations neutralized and the molarity of Na^+ adsorbed as shown in Figure 13 is thus confirmed.

Once more, we are at the same position we confronted in our three preceding sections. Invisibility to the Na^+-selective electrode by itself does not prove that the invisible fraction of the Na^+ is engaged in close-contact, one-on-one adsorption. To prove that requires additional evidence that here too the invisible Na^+ can be displaced to different degrees by other monovalent ions that have different short-range attributes. Indeed, that is precisely what the data shown in Figure 15 tell us.

The figure shows how different alkali metal ions, which differ among themselves only in short-range attributes, produce different degree of displacement of the adsorbed Na^+, making it visible to the Na^+selective electrode —, Li^+ being the most effective, Rb^+ and Cs^+ the least, with K^+ somewhere in-between. Thus the Na^+/Rb^+ selectivity ratio ($K^{oo}_{Rb\rightarrow Na}$) is 16.5; the Na^+ /Cs^+ selectivity ratio is 14.0. In contrast, the Na/Li selectivity ratio is only 2.3. Seen as a whole, there is no doubt that the Na^+ invisible to the electrode is in fact due to its close contact one-on-one adsorption on the α-, β- and γ-carboxyl groups of the hemoglobin.

2. Studies on living cells

This, the last and concluding section of this communication is divided into five subsections. In the first subsection, I shall present evidence that bulk-phase protoplasm (rather than the cell membrane and pumps postulated to exist in the cell membrane) selectively accumulates K^+ over Na^+. In the second subsection, I shall demonstrate that ATP molecules *per se* (rather than its rate of hydrolysis) control the level of selectively accumulated K^+ in living cells. In the third subsection, I shall demonstrate that K^+ in living cells are exchangeable one for one with Na^+ and other monovalent cations. In the fourth subsection, I shall demonstrate that β-, and γ-carboxyl groups carried respectively on as-

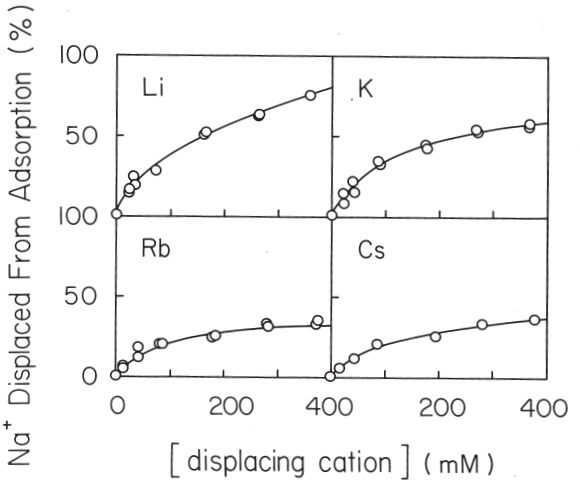

FIGUR E 15. Displacement of adsorbed Na^+ by Li^+, K^+, Rb^+ and Cs^+ with different short-range attributes . Ordinate represents percentage of "invisible" (adsorbed) Na^+ displaced by increasing concentration of the displacing ions indicated in the graph. All displacing ions were added as chlorides in a 10% hemoglobin solution containing a fixed concentration of NaOH (125 mM.) (from Ling and Zhang 1984)

partic and glutamic acid residues of cell proteins are the seat of adsorption of K^+ and its surrogate ions like Tl^+, Cs^+, Na^+. In the fifth and last subsection, I shall demonstrate that K^+ (and/or surrogate ions) are adsorbed one-on-one, in close-contact on β-, and γ-carboxyl groups of intracellular proteins.

2.1 Bulk-phase protoplasm (rather than membrane pumps) as the seat of selective K^+ accumulation

Figure 16 shows an *Effectively Membrane-less Open-ended Cell* or *EMOC* preparation of an isolated frog sartorius muscle. Only the cut end of the muscle — which does not

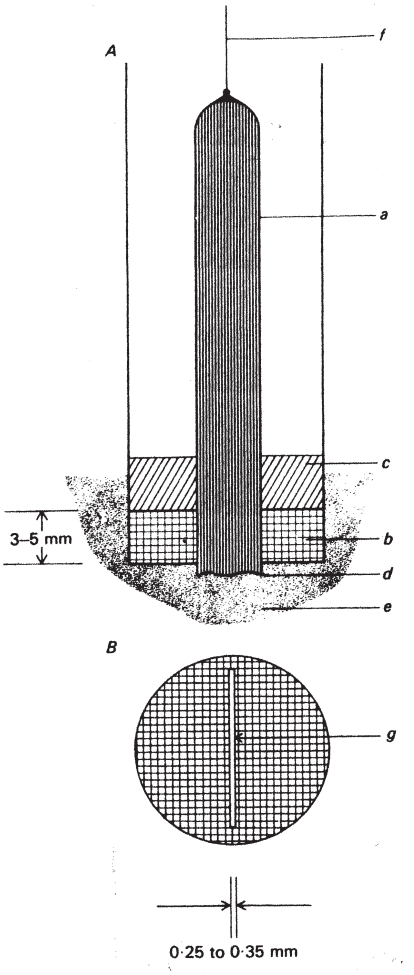

FIGURE 16. Effectively membrane-pump-less open-ended cell (EMOC) preparation of a frog sartorius muscle. (A) side view; (B) bottom view. Only the cut end (d) of the sartorius muscle (a) is in direct contact with the radioactively labeled Ringer's solution (e). Cut muscle is secured on one end by the tight-fitting slit (g) of the silicon rubber gasket (b) and on the other end by an anchoring piece of string (f). Vaseline (c) originally filling the entire lower end of the glass tube including the gasket slit effectively prevents seepage of labeled solution into and out of the gasket slit, through which the tibial end of the muscle passes. (Ling 1978, by permission of Journal of Physiology (London))

regenerate a new cell membrane (see Ling 2001, p. 20; Ling 2004, p. 14) — is exposed to a Ringer's solution (e) containing radioactively labeled K^+ and Na^+.

Now, each sartorius muscle from the North American leopard frog (Rana *pipiens pipiens*, Schreber) comprises some 1000 hair-like cells, each reaching from one end of the muscle to the other end without interruption. By far the largest part of each muscle cell in an EMOC preparation is directly exposed to either moist air or vaseline or a microscopically thin layer of Ringer's solution in the extracellular space. Neither air nor vaseline, nor this microscopically thin layer of Ringer's solution could serve as a *source* of K^+ or *sink* for Na^+. As a result, in the EMOC preparation, the postulated sodium (potassium) pump could not operate and keep the cell K^+ high and the cell Na^+ low. Yet Figure 17 shows how such an EMOC sartorius muscle preparation continues to accumulate K^+ and exclude Na^+ in the intact part of the muscle (away from the injured cut end) as if they were in their normal environment. Taken as a whole, the data show that the selective accumulation of K^+ and exclusion of Na^+ are manifestations of the properties of the bulk-phase protoplasm and not those of a sieve-like cell membrane and/or (postulated) pumps.

2.2 ATP *per se* controls the level of selectively accumulated K^+.

Figure 18 taken from Gulati *et al* (1971) shows the quantitative relationship between the equilibrium level of K^+ in a poisoned frog muscle and its ATP content. The quantitative relationship demonstrated appears indifferent to which of the arbitrarily selected metabolic poisons was used to slowly kill the muscles. In this set of data, each experimental point represents a single frog sartorius muscle. In Figure 19, in contrast, the demonstrated correlation between K^+ and ATP occurred in different parts of the same muscle cells installed in an EMOC preparation. In regions near the cut end, where the ATP concentration has fallen to zero or near-zero, virtually all the accumulated K^+ has vanished. Further toward the intact end of the muscle, the steep rise of ATP concentration paralleled a steep rise of K^+ concentration and a correspondingly steep fall of Na^+ con-

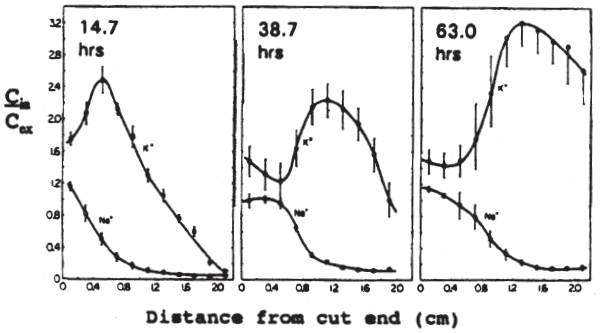

FIGURE 17. Distribution of labeled K^+ and Na^+ in segments of the muscle at different distances from the cut end (abscissa) of a frog sartorius muscle mounted in an EMOC setup (illustrated in Figure 16). Durations of incubation are indicated in the figures (25° C). Ringer's solution bathing the cut end of the muscle contained radioactively labeled K^+ and Na^+. Ordinate represents the concentration of labeled K^+ or Na^+ in cell water expressed as a ratio to their respective concentration in the Ringer's solution bathing the cut end at the conclusion of the experiment. (Ling 1978, by permission of Journal of Physiology (London))

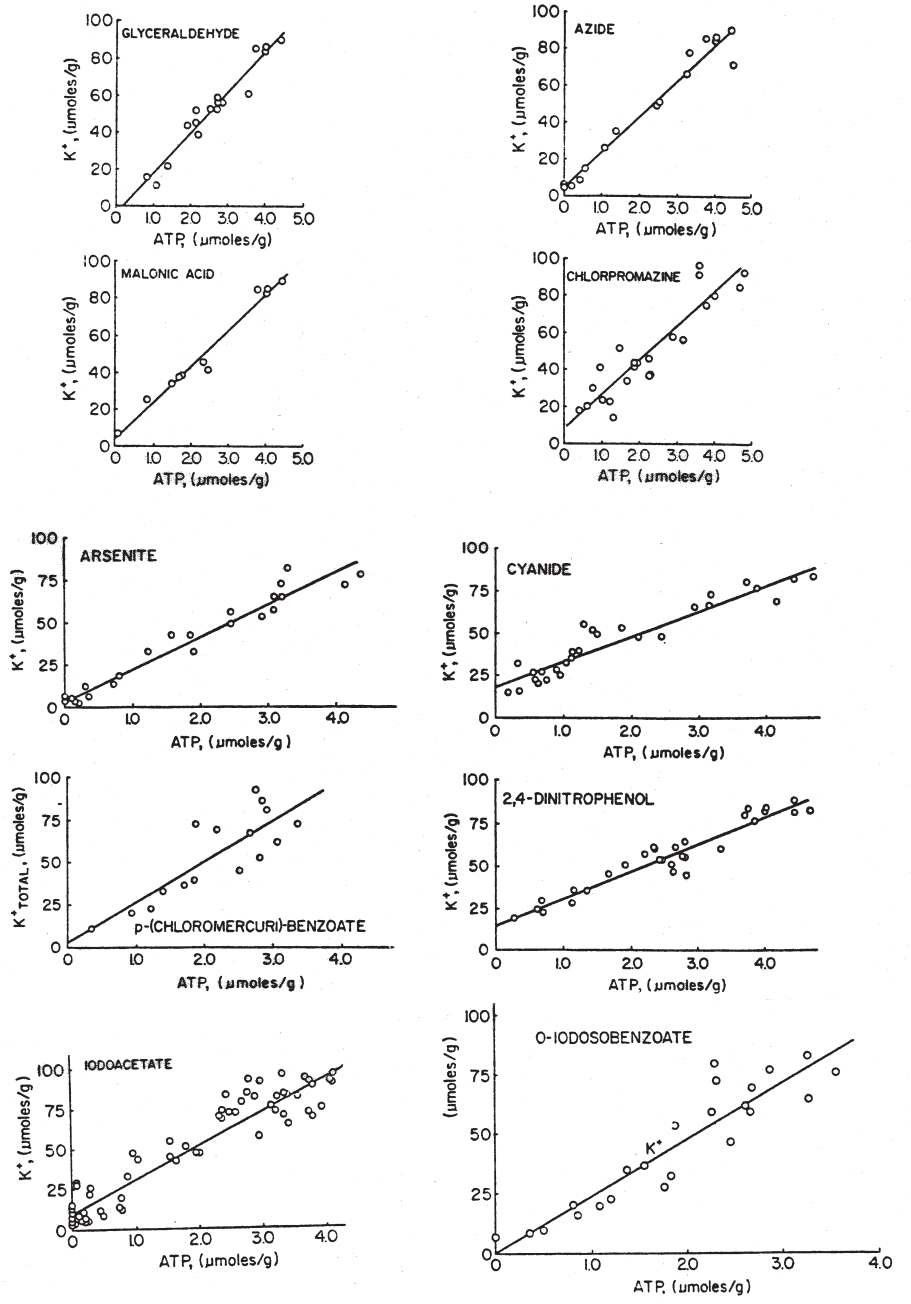

FIGURE 18. The relation between the equilibrium concentration of K^+ and the concentration of ATP in healthy, dying and dead frog muscles. These muscles were exposed to 10 different poisons (as indicted) for different lengths of time at 25°C with shaking, followed by an equilibrium period of 2 to 4 hours at 1°C also with shaking to achieve diffusion equilibrium. (Gulati *et al* 1971, by permission of Biophysical Society)

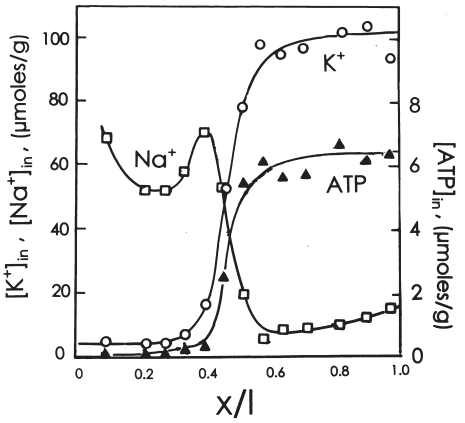

FIGURE 19. The concentration of ATP in part of a frog sartorius muscle EMOC preparation at different distances from the cut end, which alone was immersed in Ringer's solution. The muscle was in the EMOC setup for 3 days at 25°C. ATP concentration is given in μmoles per gram of fresh muscle sections. Distances from the cut end are given as a ratio of the distance from the cut surface to the center of the segment, divided by the total length of the cut muscle. ATP was analyzed using the firefly enzyme method. The K^+ (and Na^+) concentrations are given as ratios to the final concentration in the Ringer's solution bathing the cut end of the muscle. (after Ling 1992a)

centration. Both sets of data as shown in Figure 18 and Figure 19 confirm the predicted quantitative relationship between the amount of cell K^+ and the concentration of ATP as *cardinal adsorbent* — occupying key control sites called cardinal sites as illustrated in Figure 20 and Figure 21.

2.3 Cell K^+ can be stoichiometrically replaced *one-on-one* by all monovalent cations studied (e.g., Tl^+, Cs^+, Na^+) but not by divalent cations (e.g., Mg^{++})

Figure 22 shows that the total concentration of Tl^+ (thallium ion), K^+ and Na^+ in frog muscle remained constant as the ratio of external Tl^+ and K^+ varied (while the external Na^+ concentration was kept constant at 100 mM. This constancy in total monovalent cation content indicates a one-for-one exchange among all three *monovalent* cations. In contrast, Figure 23 shows that there is no one-for-one replacement of cell K^+ by the increasing concentration of both extracellular and intracellular *divalent* cation, Mg^{++}. Seen together, these two sets of data suggest that in the resting living state, virtually all the β-, and γ-carboxyl groups of the frog muscle cells exist as *isolated* anionic sites and not in pairs or clusters. (In a paper yet to be published, Ling and Ochsenfeld would describe conditions, under which this specificity for monovalent ions could be relaxed and divalent and monovalent cations become mutually exchangeable and compete for similar apparently paired or clustered sites.)

Figure 24 shows two sets of X-shaped pairs of K^+ and Na^+ curves. The points here are experimental. The lines going through and near the points are theoretical according to Equation 24 of cooperative adsorption in Appendix D. In the left-hand set of X-shaped curves, the data shows strict obedience to one for one exchange of Na^+ for K^+ when the

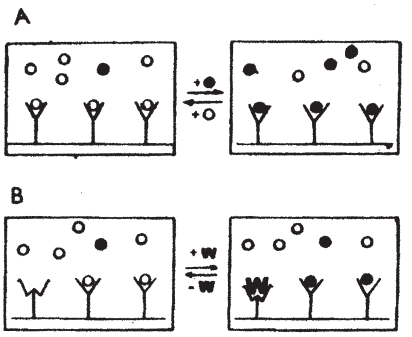

FIGURE 20. Two types of autocooperative transitions between i state in which the sites are occupied by solute i (open circles) to the j state in which the sites are occupied by solute j (solid circles). (A) In this type called "spontaneous," the transition results from a change in the relative concentrations of i and j in the surrounding medium. (B) In this type called "controlled", a similar transition occurs between the i and j state but at a constant relative concentration of i and j in the surrounding medium. The transition is caused by the interaction of a specific cardinal site with a cardinal adsorbent, W. (from Ling 2001)

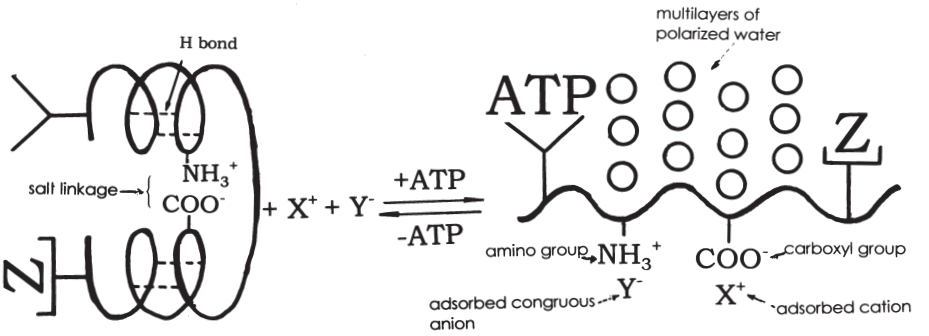

FIGURE 21. Diagrammatic illustration of how adsorption of the cardinal adsorbent ATP on the ATP-binding *cardinal site* and of "helpers" including the *congruous anions* (shown here as "adsorbed congruous anions" and Protein X (shown here as Z) unravels the *introverted* (folded) secondary structure shown on the left-hand side of the figure. As a result, selective K^+ adsorption now takes place on the liberated β-, and γ-carboxyl groups (shown on the right-hand side of the picture as carboxyl groups) and multilayer water polarization and orientation can now occur on the exposed backbone NH and CO groups. The resting living state is thus achieved and maintained. (This figure is the latest version of a basically similar but simpler one first introduced in Ling 1969.) (from Ling 2001)

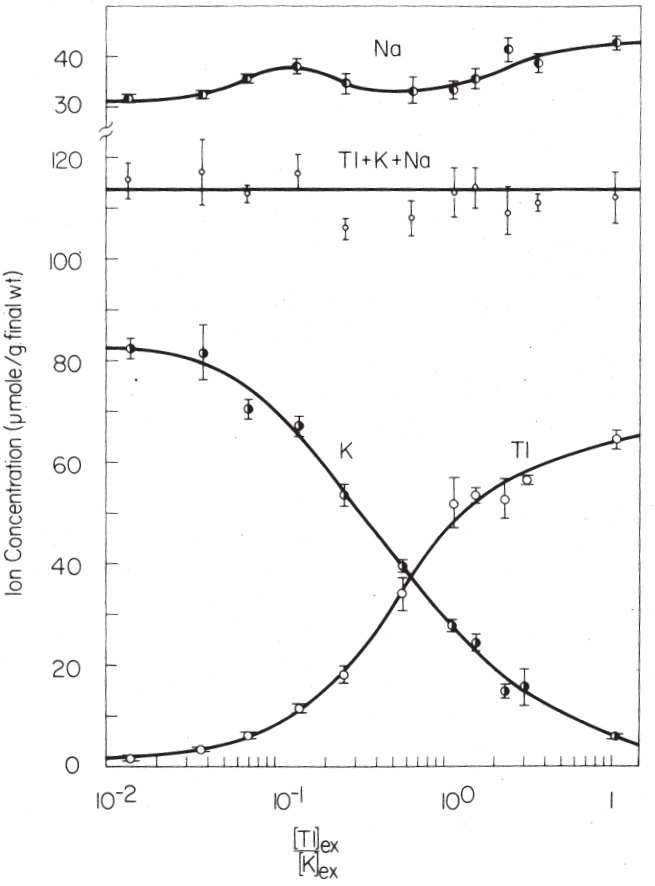

FIGURE 22. Equilibrium distribution of Tl^+, K^+ and Na^+ in frog muscles. To produce the wide range of $[Tl^+]_{ex}$ / $[K^+]_{ex}$ ratios shown on the abscissa, $[K^+]_{ex}$ was kept constant at 2.5 mM below a $[Tl^+]_{ex}$ / $[K^+]_{ex}$ ratio of unity. Above that, $[Tl^+]_{ex}$ was kept constant at 4 mM. while $[K^+]_{ex}$ varied. In all bathing solutions the external Na^+ concentration was kept constant at 100 mM. Each point is the mean of 4 or 5 determinations ± S.D. Constancy of the sum of the three ions shown in the straight horizontal line marked (Tl+K+Na) demonstrates full interchangeability among these monovalent cations on the intracellular β-, and γ-carboxyl groups. (from Ling 1977a)

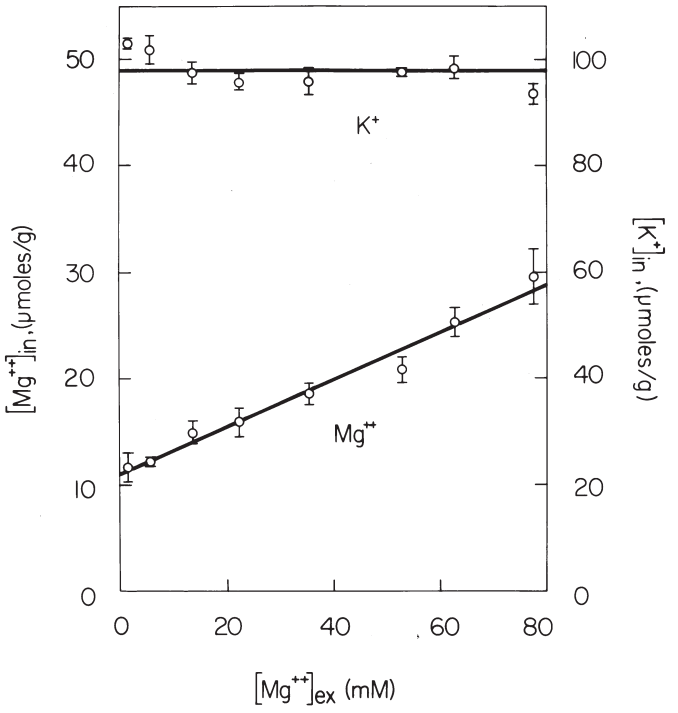

FIGURE 23. Equilibrium Mg^{++} and K^+ distribution in healthy frog muscle, demonstrating no exchange between monovalent cations and divalent cations. This specific set of experiments was conducted at 4°C. A companion study carried out at 25°C yielded similar results. Before assaying for their cellular ionic contents, the muscles were centrifuged at 1000g for 4 minutes in hermetically sealed paraffin film (parafilm) packets to remove extracellular fluid by the method of Ling and Walton, 1975. Resting frog muscle cells possess one set of adsorption sites for Mg^{++} with strong affinity. $[f]_{Mg}$ = 11.0 μmole/gram fresh muscle cell; $K^{oo}_{Mg} = 10^{-4}$ M. (from Ling *et al* 1979, reprinted by permission of John Wiley & Sons, Inc.)

ratio of external K^+/Na^+ is lowered. The data demonstrate a selectivity ratio of K^+ over Na^+ ($K^{oo}_{Na\rightarrow K}$) equal to 100. In the right-hand set, the selectivity ratio of K^+ over Na^+ ($K^{oo}_{Na\rightarrow K}$) has dropped from 100 to 21.7 — in consequence of the inclusion in the bathing solutions of a minute concentration of the cardiac glycoside, ouabain (10^{-7} M.) In the association induction hypothesis, ouabain as well as ATP are cardinal adsorbents, so are drugs and hormones in most cases and illustrated diagrammatically in Figure 20 and 21.

2.4 β-, and γ-carboxyl groups of intracellular proteins offer by far the greatest majority of adsorption sites for K^+ in frog muscle cells

This subsection comprises two parts. The first part presents evidence that β-, and γ-carboxyl groups adsorb K^+ on the basis of the known intracellular locations of the β-, and γ-carboxyl groups; the second part presents evidence that β-, and γ-carboxyl groups adsorb K^+ on the basis of the characteristic acid dissociation constant or pK_a of the β-, and γ-carboxyl groups.

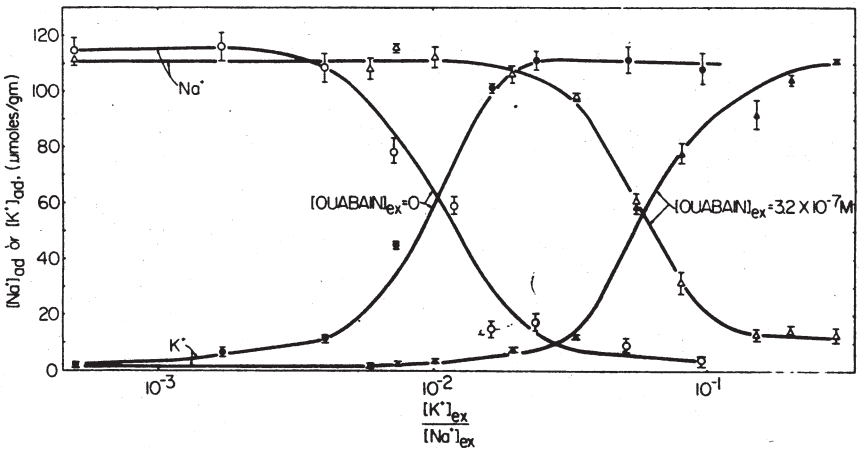

FIGURE 24. Equilibrium distribution of K^+ and Na^+ adsorbed on intracellular β-, and γ-carboxyl groups in frog muscle cells at varying external K^+ and Na^+ concentration ratio, $[(K^+)_{ex} / (Na^+)_{ex}]$ (shown on the abscissa.) As a whole, the data demonstrate full exchangeability of all adsorbed K^+ and Na^+. All points are experimental; the two sets of X-shaped lines going through or near the experimental points are theoretical according to Equation 24 in Appendix D. The muscles yielding the left-hand side pair of curves were untreated normal; the muscles yielding the right-hand side pair of curves were exposed to the cardiac glycoside, ouabain at a pharmacological (very low) concentration (10^{-7} M.) Data show that ouabain treatment has lowered the intrinsic equilibrium constant for the Na^+ to K^+ exchange ($K^{oo}_{Na \to K}$) from 100 to 21.7 with little or no change in the nearest-neighbor interaction energy ($-\gamma/2$). In parallel studies reported in the same paper, no detectable change in the concentration of ATP in the muscles was shown for ouabain concentration lower than 10^{-6} M. At ouabain concentration above 10^{-6} M, ATP concentration decline was visible. (from Ling and Bohr 1971)

2.4.1 *Identifying β-, and γ-carboxyl groups as K^+ adsorption sites from their known cytological locations.*

In presenting LFCH in 1952, I pointed out that myosin, which makes up about half of the voluntary muscle proteins, contains enough β-, and γ-carboxyl groups to adsorb all the muscle cell K^+ (Ling 1952, p. 773.) In 1977, Ling pointed out that since it has been known that myosin makes up the dark bands of striated muscle cells (Huxley 1853; Engelmann 1873; Huxley & Niedergerke 1958) the LFCH would predict that much of the muscle cell K^+ is located in the A bands (Ling 1977.)

And, once more, experimental support for this theory has been in existence long before the theory came into being. Thus using K-precipitating chemicals, Macallum (1905) and Menten (1908) have demonstrated that K^+ in various voluntary muscle cells is specifically located at the A bands and sometime at the Z-line as well.

It is true that one can raise questions about what these authors really demonstrated. However, there has been such a wealth of new experimental confirmation of the earlier-announced and later theoretically-predicted location of K^+, one cannot deny that Macallum's (and Menten's) findings were largely correct.

Nonetheless, it would be remiss if I do not mention Ludwig Edelmann's masterful and original work, nor the work of Nesterov & Tigyi-Sebes (1965), Trombitas & Tigyi-Sebes (1979.) and still others. Together, they have firmly established that most muscle cell K^+ is, as predicted on the basis of the known location of the proteins carrying most of the β-, and γ-carboxyl groups, at the edges of the A bands (and Z lines.) However, there is no way to do justice especially to Dr. Edelmann's superb work here. As the next best, I shall pick out a few highlights of his work with which I am most familiar.

Figure 25 shows my own early results of radioautographic studies of air-dried frog muscle cell preparations. The radioautographs demonstrate that the K^+ surrogates, labeled Cs^+ and Tl^+, are as predicted located mostly on the A bands (Ling 1977.)

Figure 26 was the earliest of Edelmann's transmission EM studies. Again, Tl^+ and Cs^+ were chosen as the K^+ surrogates, not for the long-life, inexpensive radioisotopes this pair of ions offer as in the study that had produced Figure 25, but for their respective high electron density and hence opaqueness to the electron beam and thus direct visibility in a transmission electron microscope. Once more, the locations of these two K^+ surrogates confirm that K^+ is normally found primarily at the edges of the A band (and at the Z-line.)

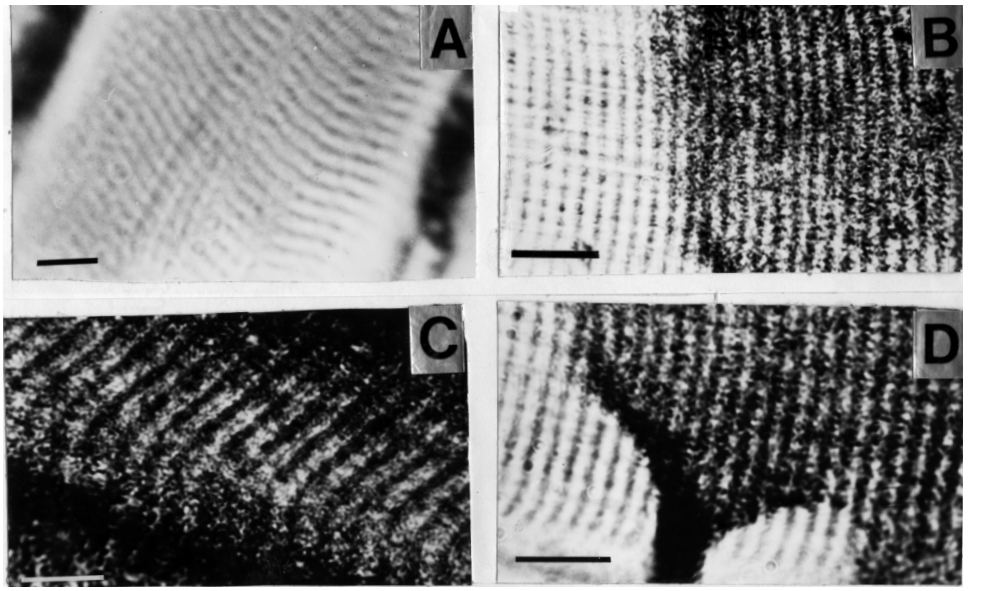

FIGURE 25. Auto-radiographs of dried single muscle fibers. (A) Portion of a single muscle fiber processed as in all the other auto-radiographs shown here but not loaded with radioisotope. (B), (C) and (D) are auto-radiographs of dried muscle fibers loaded with radioactive ^{134}Cs while living and before drying. (B) and (D) were partially covered with photo-emulsion. (B) was stretched before drying. Bars represent 10 micrometers. Incomplete coverage with photo-emulsion in B and D permits ready recognition of the location of the silver grains produced by the underlying radioactive ions to be in the A bands. Careful examination suggests that the silver grains over the A bands are sometimes double. In some cases (C), a faint line of silver grains can also be seen sometimes in the middle of the I bands, corresponding to the position of the Z line. (from Ling 1977)

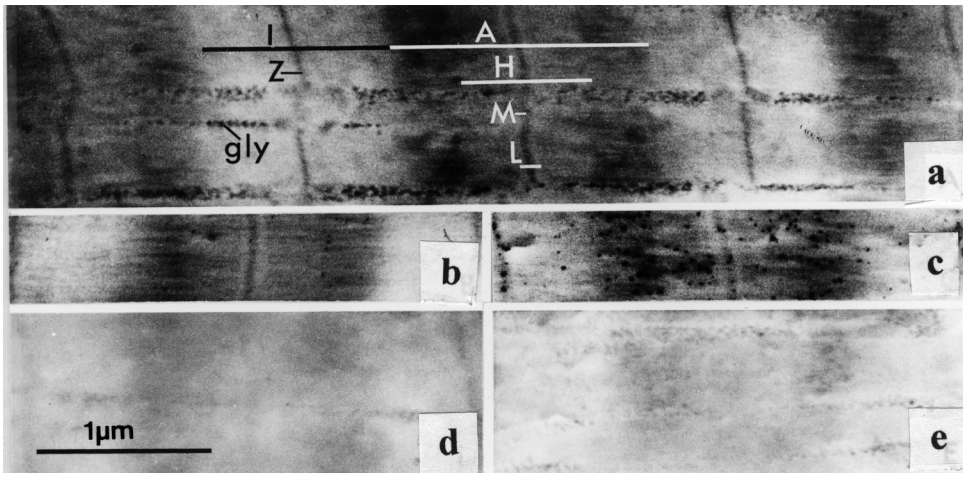

FIGURE 26. Electron micrographs of dry-cut, unstained section of freeze-dried frog sartorius muscle fibers. Muscles were loaded physiologically with Cs^+ (a) and Tl^+ (b,c) before freeze-fixation, freeze-drying and embedding. (b) was processed immediately after sectioning. (c) was obtained after exposure of a cut section to room temperature for 1 hr. (d) is the central part of (a) after storage of 2 days in distilled water. (e) is from a normal "K^+ loaded" muscle. A, A-band; H, H zone; M, M-line; L, L zone; Z, Z-line; gly, glycogen granules, Scale bar: 1.0 µm. (from Edelmann 1977)

The EM plates c and d in Figure 27 were all produced by means of a revolutionary new technique that Edelmann invented — a technique Edelmann named "adsorption staining" (Edelmann 1984.) Briefly, living muscle cells were frozen in liquid nitrogen and the frozen water in the cells replaced with pure acetone by a combinatin of feeeze-substitution and then low temperature imbedding in Lowicryl K11M. 0.1 to 0.2 µm thick sections were then dry-cut and exposed to a "staining" solution containing 100 mM LiCl, 10 mM CsCl and 0.5 mM $CaCl_2$. Lo and behold! These seemingly dead sections have maintained their resting *living state*.

And, they did exactly what intact muscles cells loaded with Cs^+ or Tl^+ in their natural living state do, selectively adsorb these surrogate ions at the two edges of the A bands.

In summary, conventional and new EM methods as well as radioautographic methods have confirmed the prediction that the K^+ surrogate Cs^+ and Tl^+ are located where most of the β-, and γ-carboxyl groups are known to be located offering further support that it is these β-, and γ-carboxyl groups carried respectively on the aspartic and glutamic acid residues of myosin and other intracellular proteins that specifically adsorb K^+ or its surrogates including Cs^+, Rb^+, Tl^+ or Na^+.

Next I shall demonstrate that the characteristic acid dissociation constant, or pK_a of β-, and γ-carboxyl groups provides another means to test the hypothesis that these β-, and γ-carboxyl groups are the seats of preferential adsorption of cell K^+.

2.4.2 *Identification of* β-*, and* γ*-carboxyl groups as the adsorption sites for* K^+ *by the carboxyl group's characteristic* pK_a

The standard way to determine the pK_a of an acid is by titration. Unfortunately, it is not easy to titrate the β-, and γ-carboxyl groups inside living cells; the cell membrane or sur-

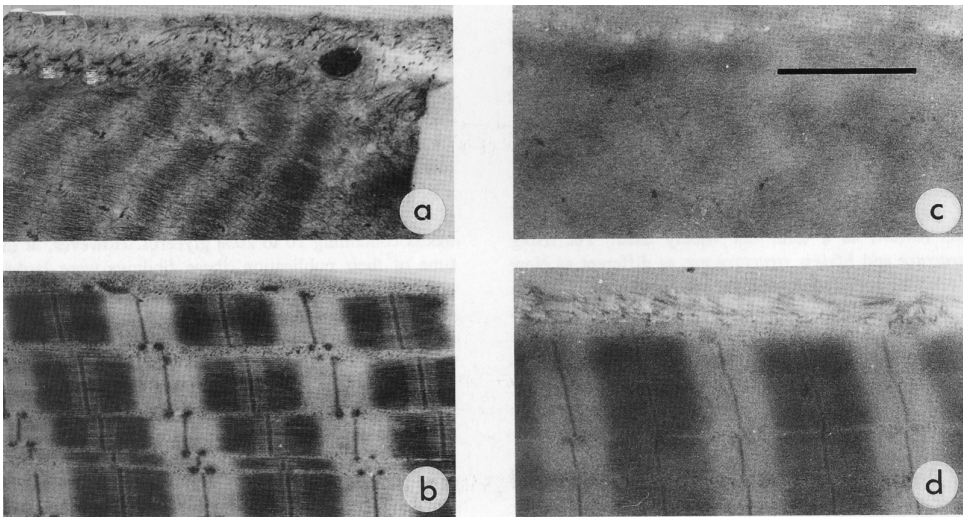

FIGURE 27. Electron micrographs of parts of a frog muscle cell near and far away from its cut end. (a) an ultrathin section stained with uranium and lead by conventional procedure, showing the cut surface of the muscle fiber at the top of the figure; (b) a similar section made at 0.4 mm away from the cut end. (c) and (d) are from 0.2 μm-thick wet-cut section (not stained with uranium and lead but) stained with electron-dense Cs^+ by Edelmann's "adsorption-staining method" in which the cut section is exposed to a solution containing 100 mM LiCl, and 10 mM CsCl. (c) obtained from the cut edge of the muscle, (d) from a section 0.4 mm away from the cut edge. Note poor or no uptake of uranium/lead in (a) nor of Cs^+ in (c), but normal uptake in both (b) and (d). (from Edelmann 1989, by permission of Scanning Microscopy)

face offers a road block to what lies inside the cell. To overcome this road block, a simple solution is to use a muscle cell preparation with its ends cut thereby directly exposing the cell interior to the outside medium. Unfortunately, as made clear in Figure 17 and 19 above, cutting a muscle cell causes a spreading deterioration of the muscle cell from the cut end toward the intact end. After many trials, I was lucky in finding a modified medium containing about 17% (w/v) of PEG-8000, which greatly prolongs the survival time of the cut muscle (Ling 1989) and it was with its help that the data shown in Figure 28 from Ling and Ochsenfeld was obtained.

The central finding here is that the (K^+-surrogate) labeled Na^+ adsorbing sites show a uniform pK_a of 3.85 (Figure 28.) Now the pK_a of the β-carboxyl groups has a pK_a of 3.65; the pK_2 of the γ-carboxyl group of glutamic acid is 4.25 (Stecher 1968, p. 107 and p. 497.) The measured value of 3.85 falls within the range of these known pK values, again confirming the theory that it is these β-, and γ-carboxyl groups that selectively adsorb K^+ and its various surrogates.

At this junction, it is relevant to point out that phosphate groups, could in amount offer alternative anionic groups to bind some cell K^+. However, the single pK_a of 3.85 also rules out that possibility because the three pK_a values of phosphoric acid are respectively 2.12, 7.21 and 12.67 and all too far removed from 3.85 to merit more attention (Hodgman *et al*

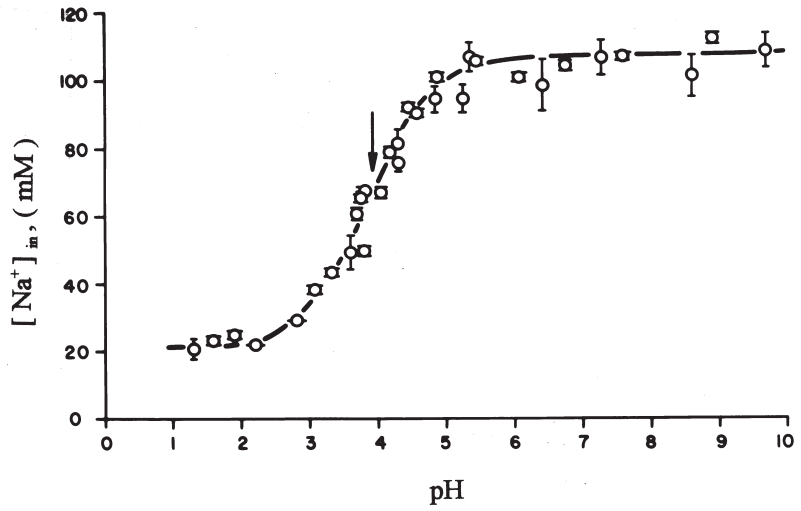

FIGURE 28. Uptake of labeled Na^+ at different pH's by 2-mm-wide muscle segments with both ends open (0°C). Incubation solution contained 16.7% (w/v) PEG-8000. Each point represents the mean ± S.E. for 4 samples. For pH 7.5 and lower, $H_2SO_4 - Na_2SO_4$ buffers were used. For pH above 7.5, glycine-NaOH buffers were used. Ordinate represents molar labeled Na^+ concentration in tissue water. Note that at pH 2.3 and lower, the curve levels off, indicating that at this and still lower pH (and corresponding *higher* H^+ concentration), all adsorbed labeled Na^+ have been chased away by the H^+ and the only labeled Na^+ in the muscle segments is *free* labeled Na^+ found in cell water. The downward arrow indicates the midpoint of the titration curve and hence the pK_a of the acidic group after the free fraction in cell water has been subtracted from the total labeled Na^+ uptake. (from Ling and Ochsenfeld 1991)

1961, p. 1757.) Indeed, there is no sign that any detectable amount of labeled Na^+ is adsorbed on acidic groups with any acidic groups characterized by these pK_a values.

2.5 K^+ (and its surrogates ions) in living frog muscle cells are engaged in close-contact one-on-one adsorption on the β- and γ-carboxyl groups on myosin or other cell proteins

As we have shown above (section 1.3), Na^+ is engaged in close contact one-on-one adsorption on the sulfonate groups of polystyrene sufonate, because different competing monovalent cations displaced Na^+ from adsorption sites to different degrees and the only difference among these displacing ions are their short-range attributes and short-range attributes cannot be perceived or felt without close contact.

By a similar combination of technique and logic, we have shown that in NaOH-titrated hemoglobin solution, the Na^+ that has become invisible to the Na^+specific electrode, is also engaged in close-contact one-on-one adsorption on the β- and γ-carboxyl groups of the hemoglobin.

In this, the concluding section of the experimental confirmation of LFCH, I shall demonstrate that K^+ (and its various surrogate ions) in living cells behave like countercations in inanimate model systems also engaged in one-on-one, close contact adsorption on these β- and γ-carboxyl groups. Again, this subsection can be divided into two parts 2.5.1 and 2.5.2.

2.5.1 *Close contact, one-on-one adsorption of K^+ from the total failure of Mg^{++} to displace any intracellular K^+ from its adsorption sites*

Let us suppose that K^+ in muscle cells exists wholly or partly as free ions in an *ion cloud* hovering around the fixed β- and γ-carboxyl groups carried on some cell proteins. In that case, that part of the K^+ that is free would be replaceable by divalent Mg^{++} because as part of the ion cloud, only the number of electric charges count and two singly charged K^+ would be fully and completely replaceable by one doubly-charged Mg^{++}.

The fact is, as shown in Figure 23, quite the opposite. The cell K^+ concentration stays entirely unchanged in the presence of increasing concentration of Mg^{++} outside and inside the muscle cells. Therefore, no cell K^+ exists in the form of free ions hovering around the fixed β- and γ-carboxyl groups.

Elementary logic dictates that the absence of no-contact, free-floating K^+ in muscle cells means that all K^+ in muscle cells are engaged in close-contact, one-on-one association with fixed sites — already estabilised above to be the β- and γ-carboxyl groups on myosin and other proteins.

2.5.2 *Close-contact, one on one adsorption of nearly all intracellular K^+ on fixed β- and γ-carboxyl groups from divergent impact of different competing cations with only short-range attribute differences among themselves*

Figure 29 shows a double reciprocal plot of the equilibrium concentration of labeled K^+ at different external labeled K^+ concentrations in the presence of varying concentration of competing non-labeled K^+. The family of straight lines converging toward the same locus on the ordinate shows that the adsorption follows what the Langmuir adsorption isotherm predicts as shown as Equation 23. However, Ling and Ochsenfeld pointed out in 1966 that converging straight lines are by themselves no proof that the ions are engaged in close contact adsorption. Countercations hovering near the fixed anions could give rise to a similar set of converging straight lines (Ling and Ochsenfeld 1966.) To prove close contact, one-on-one association, they also pointed out, we need to demonstrate different effectiveness in competing for the β- and γ-carboxyl groups among competing ions that differ only in short-range attributes. A pair of monovalent cations that meet this criterion are K^+ and Cs^+. Indistinguishable in terms of their respective *long-range* attributes as singly charged cation, they differ profoundly in their respective *short range* attributes. Most outstanding among them is in their respective Born repulsion constants, which in units of ergs/cm^9 x 10^{82} are respectively for K^+, 26.5 and for Cs^+, 82.5.

Figure 30 shows the reciprocal plots of the equilibrium concentrations of ^{134}Cs labeled Cs^+ and ^{42}K labeled K^+ against their respective concentrations in the external media. The profoundly different impact produced by the same (nonlabeled) K^+ on the equilibrium concentration of these two ions, — which differ from each other only in short term attributes — leaves no doubt that virtually all the K^+ adsorbed in frog muscle cells are engaged in one-on-one, close contact adsorption on the β- and γ-carboxyl groups.

I thank Dr. Raymond Damadian, and his Fonar Corporation and its many friendly and helpful members for their continued support, Margaret Ochsenfeld and Dr. Zhen-dong Chen for their dedicated and skillful cooperation, and librarian Anthony Colella and Michael Guarino, director of Media Services and Internet Services, for their patience and tireless assistance.

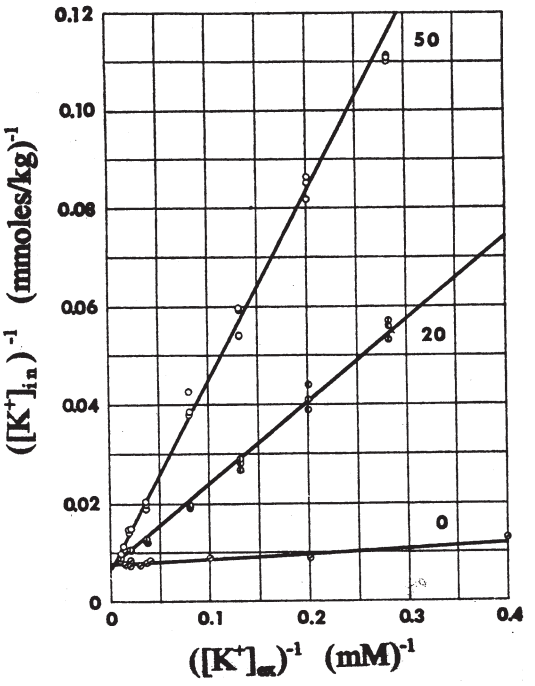

FIGURE 29. Double reciprocal plots of the equilibrium intracellular labeled K^+ concentration, $[K^+]_{in}$, against the external labeled K^+ concentration, $[K^+]_{ex}$, in the presence of 0, 20 and 50 mM of non-labeled K^+ (both labeled and non-labeled K^+ were in the form of acetate) (23–26°C). Incubation lasted 26 hours. The reciprocal of the equilibrium intracellular labeled K^+ concentration shown as $([K^+]_{in})^{-1}$ is in units of reciprocal millimoles of the ion in 1 kilogram of fresh muscle and shown as $(\text{mmoles/kg})^{-1}$; the reciprocal of the extracellular labeled K^+ concentration shown as $([K^+]_{ex})^{-1}$ is in units of reciprocal millimolarity or $(\text{mM})^{-1}$. Each point represents data from a single frog sartorius muscle. Lines obtained by the method of least squares. The total concentration of K^+-adsorbing sites in the muscle computed from the experimental data ranges from 137 to 154 mmoles per kg of fresh muscle. The average apparent adsorption constant of K^+ calculated is 665 $(\text{moles/liter})^{-1}$. (Ling and Ochsenfeld 1966, reproduced from Journal of General Physiology by permission of Rockefeller University Press)

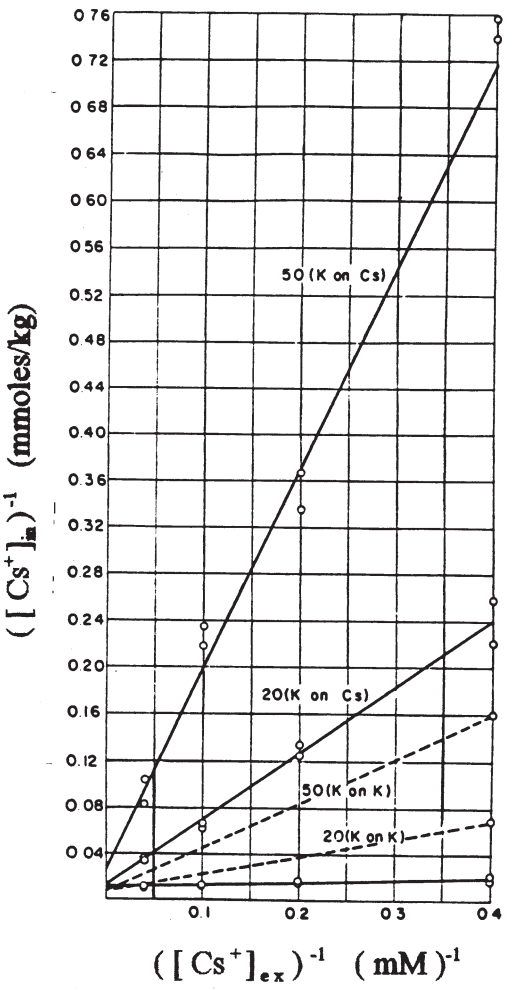

FIGURE 30. Double reciprocal plots of the equilibrium intracellular labeled Cs^+ concentration, ($[Cs^+]_{in}^{-1}$), against the reciprocal of external labeled Cs^+ concentration, ($[Cs^+]_{ex}^{-1}$), in the presence of 0, 20 and 50 mM of non-labeled K^+ (all as acetate) (23–26°C). Incubation lasted 45 hours. Each point represents data from a single sartorius muscle. Lines obtained by the method of least squares. Dotted lines are taken from Figure 29 for comparison. Taken together, the two sets of data show that the same concentration of (nonlabeled) K^+ produces dramatically different impacts on the adsorption of labeled K^+ and of labeled Cs^+ respectively. The apparent adsorption constant for Cs^+ from the single set of data shown is 488 $(moles/liter)^{-1}$. For additional explanation of units and symbols used, see legend of Figure 29. (Ling and Ochsenfeld 1966, reproduced from Journal of General Physiology by permission of Rockefeller University Press)

Endnotes

1. The experimental disproofs of the original (sieve) membrane theory include those reported by Gerard 1912, by Wu and Yang in 1931, by Kaplanski and Baldereva in 1934, by Cohn and Cohn in 1939, by Heppel in 1939 and by Steinbach in 1940. Experimental disproof of the pump version of the membrane theory includes that of Ling 1962, Jones 1965, Minkoff and Damadian 1973, and further affirmation and extension by Ling in 1997.

2. The sensible idea that electrostatic attraction between the negatively charged β- and γ-carboxyl groups and positively charged ε-amino groups and guanidyl groups caused the formation of bonds called *salt linkages* was suggested by Speakman and his coworkers for the fibrous protein, keratin (Speakman and Hirst 1931.) The idea was then extended to collagen (Lloyd *et al* 1933) and to globular proteins (Mirsky and Pauling 1936; Eyring and Stearn 1939.) For those like myself who have an interest in the history of biological sciences, it was truly astonishing to discover that the salt linkage was rarely found in the literature among protein chemists even after Perutz and his coworkers not only detected salt-linkages in crystalline hemoglobin, a *bona fide* globular protein, but described their exact locations in the protein molecule as well (Perutz *et al* 1968; Weissbluth 1974.)

This rejection of the salt linkage concept could be traced to a paper published by Jacobsen and Linderstrom-Lang (1949) on the basis of a single piece of circumstantial evidence. Namely, during acid titration of egg albumin and serum albumin, the volume change of the proteins matched the volume change measured in the titration of simple carboxylic acids. But proteins are not collections of isolated and independent chemical groups. Titration of the carboxyl groups and amino groups could produce far reaching changes in the entire protein molecules (see Ling 2003, Ling and Hu 1988.) Thus, the matching observed could be entirely coincidental — as indeed, Jacobsen and Linderstrom-Lang had themselves noted when they tried but failed to find matching in the titration of the amino groups.

Steinhardt and Zaiser offered another independent set of evidence for the existence of salt linkages in isolated hemoglobin. More specifically, they titrated hemoglobin with acid and observed the uptake of H^+ at different times thereafter (Steinhardt and Zaiser, 1951, 1953.) They found that 36 carboxyl groups were released from an inaccessible state to an accessible state in an all or none manner. They also pointed out in their 1955 review that the iso-electric point (I.E.P.) of the proteins remains near pH of 7 before and after full acid denaturation. From this unchanging I.E.P. they reached the conclusion that these carboxyl groups must be bound to an exactly equal number of cationic amino groups, which were released at the same time. This is another way of saying that the fixed carboxyl groups were engaged in salt linkages in native hemoglobin (Steinhardt and Zaiser 1955; Edsall and Wyman 1958, p. 539.)

Then in 1984, thirty-nine years after the publication of the Jacobsen and Linderstrom-Lang paper, an unequivocal confirmation of the salt linkage hypothesis was provided by Ling and Zhang (1984.) Here they demonstrated that for each fixed cationic group neutralized, exactly one fixed anionic group is set free and that freed fixed anionic group then adsorbs exactly one Na^+ (see Figures 13 and 14 of the present paper.)

Finally, I want to explain why it is important to review this history of the salt-linkage hypothesis. The myth of the non-existence of salt linkages was a part of the foundation for the mistaken notion of free ions surrounding proteins as proposed by Linderstrom-Lang mentioned earlier.

References

Arrhenius, S. (1887) *Zeit. physik. Chem.* 1: 631.
Arrhenius, S. (1888) *Phil. Mag.* 21: 81.
Beatley, E.H. and Klotz, I.M. (1951) *Biol. Bull*. 101: 205.
Bjerrum, N. (1923) *Zeit. physik. Chem*. 196: 219.
Bjerrum, N. (1926) *Kgl. Danske Vid. Selsk. Math. fys. Medd*. 7, No. 9, 1.
Boyle, P.J. and Conway, E.J. (1941) *J. Physiol.* (London) 100: 1
Bradley, A.P. and Sulley, D.J. (1948) *J. Amer. Chem. Soc.* 70: 914
Bregman, J.I. (1953) *Ann. N.Y. Acad. Sci*. 57: 125.
Carr, C.N. (1956) *Arch. Biochem. Biophys*. 62: 476.
Cohn, W. and Cohn, E.F. (1939) *Proc. Soc. Exp. Biol. Med*. 41: 445.
Debye, P. and Hhckel, E. (1923) *Physik. Z.* 24: 185.
Debye, P. and Hhckel, E. (1927) *Trans. Faraday Soc.* 23: 334.
Debye, P. and Pauling, L. (1925) *J. Amer. Chem. Soc.* 47: 2129.
Edelmann, L. (1977) *Phyiol. Chem. Phys*. 9: 313.
Edelmann, L. (1984) *Scanning Electron Microscopy* II: 875.
Edelmann, L. (1989) *Scanning Microscopy* 3: 1219.
Edsall, J.T. and Wyman, J. (1958) *Biophysical Chemistry* Vol. 1, Chapter 9 and 11, Academic Press, New York, pp. 512–522.
Engelmann, T.W. (1873) *Pflhgers Arch. Ges. Physiol.* 7: 155.
Ernst, E. (1963) *Biophysics of the Striated Muscle*, 2nd ed., Hungarian Acad. Sci., Budapest, p. 112.
Eyring, H. and Stearn, A.E. (1939) *Chem. Rev.* 24: 253.
Faraday, M. (1834) *Faraday-Whewell Correpondene 6, Faraday to Whewell R. I.,* Trinity College.
Fenn, W.O. (1936) *Physiol. Rev.* 16: 450.
Fenn, W.O. (1940) *Physiol. Rev.* 20: 377.
Fowler, R. and Guggenheim, E.A. (1960) *Statistical Thermodynamics,* Cambridge University Press, Cambridge.
Frost, A.A. and Pearson, R.G. (1962) *Kinetics and Mechanism: A Study of Heterogeneous Reactions,* 2nd ed., John Wiley & Sons, Inc., New York.
Fuoss, R.M. (1934) *Trans. Faraday Soc.* 30: 967.
Gerard, P. (1912) CR 154: 1305.
Glasstone, S. (1946) *Textbook of Physical Chemistry*, D. van Nostrand Co. Inc., New York.
Graham, D. C. (1950) *J. Chem. Phys.* 18: 903.
Graham, T. (1861) *Philos. Trans. Roy. Soc.* (London) 151: 183
Gregor, H. (1948) *J. Amer. Chem. Soc.* 70: 1293.
Gregor, H. (1951) *J. Amer. Chem. Soc.* 73: 642.
Gulati, J., Ochsenfeld, M.M. and Ling, G.N. (1971) *Biophys. J.* 11: 973.
Guggenheim, E. A. (1950) *Thermodynamics: An Advnaced Treatment for Chemists and Physicists*, 2nd ed., Intersience Publishers, Inc. New York.
Güntelberg, (1926) *Zeitschr. Physik. Chem*. 123: 243.
Gurney, R.W. (1949) *Introduction to Statistical Mechanics,* McGraw-Hill, New York.
Harris, F.E. and Rice, S.A. (1956) *J. Chem. Phys.* 24: 1208.
Hartley, G.S., Collie, B. and Samis, C.S. (1936) *Trans. Farad. Soc*. 32: 1795.
Helfferich, F. (1962) *Ion Exchange,* McGraw-Hill, New York.
Heppel, L.A. (1939) *Amer. J. Physiol.* 127: 385.
Hill, A.V. (1930) *Proc Roy. Soc.* (London) Ser. B 106: 477.
Hill, A.V. and Kupalov, P.S. (1930) *Proc. Roy. Soc.* (London) Ser. B 106:445.
Hill, R. and Wolvekamp, H.P. (1936) *Proc. Roy. Soc.* (London) B143: 81.
Hodgman, C.D., Weast, R.C. and Selby, S.M. (1961) *Handbook of Chemistry and Physics,* The Chemical Rubber Publishing Co., Cleveland.
Hückel, E. (1925) *Physik. Zeit.* 26: 91.
Huizenga, J.R., Grieger, P.F. and Wall, F.T. (1950) *J. Amer. Chem. Soc.* 72: 2636.
Huxley, A.F. and Niedergerke, R. (1958) *J. Physiol. (London)* 144: 403.

Huxley, T.H. (1853) *Review I, The British and Foreign Medico-Chronological Review* 12: 285.
Jacobsen, C.F. and Linderstrom-Lang, K, (1949) *Nature* 164: 411.
Jenny, H. (1927) *Kolloidchem. Beihefte* 23: 428.
Jenny, H. (1932) *J. Phys. Chem.* 36: 2217.
Jones, A.W. (1965*)* *Ph.D. Thesis, Appendix*, University of Pennsylvania, Phildelphia.
Kaplanski, S. Ya. and Boldereva, N. (1934) *Fisiol. Zh*. 17: 96.
Katchalsky, A. (1954) *Progr. Biophys*. 4: 1.
Kern, W. (1948) *Makromol. Chem.* 2: 279.
Klotz, I. (1953) in *The Proteins: Chemistry, Biological Activity and Methods*, The Academic Press, New York Chap. 8, p. 795.
Langmuir, I. (1918) *J. Amer. Chem. Soc.* 40: 1370.
Lillie, R.S. (1923) *Protoplasmic Action and Nervous Action,* 1st ed., University of Chicago Press, Chicago.
Linderstrom-Lang, K. (1924) *Compt. rend. trav. lab. Carlsberg* (Ser. chim.) 15, No. 7.
Ling, G.N. (1951) *Amer. J. Physiol.* 167: 806.
Ling, G.N. (1952) in *Phosphorus Metabolism* (Vol. II) (W.D. McElroy and B. Glass, eds.) The Johns Hopkins University Press, Baltimore, p. 748.
Ling, G.N. (1962) *A Physical Theory of the Living State: the Association-Induction Hypothesis*, Blaisdell Publishing Co, Waltham, MA.
Ling, G.N. (1964) *Biopolymers* 1: 91.
Ling, G.N. (1965) *Ann. N.Y. Acad. Sci.*125: 401.
Ling, G.N. (1969) *Intern. Rev. Cytol.* 26: 1.
Ling, G.N. (1977) *Physiol. Chem. Phys.* 9: 319.
Ling, G.N. (1977a) *Physiol. Chem. Phys.* 9: 217.
Ling, G.N. (1978) *J. Physiol. (London)* 280: 105.
Ling, G.N. (1980) in *Cooperative Phenomena in Biology* (George Karreman, ed.), Pergamon Press, New York, pp. 39–70.
Ling, G.N. (1984) *In Search of the Physical Basis of Life,* Plenum Publishing Co., New York.
Ling, G.N. (1989) *Physiol. Chem. Phys. & Med. NMR* 21: 13.
Ling, G.N. (1992) *A Revolution in the Physiology of the Living Cell,* Krieger Publishing Co., Malabar, Fl.
Ling, G.N. (1992a) *Scanning Microscopy* 6: 405.
Ling, G.N. (1993) *Physiol. Chem. Phys. & Med. NMR* 25: 145.
Ling, G.N. (1997) *Physiol. Chem. Phys. & Med. NMR* 29: 12. <http://www.physiologicalchemistryphysics.com/pdf/PCP29-2_ling.pdf.>
Ling, G.N. (1997a) <http://www.gilbertling.org>
Ling, G.N. (2001) *Life at the Cell and Below-Cell Level: the Hidden History of a Fundamental Revolution in Biology*, Pacific Press, NY.
Ling, G.N. (2003) *Physiol. Chem. Phys. & Med. NMR* 35: 91. <http://www.physiologicalchemistryphysics.com/pdf/PCP35-2_ling.pdf>
Ling, G.N. (2004) *Physiol. Chem. Phys. & Med. NMR* 36: 1. <http://www.physiologicalchemistryphysics.com/pdf/PCP35-2_ling.pdf>
Ling. G.N. (2005) in *Water in Cell Biology* (G. Pollack, I. Cameron and D. Wheatley, eds.) Springer, New York (in press).
Ling, G.N. and Bohr, G. (1970) *Biophys. J.* 10: 519.
Ling, G.N. and Bohr, G. (1971) *Physiol. Chem. Phys* 3: 431.
Ling, G.N. and Gerard, R.W. (1950) *Nature* 165: 113.
Ling, G.N. and Hu, W.H. (1988) *Physiol. Chem. Phys. & Med. NMR* 20: 293.
Ling, G.N. and Ochsenfeld, M.M. (1966) *J. Gen. Physiol.* 49: 819.
Ling, G.N. and Ochsenfeld, M.M. (1991) *Physiol. Chem. Phys. & Med. NMR* 23: 133.
Ling, G.N. and Walton, C. (1975) *Physiol. Chem. Phys.* 7: 215
Ling, G.N. and Zhang, Z.L. (1983) *Physiol. Chem. Phys. & Med. NMR* 15: 251.
Ling, G.N. and Zhang, Z.L. (1984) *Physiol. Chem. Phys. & Med. NMR* 16: 221.

Ling, G.N., Niu, Z. and Ochsenfeld, M.M. (1993) *Physiol. Chem. Phys. & Med. NMR* 25: 177.
Ling, G.N., Walton, C. and Ling, M.R. (1979) *J. Cell. Physiol*. 101: 261.
Ling, G.N., Zodda, D. and Sellers, M. (1984) *Physiol. Chem. Phys. & Med. NMR* 16: 381.
Lloyd, D.J., Marriott, R.H. and Pleass, W.B. (1933) *Trans. Farad. Soc.* 29: 554.
Macallum, A.B. (1905) *J. Physiol. (London*) 32: 95.
McBain, J.W. (1932) *The Sorption of Gases and Vapor by Solids*, George Rutledge & Sons, London.
Menten, M.L. (1908) *Trans. Canad. Inst.* 8: 403.
Michaelis, L. and Rona, P. (1919) *Biochem. Zeitschr*. 97: 57.
Minkoff, L. and Damadain, R. (1973) *Biophys. J*. 13: 167.
Mirsky, A.E. and Pauling, L. (1936) *Proc. U.S. Nat. Acad. Sci*. 22: 439.
Moelwyn-Hughews, E.A. (1949) *Proc. Cambridge Phil. Soc.*45: 477.
Moore, B. (1906) *Recent Advances. in Biochemistry* (Leonard Hill, ed.), Edward Arnold, London.
Moore, B., Roaf, H.E. and Webster, A. (1912) *Biochem. J.* 6: 110.
Nesterov, V.P. and Tigyi-Sebes, A. (1965) *Acta. Physiol. Hung*. 28: 97.
Pauley, J.L. (1954) *J. Amer. Chem. Soc.* 76: 1422.
Perutz, M., Muirehead, H., Cox, J.M., Goaman, L.C.G., Mathews, F.S., McGandy, E.L. and Webb, L.E. (1968) *Nature* 219: 29.
Rothmund, V. and Kornfeld, G. (1918) *Zeitschr. anorg. allgem. Chem*. 103: 129.
Speakman, J.B. and Hirst, M.C. (1931) *Nature* 128: 1073.
Stecher, P.G. (1968) *Merck Index,* Merck & Co., Rahway, NJ.
Steinbach, B. (1940) *J. Biol. Chem*. 133: 695.
Steinhardt, J. and Zaiser, E.M. (1951) *J. Biol. Chem.* 190: 197.
Steinhardt, J. and Zaiser, E.M. (1953) *J. Amer. Chem. Soc*. 75: 1599.
Steinhardt, J. and Zaiser, E.M. (1955) *Adv. Protein Chem*. 10: 151.
Thompson, H.S. (1850) *J. Roy. Agr. Soc., England* 11: 68.
Trombitas, C. and Tigyi-Sebes, A (1979*) Acta Biochim. et Biophys. Acad. Sci. Hung*. 14: 271.
van't Hoff, J.H. (1885) *Kon. Svensk. Vetenskap. Akad. Handl.* 21: 42.
van't Hoff, J. H. (1887) *Z. physik. Chem.* 1: 481.
Way, J.T. (1850) *J. Roy. Agr, Soc., England* 11: 313.
Webb, T.J. (1926) *J. Amer. Chem. Soc.* 48: 2589.
Weber, H.H. and Nachmansohn, D (1929) *Biochem. Z.* 294: 215.
Weissbluth, M. (1974) *Hemoglobin,* Springer-Verlag. New York, p. 23.
Whewell, William Rev. (1834) *Trinity College, Faraday-Whewell Correspoondence, Faraday to Whewell,* 6.
Wiegner, G. (1925) *Kolloid Zeitschr.* 36: 341.
Wu, H. and Yang, E.F. (1931) *Proc. Soc. Exp. Biol. Med*. 29: 248.
Yang, C.N. and Ling, G.N. (1964) see Ling, G.N. 1964.
Zheng, J. and Pollack, G.H. (2003) *Phys. Rev*. E 68: 031408.

Received June 7, 2004;
accepted December 8, 2004.

Appendix A

How the idea of ionic dissociation, which began as a brilliant scientific achievement has inadvertently degenerated into a misleading dogma and roadblock to progress

At one time, natural philosophers thought that sodium chloride exists as intact molecules just as sucrose does when dissolved in water. However, this idea was to make a 180 degree turn by the middle of the 20th century — as the reader of the earlier pages of this article have begun to suspect already.

Though ionic association and dissociation are *bona fide* physical chemistry, the story actually began in the research on (muscle) physiology. Two centuries later, it has returned to the science of (cell) physiology.

Aloisius Galvani (1737–1798) studied the way electricity brought about contractions of isolated frog legs. One day he was on the way out to carry out an experiment with electricity brought down from thunderclouds as Benjamin Franklin did in his famous kite experiment. To Galvani's astonishment, the frog legs suddenly contracted violently before he got to the thunderclouds — when the brass hook on which he had skewered his frog legs accidentally touched the iron railing of the building.

This surprising discovery eventually prompted Galvani to propose — for a while highly controversial — theory of animal electricity. It also set the stage for his detractor, physics professor, Alessandro Volta (1745–1827) to verify and extend his idea that it was entirely the result of electric activities at the point of contract between two different metals that caused the muscle to contract.

In time, Volta's study led him to invent what is known as his "Voltaic Pile". This primitive electric battery, in turn, played an important role in the discovery of *electrolysis* by Michael Faraday.

With the help of Rev.William Whewell of the Trinity College, Faraday then introduced the name cations for positively charged ions (like Na^+) and the name anions for negatively charged ions (like Cl^-.) Obviously, Faraday must have known and known well that electrolytes could dissociate in water; or else he would have no need to invent the names of the products of dissociation: cations and anions. The time was 1834 (Faraday 1834.)

Twenty seven years later, Thomas Graham — in his historic paper introducing the concept of *colloid* (Graham 1861) — described results of a relevant observation. Here, he showed that "a mixture of chloride of potassium and sulphate of soda is the same thing as a mixture of sulphate of potash and chloride of sodium, when the mixtures are in a state of solution." Graham went on to point that this finding is "in harmony with (Claude-Lewis) Berthollet's view, that the acids and bases are "indifferently combined." (Graham 1861, p. 197.) Graham gave no date when Berthollet's expressed this view (and where) but it must be earlier than 1861.

Most textbooks, however, made no mention of Berthollet, Graham or Faraday in their earlier discovery of electrolyte dissociation. Instead, the textbooks tell us that it was to Svante August Arrhenius (1858–1927) that we owe the knowledge that sodium chloride exists in water as dissociated sodium and chloride ions (Arrhenius 1887, 1888.)

Credit was also given to J.H. van't Hoff. van't Hoff suspected dissociation of salt in water when he found that the osmotic pressure of a solution of sodium chloride exceeds that of an equi-molar concentration of sucrose. But van't Hoff's work was published at

about the same time as Arrhenius's theory (van't Hoff 1885, 1887) and therefore also years after the same idea was expressed by Berthollet and by Graham. One asks, Is it pure coincidence that van't Hoff was the recipient of the first Noble Prize for Chemistry in 1901 and his pupil, Svente Arrhenius got the third Nobel Prize for Chemistry three years later?

In broad terms, the theory of ionic dissociation in water has largely proved correct. It is worth pointing out at this juncture that there are in fact two separate events underlying what we refer to as ionic dissociation. The first event is *ionization*. That is, the sodium atom gives off one of its valence electrons, thereby becoming a positively charged ion or cation and the chlorine atom gains an extra electron, thus becoming a negatively charged ion or anion. On this subject, there is now no dissension known to me.

Today, all agree that even in the form of (the most concentrated) solid crystal forms, all Na and Cl exist in the ionized Na^+ and Cl^- forms respectively — as X-ray crystallography studies carried out in the 1920's clearly showed. However, in his proof of his ionic dissociation theory, what Arrhenius called dissociation (in support of his theory) was in fact ionization. Accordingly, the accord he reported between theory and (that part of the) experimental observation is fortuitous (see Glasstone, 1946. p. 888.)

It is on the second event that difference in opinion exists — namely, the dissociation of a cation or an anion from an associated ion pair. Again, there is little dissension that in an infinitely dilute solution of NaCl, for example, all the Na^+ and Cl^- are fully dissociated. However, *a profound difference in opinion exist in regard to an electrolyte as found in living cells, in soils, in permutit, and in cation exchange resins.*

As pointed out earlier, Moore, Roaf and Webster believed that soil and proteins in living cells have special affinity for K^+. Wiegner and Jenny also believed that K^+, Na^+ and other cations in permutits could be preferentially adsorbed. In contrast, most textbooks of biology teach as established truth that ions in living cells are all free. And in the popular theories, counter-ions in exchange resins, near proteins and in living cells are all free. That, despite the fact that in the case of the cation exchange resin, the concentration of counter-ions could be as high as 3 Molar or higher.

How and when did this profound divergence on full ionic dissociation and association begin? And I repeat what specific evidence was there that has so thoroughly convinced some of the best scientific minds to their extreme view on the subject? Again, I repeat what I said above that I searched and searched but found none. No one denies that Faraday, Berthollet, Graham, Arrhenius, and van't Hoff have all played brilliant roles in establishing ionic dissociation in aqueous media. *But none of them suggested that full ionic dissociation is an absolute truth under all conditions.*

So common sense dictates that perhaps this extreme view on universal ionic dissociation as an immutable truth came about as a mistake. And, that once adopted by the opinion makers of the time, it acquired a life of its own. Next thing you know it has taken on the stern face of absolute and categorical truth. While the full story behind may never be known, I would venture a guess that it began with the work on ionic dissociation by van't Hoff and Arrhenius discussed above but in particular the famous *Limiting Law* of ionic dissociation of P. Debye and E. Hückel of 1923.

For what this Limiting Law tells us is that ions like Na^+ and Cl^- are fully dissociated in an infinitely dilute concentration. However, though they are fully dissociated, they are not entirely independent of each other Rather, each ion is surrounded by an ion cloud bearing an excess of oppositely charged ions. It is this ion cloud that causes the ions in

even an extremely dilute solution to behave in a way other than ideal. The factor that describes this non-ideality is known as the *activity coefficient*. For an electrolyte carrying a cation R and an anion X, the activity coefficient γ_{RX} is according to Debye-Hückel's limiting law, described by the following formula:

$$\ln \gamma_{RX} = a\, z_+ \mid z_- \mid I^{1/2} . \tag{A1}$$

In an aqueous solution at 25°C, the term, "a" equals 1.17 for an one-one electrolyte like NaCl. The product of the valence of the positive ion, z_+ and the absolute value of the valence of the anion $|z_-|$ is in this case equal to +1. I, the ionic strength, is equal to $^1/_2\Sigma_i\, z_i^2\, m_i$, which is 1/2 of the sum of the squares of the valence of the ith (and other) ion(s) multiplied by its respective molal concentration, m. Again, for an one-one electrolyte like NaCl, $I^{1/2}$ is equal to $m^{1/2}$. Therefore,

$$\ln \gamma_{RX} = 1.17\, m^{1/2} . \tag{A2}$$

For a more concentrated solution, Debye introduced a modification,

$$\ln \gamma_{RX} = a\, z_+ \mid z_- \mid \{I^{1/2} / (1 + \varrho_{RX}\, I^{1/2})\} , \tag{A3}$$

where ϱ_{RX} could be seen as proportional to the diameters of the X and R ions if they are seen as rigid spheres of equal size. However, as pointed out by Guggenheim, it would be safer to regard ϱ_{RX} as an empirical parameter. In 1925 Hückel introduced still another equation containing a second added parameter, β_{RX}:

$$\ln \gamma_{RX} = a\, z_+ \mid z_- \mid \{I^{1/2} / (1 + \varrho_{RX}\, I^{1/2})\} + 2\beta_{RX}\, m . \tag{A4}$$

Once more in the words of Guggenheim, "in spite of what Hückel might have thought," β_{RX} is yet another empirical parameter (Guggenheim 1950, p. 314.) In 1926 Güntelberg also suggested another equation in which ϱ_{RX} of Equation 4 is set to unity (1926). In 1935, Guggenheim himself introduced still another equation with only one empirical parameter, β_{RX}:

$$\ln \gamma_{RX} = z_+ \mid z_- \mid \{I^{1/2} / (1 + I^{1/2})\} + 2\, \beta_{RX}\, \tilde{\nu} m\} , \tag{A5}$$

where $\tilde{\nu}$ is the harmonic mean of the number of positive and negative ions in the electrolyte, ν_+ and ν_- through the relation

$$2 /\tilde{\nu} = 1/ \nu_+ + 1/ \nu_- . \tag{A6}$$

For an one-one electrolyte like NaCl, ν_+, ν_- and $\tilde{\nu}$ are all equal to unity. As pointed out by Guggenheim, his β_{RX} too is a purely empirical parameter. To find its value, one has to obtain the experimental data first.

I have chosen to quote all these improvements of the original limiting law of Debye and Hückel to cover not just very dilute solutions but concentrated electrolyte solutions as

well. With no exception, every equation dealing with the higher electrolyte concentrations is (partly) empirical.

Unfortunately, what these various empirical extensions of a rigorously derived limiting law could have done might not be what was intended. Thus, they could have misled others into believing that the absence of significant association between cations and anions covers the entire range of concentrations from the infinitely dilute to near saturation or not too far from it (e.g., 3 M or even higher.)

In my view, this misinterpretation might have occurred this way. The empirical parameters to describe activity coefficient at the higher end of the concentration spectrum were not accompanied by a clear warning. That is, a warning to the effect that *these parameters could hide from view the impact of significant association of the cations and anions on the activity coefficient*. As a result, readers could have been inadvertently led to believing that the introduction of the empirical parameter(s) does not in any way alter the validity of the assumption of full ionic dissociation — intended for the infinitely dilute solutions only.

Take as an example the superb *Textbook of Physical Chemistry* by Samuel Glasstone. It refers to Hückel's equation (Equation 4) as the Complete Debye-Hückel Equation (Glasstone 1946, p.966.) Even though Glasstone correctly pointed out that ϱ_{RX} and β_{RX} can only be determined empirically, he did not mention that these parameters could be covering up ion-to-ion direct-contact association.

To make my point that this is more than speculation, I quote Bjerrum (1926) and Fuoss (1934). Both have long believed and expressed the view that a fraction of the ions in aqueous solution stronger than the infinitely dilute are associated with their oppositely charged partners. Unfortunately, most popular textbooks do not cite their opinions.

In summary, there still is a widespread belief that alkal-metal ions like K^+ and Na^+ do not associate with anions regardless of the concentration and regardless of whether or not the anion may be fixed in space. The mistaken notion could be traced to the misunderstanding of the significance of the empirical parameters in the several equations. In all probability those empirical parameters hide the impact of ionic association.

Finally I add that this notion of full dissociation under all conditions is wrong will be made still clearer from additional new theoretical reasons presented in the main text and in Appendix B but especially from the extensive experimental evidence showing full ionic association with site fixation as observed in living cells and in inanimate systems of soil, permutit and ion exchange resin.

Appendix B

A kinetic interpretation of enhanced association with the spatial fixation of one species of the interacting particles

The reasons I offered for the enhancement of association between a pair of interacting particles due to the spatial fixation of one species applies to particles bearing net electric charges as well as particles bearing no net electric charges. But as a rule, interaction between oppositely charged particles tend to be stronger.

Consider a pair of particles A and B, which exist partly in a dissociated state as free A and free B and partly in the associated state, AB. Under constant temperature and pressure, the total percentage of A and B in the dissociated state and in the associated state are constant. That is to say, at any given moment, the number of A and B associating is equal to the number of AB dissociating. What we have here is then a direct second order reaction from left to right with a specific rate constant k opposed by a first order reaction from right to left with a rate constant k′:

$$A + B \rightleftarrows AB \ . \tag{B1}$$

At equilibrium, the reversible reaction is described by an association constant, $K_{A,B}$, and

$$K_{A,B} = k / k' , \tag{B2}$$

where

$$k = pZ \exp (-\Delta E/RT) \tag{B3}$$

and

$$k' = p'Z' \exp (-\Delta E'/RT) \ . \tag{B4}$$

p and p′ are the *steric factors* for the forward and reverse reaction respectively; Z and Z′ are their respective *collision numbers*; ΔE and ΔE′ their respective *activation energies*. The difference between ΔE and ΔE′ is equal to χ, which is often considered as the total energy change of the reaction. In fact, that is true only when the activation energies in opposing directions are exactly equal. Otherwise, χ contains the difference in the activation energies.

Having put down the well-known basics of chemical kinetics, I now replace it with a more specific model. Here A would be replaced by a positively charged mono-valent cation, K^+ and B would represent a carboxyl anion represented as $XCOO^-$ in a moderately dilute aqueous solution.

$$K^+ + XCOO^- \rightleftarrows XCOO^- - K^+ \ . \tag{B5}$$

Assuming that $XCOO^-$ is the anionic component of a strong acid, the salt $XCOO^- - K^+$ is fully ionized under all conditions. Furthermore, strong electrostatic attraction between $XCOO^-$ and K^+ makes the forward reaction exothermic and the reverse reaction endothermic. Nonetheless, we also know well that at room temperature and atmospheric pressure, the reaction is in favor of the reverse direction toward dissociation.

From the kinetic viewpoint, the extensive dissociation speaks for a much larger value of k′ when compared to k. Now, the electrostatic attraction is very powerful at close range, especially if one takes into consideration the phenomena of *dielectric saturation*. That makes $-\Delta E'$ much larger than $-\Delta E$, and by necessity, $p'Z'$ must be much larger than pZ. Yet as a first order reaction involving one kind of "molecules", the collision number Z′ would be equal to 2 $(\pi\ kT/m)^{1/2}\ \sigma^2\ n^2$, where π is 3.1416; k, the Boltzmann constant; T, the absolute temperature; m, the mass of a molecule; σ, its *collision diameter*; n, the concentration of the reactant expressed as number of molecules per ml. (Frost and Pearson 1962.) In a moderately dilute solution of say 0.1 M, the concentration of the associated $XCOO^- - K^+$ is a very small number. Thus as a whole, there must be another hidden factor that would make $p'Z'$ a large number. Most likely, this expected large $p'Z'$ is the consequence of the reaction taking place not in air but in water, which exists at the enormous concentration of over 55 Molar.

As such, what is represented, as a first-order dissociation reaction is in fact a reaction of a second or even higher order. It is the fraction of high-energy waters molecules that by its collision with the associated $XCOO^- - K^+$ that causes its dissociation to its components. In other words, what we may vaguely refer to as dissociation by thermal agitation, the energy that creates the agitation must be mostly provided by high-energy water molecules — going in the correct direction with a correct orientation and hence with a favorable p factor.

To cause the dissociation of the ion pair, $XCOO^- - K^+$, the effectiveness of a high-energy water molecule depends strongly upon its orientation and direction of movement in reference to the orientation of the associated ion pair at that moment. In addition, we must also keep in mind that a water molecule is not electrically neutral but is a strong *electric dipole* with what one may visualize as one positive end and one negative end. To approach the associated ion pair $XCOO^- - K^+$ from its anionic end, the minimum energy path would be along the axis joining the centers of the two oppositely-charged ions with the positive pole of the water molecule in the lead toward the anion of the associated ion pair. This way the approaching water dipole would be drawn to, and in the process weaken the electrostatic attraction between the ion pair. And this twofold action would in turn lower the value of $-\Delta E'$, thereby enhancing the probability of dissociation.

In summary, the high degree of ionic dissociation in a dilute aqueous solution of monovalent salts like $XCOO^- - K^+$ is seen as due to a large extent to the relative high value of k′. This in turn reflects the highly favorable steric factor and collision number on account of the participation of the enormous number of water molecules. Together, the favorable p′ and Z′ are able to overcome the strong electrostatic attraction between the ion pairs, which would have kept the ions in an associated state.

In the following, I shall present the hypothesis that spatial fixation of one species of the interacting ion is able to cause a dramatic change in the balance of the forward and backward reactions shown in Equation B1 — leading to strong association.

1. The influence of spatial fixation on the rate of association.

If a pair of ions, R and X, are represented as rigid spheres with respective radius of σ_R and σ_X then the collision number will be $\pi\,\sigma_{RX}^2\ r\ n_X$, where σ_{RX} is equal to the sum of σ_R and σ_X. n_X is the number of X in one cubic centimeter. r represents the relative mean velocity of the ion R in reference to X and it is a deciding factor in the rate of the reaction.

One asks, would the spatial fixation of one of the interacting species strongly slow down r? In fact we already have a clear answer. And J.C. Maxwell provided it.

What Maxwell did was to show that the actual velocity is in fact smaller than the velocity measured against stationary molecules by a factor of $\sqrt{2}$ (see Glasstone 1946, p. 275.) What this tells us is that spatial fixation of one species of the interacting ions does not slow down the relative velocity between the pair of ions X and R. On the contrary it actually accelerates it.

All in all, the collision number of R and X encounters and hence the *rate of association* is not adversely affected if X is fixed in space. On the other hand, fixation of X would have profound influence on *the rate of dissociation* of the associated ion pair RX as shown next.

2. The influence of spatial fixation of one species of ion on the rate of dissociation.

As explained in the preceding section, when both R and X are free, their predominantly dissociated state in an aqueous solution bespeaks of many collisions with the (numerous) water molecules. If now X is rigidly fixed in space, the consequence that is most obvious is that half of the collisions with water molecules will be made futile. This simple fact would by itself reduce the rate of dissociation of RX by a factor of two. But the impact on dissociation by the fixation of X is far more.

To get a better visual image of the impact of a collision, one must change our visual image. That is, to replace one in which two billiard balls sitting next to each other are being hit and hence knocked apart by a third one — by one in which the two juxtaposed balls are actually tied to each other with a breakable rubber band and they are being hit by a third ball.

Accordingly, the reduction of dissociation will be reduced to far beyond a factor of two, because only a portion of the collisions are effective enough to break that rubber band. And, the most effective collisions, as mentioned above, are those in which the collision is along the minimum energy paths. With the fixation of X in space not only are the collision of the kind R X $\leftarrow$ H_2O — where the high-energy water molecule collides with the fixed entiry, X — made less effective, the collision of the kind, XR $\leftarrow$ OH_2 — where the high-energy water molecule collides with the adsorbed entity, R — are also made ineffective. Since these are the main pathways leading to dissociation, the p factor for the dissociation reaction is reduced to a factor far lower than 1/2. But there is still another factor that contributes to the further reduction of the number of successful collisions between RX and the water molecules. This originates from the water of hydration.

Thus far, we have considered X, R as well as RX as simply themselves. In truth, each is clothed in a shell of water molecules, comprising k, l and m water molecules for each of the interacting entities (see Equation B6). Indeed, in constructing my 1952 model depicted in Figure 4, I have already encountered the problem. The assumption I made was that if R represents either K^+ or Na^+, then the number of water molecules for either ion would remain unchanged when each comes into contact with the fixed anions, X. It turned out that this was a lucky choice, when considered from a later date after a much broader approach was taken on this problem and limited to the special case considered (see Ling 2001, p.143.)

$$R(H_2O)_k + X(H_2O)_l \rightleftarrows RX\ (H_2O)_m \tag{B6}$$

in which the sum of k and l equals m. In a more comprehensive approach introduced in 1962, I realized that if we return to the more specific model cited above, then it is the number of water molecules that exist between the interacting ions that is not constant but that variations then determine the degree of association and the energy of adsorption. This is expressed in the simple equation form as follows

$$COO^-\ (H_2O)_k + K^+\ (H_2O)_m \rightleftarrows XCOO^-\ (H_2O)_n\ K^+ + o\ (H_2O)\ . \tag{B7}$$

I then found that for a given X in the entity $XCOO^-$, the energy of what is referred to as Configuration 0 with no water molecules between the interacting ion pair, or Configuration 1, 2 or 3 respectively with 1, 2 or 3 water molecules in between (Figure B1), the total energy difference may not be very large as shown in Figure B2.

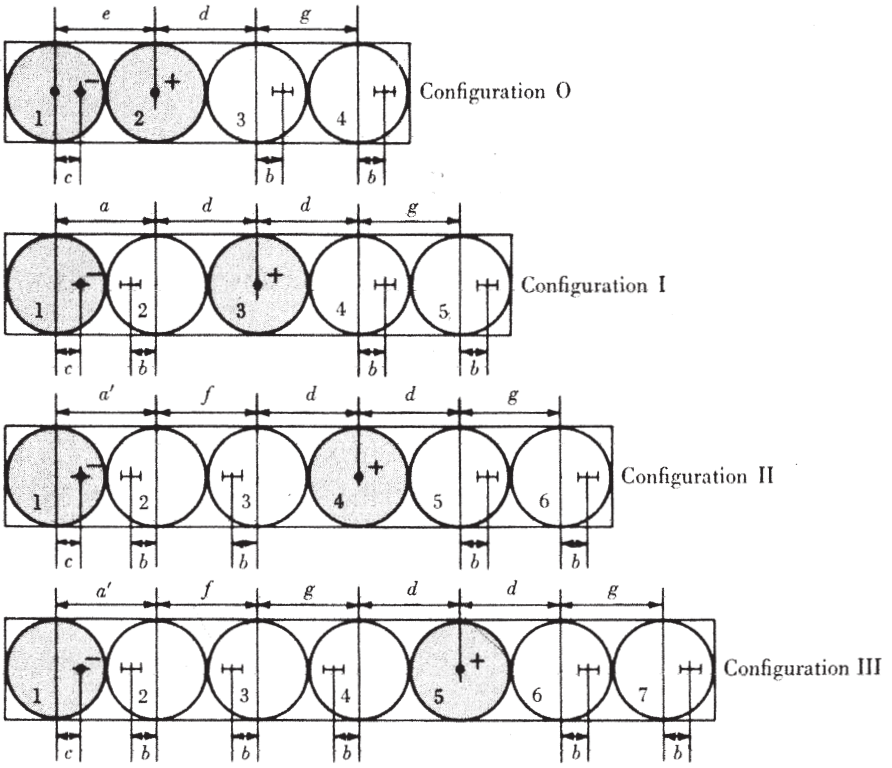

FIGURE B1. The linear model. The total interaction energies were computed (but not shown here) for each monovalent cation in each of the four confirgurations of fixed anions and water molecules. (from Ling 1962)

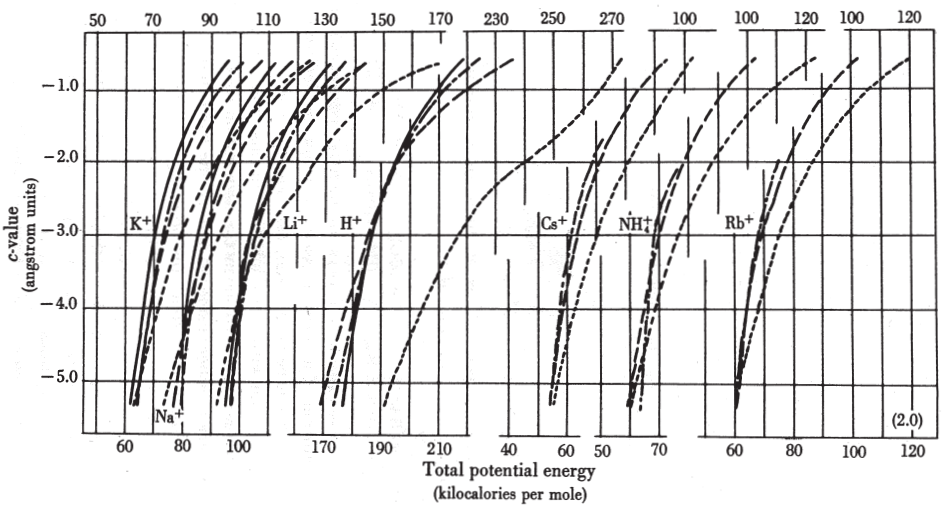

FIGURE B2. The variation of the total potential energy $\mathcal{U}$ of the fixed anion-counter-cation-water system as a function of the c-value at near 0°K. In this figure, the fixed anion has a polarizability of 2.0 x 10^{-24} cm^3.Values are plotted for each cation in each of the 0 — , I — , II— and III — configurations (see Figure B1.) Roughly speaking, the c-value is a quantitative measure of the electron density of the singly-charged carboxyl oxygen. High c-value denotes a weak acid (e.g., acetic acid with a pK_a of 4.76); low c-value denotes a strong acid (e.g., trichloroacetic acid with a pK_a of less than 1.0.) (from Ling 1962)

Accordingly, a collison which would have knocked away one of the intervening water molecules will only shift the ion pair-water assembly into a different Configuration and not full dissociation. In other words, only a succession of multiple collisions would bring about dissociation. Since each of these needed steps would be hampered or made impossible by the fixation of one the interacting ions, this requirement of multiple collision, further reduces the chance of dissociation with the fixation of one of the pair of interacting entities.

Again, the cited example here deals with ions having net charges. But the principle should operate if the interacting pair does not carry net changes, though conceivably in degree it could be weaker.

Appendix C

We began with a mixture of three kinds of particles or molecules, free A, free B and their associated product, AB. We ask what would happen if all the free A's are rigidly fixed in space and made into a network of fixed A's. First, by rigidly fixing and arresting all the A's motional freedom, their W_{th}^{A} becomes or approaches unity and ln W_{th}^{A} becomes or approaches zero. At the same time, a new configurational entropy is created corresponding to what we shall designate as W_{cf}. Meanwhile, the B's would either remain free or associated one on one to a now immobilized A site. Because of the fixation of A's, the total ln W of the assembly will change from

$$\ln W_{th}^{A(free)} + \ln W_{th}^{B(free)} + \ln W_{th}^{AB} \tag{4}$$

to

$$\ln W_{th}^{B(assoc)} + \ln W_{th}^{B(free)} + \ln W_{cf} \,. \tag{5}$$

Let us now focus our attention on ln W_{cf}. When we have rigidly immobilized all the A's into a network, the total number of these fixed A sites would become a constant, to be called N_s. Now, a number of these sites would be associated with B particles, others would be vacant. Let us designate these numbers respectively as N_B, and $N_S - N_B$. Thus the number of recognizably different ways of distributing N_S number of sites to B and to vacant sites would be

$$W_{cf} = \frac{N_s\,!}{N_B\,!\,(N_s - N_B)!}\,. \tag{6}$$

The complete partition function of adsorbed molecules would be

$$\frac{N_S\,!}{N_B\,!\,(N_S - N_B)!}\cdot\left[(\text{p.f.})_B \exp\left(\frac{\chi}{kT}\right)^{N_B}\right]. \tag{7}$$

where χ is the minimum energy needed to dissociate the B molecules from its adsorption on the fixed site at its lowest energy level and take that lowest energy level as zero.

The free energy, F^{ads} of the adsorbed molecules can then be written out as

$$\frac{F^{ads}}{kT} = -\log\left[\frac{N_S\,!}{N_B\,!\,(N_S - N_B)!}\cdot\left[(\text{p.f.})_B \exp\left(\frac{\chi}{kT}\right)\right]^{N_B}\cdots\right] \tag{8}$$

$$= -N_S \log N_S + N_B \log N_B + (N_S - N_B)\log(N_S - N_B)$$
$$-N_B \log\left[(\text{p.f.})_B \exp\left(\frac{\chi}{kT}\right)\right]. \tag{9}$$

Now, the chemical potential or what Fowler and Guggenheim call partial potential of free B paricles, μ_B, is described by the following equation:

$$\frac{\mu_B}{kT} = \frac{1}{kT}\left(\frac{\partial F}{\partial N_B}\right)_T \tag{10}$$

$$= \log\left(\frac{N_B}{N_S - N_B}\right) - \log\left[(p.f.)_B^{ads} \cdot \exp\left(\frac{\chi}{kT}\right)\right]. \tag{11}$$

If we designate the fraction of sites occupied by B as θ and the fraction of vacant sites as $1-\theta$, then

$$\frac{\mu_B}{kT} = \log\left(\frac{\theta}{1-\theta}\right) - \log\left[(p.f.)_B^{ads} \cdot \exp\left(\frac{\chi}{kT}\right)\right]. \tag{12}$$

We can then calculate the absolute activity of adsorbed B, λ_B^{ads} as follows:

$$\lambda_B^{ads} = \exp\left(\frac{\mu_B}{kT}\right) = \left(\frac{\theta}{1-\theta}\right) \cdot (p.f.)_B^{ads} \cdot \exp\left(\frac{\chi}{kT}\right) \tag{13}$$

and the absolute activity of free B as

$$\lambda_B^{free} = \frac{p_B}{kT(p.f.)_B^{free}}. \tag{14}$$

where p_B is the pressure of free B; $(p.f.)_B^{free}$ is its partition function.

At equilibrium, the absolute activities of free and adsorbed B molecules are equal,

$$\lambda_B^{ads} = \lambda_B^{free}. \tag{15}$$

From this, we derive

$$\frac{\theta}{1-\theta} = \frac{p}{p^o}, \tag{16}$$

where p replaces p_B and p^o is defined as follows

$$p^o = \frac{kT(p.f.)_B^{free}}{(p.f.)_B^{ads} \cdot \exp\frac{\chi}{kT}}. \tag{17}$$

Equation 16 can be transformed to read

$$\theta = \frac{p}{p^o + p}. \tag{18}$$

Appendix D

The Yang-Ling Cooperative adsorption isotherm

Based on the one-dimensional Ising model, Yang and Ling published in 1964 their cooperative adsorption isotherm of proteins and other linear polymers containing a liner chain of similar adsorption sites (Ling 1964):

$$[p_i]_{ad} = \frac{[f^-]}{2}\left\{1 + \frac{\xi - 1}{\sqrt{(\xi-1)^2 + 4\xi \exp(\gamma / RT)}}\right\} \tag{24}$$

where $[p_i]_{ad}$ and $[p_i]_{ex}$ are respectively the concentration of adsorbed and free ith solute. $[f^-]$ is the concentration of fixed adsorption sites. R is the gas constant and T, the absolute temperature. $-\gamma/2$, the nearest neighbor interaction energy, is equal to the additional energy each time a new i–j pair of nearest neighbors of adsorbed solutes is formed. ξ is defined as follows:

$$\xi = \frac{[p_i]_{ex}}{[p_j]_{ex}} K^{oo}_{j\to i} \tag{25}$$

where $K^{oo}_{j\to i}$ is the *intrinsic equilibrium constant.* It is related to *the intrinsic free energy change,* $\Delta F^{oo}_{j\to i}$ involved in an j→i exchange adsorption by the following equation

$$\Delta F^{oo}_{j\to i} = RT \ln K^{oo}_{j\to i} . \tag{26}$$

The Yang-Ling isotherm presented above as Equation (24), can also be written in the following form:

$$\frac{[p_i]_{ad}}{[p_j]_{ad}} = \frac{\sqrt{(\xi-1)^2 + 4\xi \exp(\gamma / RT)} + \xi - 1}{\sqrt{(\xi-1)^2 + 4\xi \exp(\gamma / RT)} - \xi + 1} \tag{27}$$

A plot of log $\{[p_i]_{ad}/[p_j]_{ad}\}$ against log$\{[p_i]_{ex}/[p_j]_{ex}\}$ at varying values of the nearest neighboring interaction energy, $-\gamma/2$, is shown in Figure D1. A tangent along each curve at the point when half of the sites are occupied by i and the other half by j, is of the following form:

$$\log \frac{[p_i]_{ad}}{[p_j]_{ad}} = n \log \frac{[p_i]_{ex}}{[p_j]_{ex}} + n \log K^{oo}_{j\to i} . \tag{28}$$

Note that this equation has essentially the same form as one introduced by Rothmund and Kornfeld (1918) for ion exchange in soils:

$$\log\left[\frac{[A]_{ad}}{[B]_{ad}}\right] = n\left[\frac{[A]_{free}}{[B]_{free}}\right] + n \log K' \tag{29}$$

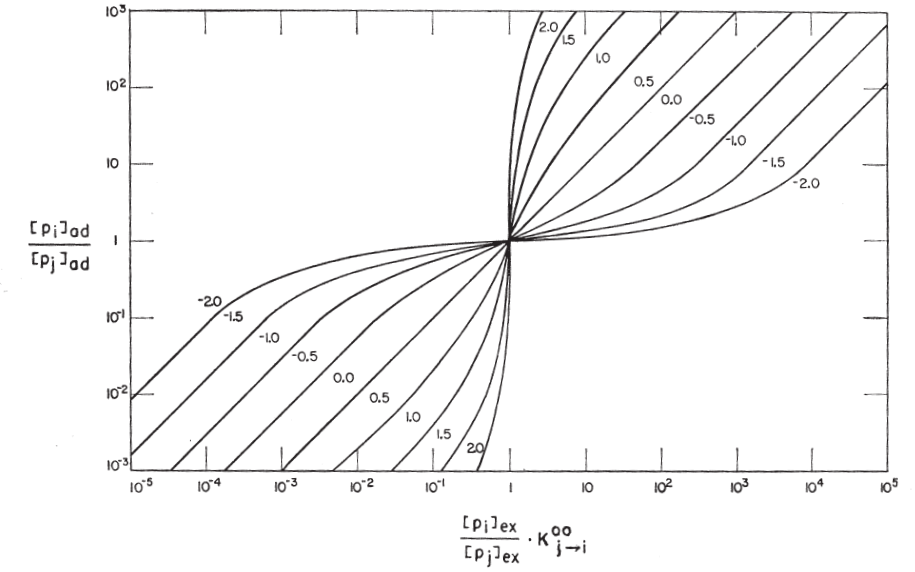

FIGURE D1. Theoretical plot of the cooperative adsorption isotherms of two competing solutes according to Equation 19. The number near each curve is the free energy of nearest neighbor interaction ($-\gamma/2$.) and is in units of kcal/mole at 25°C. (from Ling and Bohr 1970, by permission of Biophysical Society)

as well as that of Hill and Wolvekamp (1936) for oxygen binding on hemoglobin:

$$\log \frac{y}{1-y} = n \log pO_2 + n \log K \tag{30}$$

where y represents the fraction of (hemoglobin) sites occupied by oxygen and (1 − y) represents the fraction not occupied by oxygen. In both the Rothmund-Kornfeld equation and the Hill-Wolvekamp equations, the constants n's are empirical. This is, of course, not true in the (analogous) n of Equation 28 derived from the Yang-Ling isotherm, Indeed, the parameter, n, here is explicitly related to the nearest neighbor interaction energy, $-\gamma/2$ by the following relation

$$n = \exp(-\gamma/2RT) \tag{31}$$

when $-\gamma/2$ is larger than 0, n is larger than 1. In this case, the adsorption is what is conventionally called *ferro-magnetic* type of cooperative interaction but called *auto-cooperative* in the lingo of the AI Hypothesis. It signifies that each time an ith solute is adsorbed it would favor the adsorption of another pair of ith solute on the two nearest neighboring sites. When $-\gamma/2$ is less than 0, n is less than 1, we have what I call *hetero-cooperative* interaction. It means that each ith solute adsorption favors the adsorption of the alternative jth solutes. When $-\gamma/2$ is equal to 0, n is equal to 1, in this case, the Yang-

Ling cooperative adsorption isotherm and the tangent equation at half saturation are not distinguishable. Both are in fact become a simple version of the Langmuir adsorption isotherm.

For easy recognition of the nature of a set of adsorption data, I have reproduced in Figure D2 typical cases of auto-cooperative interaction ($-\gamma/2 > 0$), hetero-cooperative interaction ($-\gamma/2 < 0$) and non-cooperative (or Langmuir) adsorptions ($-\gamma/2 = 0$) in reciprocal plots (A) and in what is known as Scatchard plots (B).

As Langmuir first introduced this theory, its most distinction feature is that each adsorbent molecule occupies a single localized site. At the time, he was referring to adsorption on a solid surface. However, as time went by, it has become broadly applied to adsorption in other types of systems. The approach I have given here, which is essentially that given by Fowler and Guggenheim, did not suffer any restriction to two dimensional systems. But, the main reason it is given here is to show how the fixation of one species of an interacting pair of molecules or ions has transformed what one may see as an aberration from the limiting law of full dissociation to the critically important phenomenon of association or *adsorption*. What caused this transformation is the fixation and aggregation of one of the interacting species.

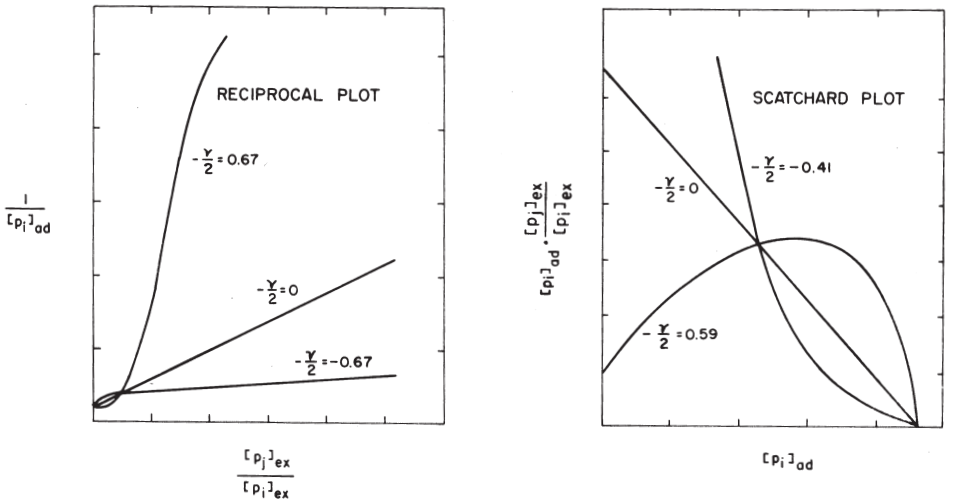

FIGURE D2. Reciprocal plot (left) and Scatchard plot (right) of adsorption isotherms in which the free energy of nearest neighbor interaction ($-\gamma/2$) is positive, negative or zero. *In the reciprocal plots*, the reciprocal of the ith adsorbent is plotted against the ratio of the ith and jth solute in the bathing solution, $[p_i]_{ex} / [p_j]_{ex}$. The sigmoid curve indicates auto-cooperativity with $(-\gamma/2) > 0$. Heterocooperative adsorption with $(-\gamma/2) < 0$ assumes a hyperbolic shape. When the plot is in the form of a straight line, it is non-cooperative or a Langmuir isotherm with $(-\gamma/2) = 0$. *In the Scatchard plot* again the non-cooperative (Langmuir) isotherm appears as a straight line; heterocooperative isotherm concaves upward and autocooperative isotherm concaves downward. (from Ling 1980 with permission from Elsevier)

Physiol. Chem. Phys. & Med. NMR (2005) *37*: 65–69

Studies on the Amount of Aluminum and Calcium in Urine following Aluminum Administration with and without Amino Acids

Hiromi Aikoh, Kazuhiro Nakamura, Masaaki Yamato and Takashi Shibahara

Department of Chemistry, Faculty of Science, Okayama University of Science, 1-1 Ridai-cho, Okayama City 700-0005, Japan.
E-mail: aikoh@chem.ous.ac.jp

Abstract: The evidence implicating aluminum as a neurotoxin is mounting. Research with animals and humans has linked aluminum with neuro-cognitive dysfunction and, in some cases, death. Although the relationship between aluminum intake and Alzheimer's disease is still unclear, some experts have recently issued a strong warning that human exposure to aluminum should be limited. The results indicate that the amount of aluminum decreased in the urine in mice that were administered glycine or glutamic acid together with aluminum ion. In the mice in which the amounts of aluminum decreased in the urine, the amount of calcium conversely increased.

IN PAST YEARS infant formulas and parenteral nutrients were found to contain excessive quantities of aluminum but this potential hazard has supposedly been corrected. Known sources of aluminum include air[1], antacids[2], antiperspirants[2], cosmetics[3], dental preparations[4], food additives[5], vaccines and allergenic extracts[4], tea[6], and water. The evidence implicating aluminum as a neurotoxin has been continuously mounting. Research with both animals and humans has linked aluminum with neuro-cognitive dysfunction and, in some cases, death[7].

Although the relationship between aluminum intake and Alzheimer's disease is still unclear, some experts have recently issued the strong warning that 'human exposure to aluminum should be limited'.

Our working hypothesis is that the materials in some drinking water and food additives combine with the aluminum and may promote the internal absorption of aluminum.

The present report is concerned with the *in vivo* absorption of aluminum and the urinary metabolites in experimental mice that had received aluminum-ion-containing samples.

Materials and Methods

Aluminum (1000 ppm-Al in 0.2M-HNO_3 and Calcium (1000 ppm $CaCO_3$ in 0.1M-HNO_3 standard solutions were purchased from Kanto Chemicals. Amino acids were purchased from Kanto Chemicals (glycine) and Nakalai Tesque (L-glutamic acid).

Three-month-old female mice with a body weight of 25~30 g were used for the experiment. Sixteen mice were divided into four groups (four mice in each). The mice in the control group were administered water. The mice in the other groups were administered aluminum ion (Al^{3+}) only (0.5 ppm), or glycine (Gly) at 1 x 10^{-4} mol/l together with the Al^{3+}, or glutamic acid (Glu) at 1 x 10^{-4} mol/l together with the Al^{3+} (0.5 ppm). These mice were used as an oral administration group during the feeding period; the sample containing 0.5 ml of aluminum ion was compulsorily administered orally with a catheter.

Mice were kept in a metabolic cage to collect urine. The urine was collected during the feeding period once at the end of the week. The volume measured the quantity of urine that a mouse drained in a day and night (24h). Urine was gathered for 24 hours so that the mean of a night and day ion content could be determined.

Pretreatment of the urine for the measurement of aluminum and calcium was as follows: the urine sample was centrifuged to remove any solid materials. A PFA jar (Hagitec Co. Ltd., Japan) containing the supernatant solution (0.5 ml) and concentrated nitric acid (1 ml) was placed in an oven for 5 min to decompose the urine sample. The decomposed sample was transferred into a measuring flask (50 ml) and brought to volume with water.

The urinary aluminum or calcium content excreted from each mouse was measured by ICP-MS spectrometer (Model SPQ6500, SEIKO) or atomic absorption spectrophotometer (Model Z6100, Hitachi).

Results

Amount of aluminum and calcium in the urine

The amount of aluminum in the urine was measured in those mice that had been administered various samples orally. The results are shown in Figure 1. The amount of aluminum (1.83 ± 0.20 μg/g) in the urine excreted from mice that had received an aqueous solution of Al^{3+}, or Gly or Glu including Al^{3+} had a higher value than that measured in the control mice (0.85 ± 0.12 μg/g), which had received tap water only. The amount of aluminum (1.48 ± 0.16 μg/g or 1.41 ± 0.21 μg/g) in the urine of mice that had received the Al^{3+} + Gly or Al^{3+} + Glu had a lower value than that of mice that had received Al^{3+} only. All differences were significant at the $p < 0.01$ level, at which the difference between the amount of aluminum in the urine excreted from mice which had been administered Al^{3+} and those which had been administered Al^{3+} + Gly or Al^{3+} + Glu could be observed. These results suggest that the aluminum ion with Gly or Glu is accumulated *in vivo* but the aluminum ion without Gly or Glu is discharged extracorporeally.

The amount of calcium in the urine was investigated in the mice that had received the various samples. The results are shown in Figure 2. The amount of calcium (26.2 ± 3.4 μg/g) excreted in the urine from mice that had received the Al^{3+} only was almost the same as that in the control mice (25.5 ± 3.6 μg/g). However, the amount of calcium (85.6 ± 3.1 μg/g

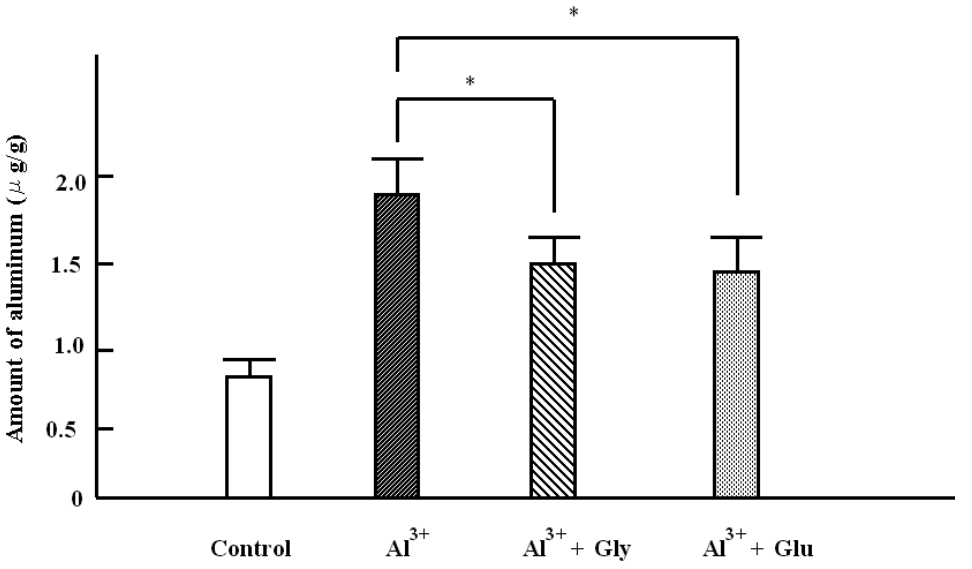

FIGURE 1. Amount of aluminum in the urine excreted from mice. Values are mean ± SD, *: $p < 0.01$ significantly different.

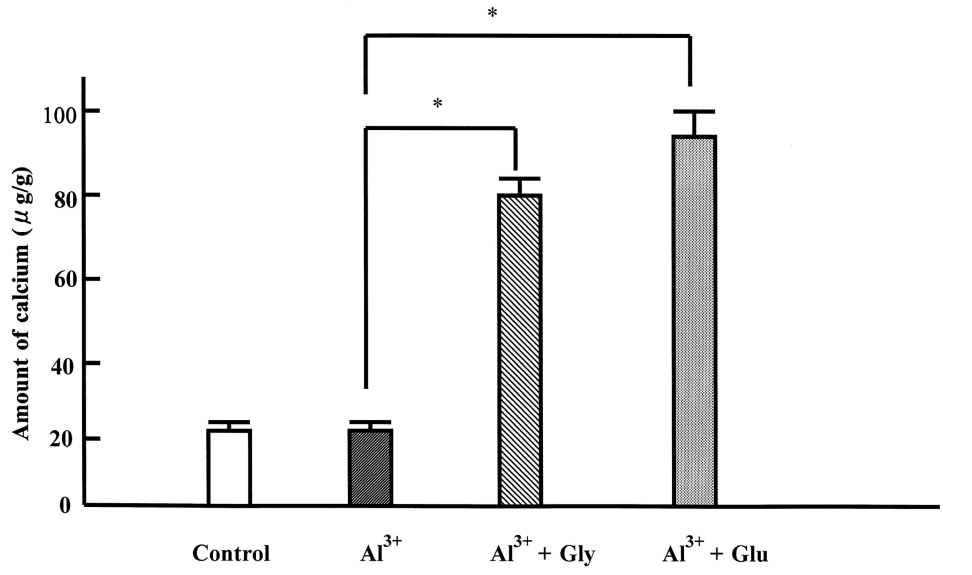

FIGURE 2. Amount of calcium in the urine excreted from mice. Values are mean ± SD, *: $p < 0.01$ significantly different.

or 95.5 ± 3.0 μg/g) in the urine excreted from mice that had received the aqueous solution of Gly or Glu including Al^{3+} was about 4~5 times higher than that in the control mice. These results suggest that there is some link between calcium loss and the absorption of aluminum ion in the living body.

Discussion

The chemical properties of aluminum are very similar to those of iron and materials that naturally combine with iron also combine strongly with aluminum. Iron combined with transferrin is thought to be transported to the neurons that pass through the blood-brain barrier. Aluminum is present in some drinking water[8–10] and foods. When the aluminum in drinking water is absorbed by the body similarly to iron, about 80% may be combined with transferrin and transported to the internal organs[11].

Our results indicate that the amounts of aluminum decreased in the urine of mice that had received glycine or glutamic acid including aluminum ion. This result suggests that aluminum may form coordination compounds with some amino acids and accumulate in the body more easily than aluminum only. Therefore, this amino-acids-coordinated aluminum may pass through the blood-brain barrier easily, thus being absorbed into the brain and carried to the neurons, where the aluminum acts as a neurotoxin that has important effects on nerve cells. We speculated that the decreased urinary excretion of aluminum in mice given aluminum together with glycine or glutamic acid was due to the accumulation of aluminum-amino acid complex in the body. The result suggests that aluminum passes intestinal mucous membrane as aluminum-amino acid complex and is absorbed into the body. The amount of aluminum in feces is considered to be a very small value in comparison with that in urine, though aluminum in feces was not measured. However, we confirmed previously that there are higher amounts of mercury in urine than that in feces of mice administered mercuric ion orally. Amount of aluminum in intestine or feces, and the formation of aluminum-amino acid complex is now under investigation.

The relationship between aluminum and Alzheimer's disease is quite controversial. As has been pointed out by other researchers, some people may consume up to 1~30 mg of aluminum per day in the form of antacids[1] yet no association has been found between dementia and the use of antacids[12]. There is, however, evidence to indicate that aluminum may be more bioavailable when dissolved in water as opposed to being ingested in foodstuffs[6]. There are also several other factors[2–5] that may increase the bioavailability of aluminum and these are of concern when considering the results of the current study. On the other hand, the amount of calcium increased in the urine of the mice that were administered the glycine or glutamic acid including aluminum ion. The result suggest that aluminum absorbed by the body may erode bones and as a result, contribute to osteoporosis. The result is now under investigation.

References

1. Epstein, S.G. (1987) Aluminum and health: an update on Alzheimer's Disease. Washington, DC: *Aluminum Association*.

2. Graves, A.B., White, E., Koepsell, T.D., Reifler, B.V, Van Belle, G., Larson E.B. (1990) The association between aluminum-containing products and Alzheimer's disease. *J. Clin. Epidemiol. 43:* 35–44.
3. Walton, L. (1992) Alzheimer's disease and the environment(editorial). *J. Royal Soc. Med. 85:* 69–70.
4. McLachlan, D.R.C., Kruck, T.P., LuKiw, W.J., Krishnan, S.S. (1991) Would decreased aluminum ingestion reduce the incidence of Alzheimer's disease? *Canad. Med. Assoc. J. 145:* 793–804.
5. Greger, J.L. (1985) Aluminum content of the american diet. *Fd. Technol. 39:* 73.
6. Kawachi, I., Pearce, N. (1991) Aluminum in the drinking water — is it safe? *Australian J. Public Health 15:* 84–87.
7. Murray, J.C., Tanner, C.M., Sprague, S.M. (1991) Aluminum neurotoxicity: A reevaluation. *Clin. Neuropharm. 14:* 179–185.
8. Greger, J.L. (1992) Dietary and other sources of aluminum intake. *Ciba. Found. Symp. 169:* 26–49.
9. Greger, J.L. (1993) Aluminum metabolism. *Annu. Rev. Nutr. 13:* 43–60.
10. Bakir, A.A., Hryhorczuk, D.O., Ahmed, S., Hessl, S.M., Levy, P.S., Spengler, R. and Dunea, G. (1989) Hyperaluminemia in renal failure: the influence of age and citrate intake. *Clin. Nephrol. 31:* 40–44.
11. Slanina, P., Frech, W., Ekstrom, L., Loof, L., Slorach, S. and Cedergren, A. (1986) Dietary citric acid enhances absorption of aluminum in antacids. *Clin. Chem. 32:* 539–541.
12. Jonstone, T. (1992) Aluminum and Alzheimer's disease (letter). *Canad. Med. Assoc. J. 146:* 431–432.

Received February 8, 2005;
accepted August 29, 2005.

Physiol. Chem. Phys. & Med. NMR (2005) *37*: 71–84

Electrical Properties of Hornet Silk: Temperature Dependence

Marian Plotkin[1], Natalya Y. Ermakov[1], David J. Bergman[2] and Jacob S. Ishay[1*]

[1]*Department of Physiology and Pharmacology, Sackler Faculty of Medicine and*
[2]*School of Physics and Astronomy, Raymond and Beverly Faculty of Exact Sciences,*
Tel Aviv University, Ramat Aviv 69978, Israel
** Address for correspondence*
E-mail:physio7@post.tau.ac.il

Abstract: Hornet silk is a polymer of amino acids. One of the known properties of polymers is their electrical activity. The present study describes the results of electrical measurements carried out vertically on the silk cap of pupae of the Oriental hornet *Vespa orientalis* (Hymenoptera, Vespinae). The measurements undertaken were the temperature-dependent electric current, voltage and resistance, all measured within the range of biological temperatures, as well as the capacitance. The temperature-dependent spontaneous current attained values up to 327 nano Amperes (nA) while the maximal voltage reached 347 millivolt (mV). The electrical resistance was low and steady (1–20MΩ) at temperatures ranging between 19–32°C, but at lower or higher temperature it increased fairly sharply by about three orders of magnitude. The electrical capacitance, computed according to the discharge curve (decay curve) amounted to 0.4 microFarad (μF). The paper also discusses the role of the pupal silk as producer of a 'clean room' while the cuticle is being laid down by the pupae after undergoing metamorphosis, as well as the significance of the measured electrical parameters *vis-à-vis* the developing pupae.

A CONSIDERABLE part of the known insects produce a 'silk', that is they secrete a proteinaceous, stringy material that can serve various purposes, to wit: to protect the larval stages (Nation, 2002), to retain the oviposited eggs (ootheca) (Rudall and Kenchington, 1971), or most commonly to enwrap the developing larva as it undergoes metamorphosis (Wilson, 1971; Spradbery, 1973; Edwards, 1980; Matsuura and Yamane, 1990).

In the case of hornets, this silk is produced both by the larval stages as well as by the adults (Joseph and Ishay, 2004). The source of the silk in insects is the same gland that also produces the insect's cuticle (Imms, 1960). In social wasps and hornets (Vespinae), the pupating larva produce and secrete a silk from their labial glands, and this silk provides both

a padding and a casing for them, and underneath it is formed the cuticle of the future imago. The silk thus serves also, *inter alia*, as a 'clean room', that is, a barrier against dust particles or air currents that may hamper the creation of hornet cuticle which has the properties of a semiconductor (Gutmann *et al.*, 1983; Shabtai and Ishay, 1998). Generally speaking, much more is known about the silk produced by the larval hornets than about that of the adults. Thus the silk of the pupating larva is released as a string comprised of a central fiber composed of fibroin fibrils arranged longitudinally, and this central fiber (and its longitudinal fibrils) is in turn enwrapped in sericin proteins which are arranged transversally across the central fiber (Prudhome *et al.*, 1985). In previous studies, we have dealt to some extent with the electrical properties of the silk strings of hornet larvae, and what we know so far is the following: each silk casing formed around a pupating larva bears a cap with a central button containing a sizeable amount of silk, that covers the head of the larva, whereas at the margins of the cap and along the length of the larval cell there is a thin silk sleeve that houses the rest of the larval body (Kirshboim and Ishay, 2000). The larval silk is immiscible in water, be it at room temperature or at 100°C, nor is it soluble in ordinary organic solvents like ether, but it is soluble in acetone and acids (Magoshi *et al.*, 1979; Ayub *et al.*, 1994; Ishay, unpublished observations). The young vespan imagines ecloding from their puparia do not consume the encasing silk and apparently are incapable of digesting it, but they do cut the cap as they emerge, leaving the nursing worker hornets to remove the remaining silk cap traces from the vacated cell. Interestingly, however, these cleaning workers do not remove the silk sleeve proper but rather retain it within the cell so as to raise the next brood upon it (Ishay and Ganor, 1990).

The present study was undertaken in order to ascertain more precisely the electrical properties of larval silk, namely, current, voltage, resistance and capacitance, mainly but not exclusively within the optimal temperature range for hornets (19–35 °C). Our results are presented herein.

Materials and Methods

Silk caps were collected from the cells of various Oriental hornet combs in the Tel-Aviv district in the summer of 2004. After subjecting the adult hornet population to ether anesthesia, the complete silk caps were snipped off by use of scissors. Care was taken to remove the caps at their juncture point with the comb cell, without the thin inner part. The time at which the collected silk caps were formed, as estimated from their color, ranged from a few days up to a week, which leads us not to expect uniform results. The snipped caps were immediately stored under refrigeration at 4°C, in the dark.

As for 'age' of the caps we noted that young caps had a light cream color whereas the 'older' caps acquire an increasingly darker-blackish coloration. For study we chose caps, 25 similar looking ones with a mean weight of 1.4 milligram (mg) and standard deviation (SD) = 0.15mg. The average thickness of a silk cap at its center button (averaged over 14 specimens) is approximately 210 μm. The electrical properties, including resistance, voltage, current and capacitance, were measured with the aid of a Keithely 617 programmable electrometer. All measurements were carried out in a Revco incubator (Revco, NC,USA) under conditions simulating the normal state of the hornet nest (i.e., darkness and a relative humidity (RH) of about 90%).

The measurement of current, voltage and resistance was undertaken at temperatures ranging between 10–60°C. The resistance was not measured directly since the spontaneous current influenced the correct reading. Instead, the current was measured under a steady voltage of about 15 volts, and the resistance was then computed from the formula $R = V/I$. We performed a values control assessment by substituting a commercial resistor for the silk cap. The resistor remained highly stable throughout the thermal increase, with the maximal change in its resistance amounting to a 0.4%, as expected from its technical specifications. The capacitance was measured at a steady temperature of 25°C, by using two electrodes and charging the silk up to a voltage of 25 volts for 10 minutes before allowing it to discharge through its natural resistance R. In order to assess the results of the capacitance measurements, use was made of a computer as previously described, (Ishay and Barenholz-Paniry, 1995) and the capacitance value was computed from the equation $C = \tau/R$. Here the parameter τ is the time needed for the voltage to reach 37% (or 1/e) of its initial value. The static resistance (R) of the silk cap was measured, using the same two electrodes, at the end of this discharge. In all these procedures the silk cap was fastened to the measuring instruments in such manner that one circular metallic electrode was attached to the outer surface of the central button and the other electrode was attached to its inner surface. The diameter of each electrode was 2mm. Infra-red (IR) photographs of combs, with filled and empty comb cells, were taken using a Thermacom Model 290pm camera. These photographs were processed by commercial Thermonitor 95 software. Both the software and the hardware are products of Inframetrics USA.

Preliminary measurements of Raman spectroscopy of hornet silk, from the internal and external site were preformed (Galushko *et al*., in prep.) for the Raman measurement a single filament, about 10 μm thick, was glued on the viewing frame, and aligned perpendicular to the direction of polarization of the laser beam. We used a 488nm laser (Yu *et al*., 1973; Barry *et al*., 1993).

Results

Current. (Spontaneous thermoelectric effect) A typical current measurement under changing temperature is shown in Figure 1 .

Measurements were taken under condition of darkness. In the temperature range of 14–46°C, the temperature was increased at an average rate which varied from 0.44°C/min at the lower temperature down to 0.33°C/min at the higher temperature. The (–) electrode was fastened to the inner (concave) side of the silk cap and the (+) electrode to the outer (convex) side of the cap. At a relative humidity(RH) of 90%, the following results were obtained: Starting at a temperature of 17.5°C and up to 20°C there was a moderate increase in the current (1 nA – 19 nA); between 20–25°C, the current increased at a greater rate (up to 200 nA); between 25–37.8°C, there was a drop in rate, with maximum current of 327.4 nA recorded at 37.8°C; between 37.8–39.5°C there was moderate drop in the current and at 39.5–43°C a sharp drop in the current which subsequently tapers off to reach 2 nA at 46°C (i.e., equal to the starting current level). Graphs of the current, similar or even identical to the one shown in Figure 1, were obtained on different samples throughout the year.

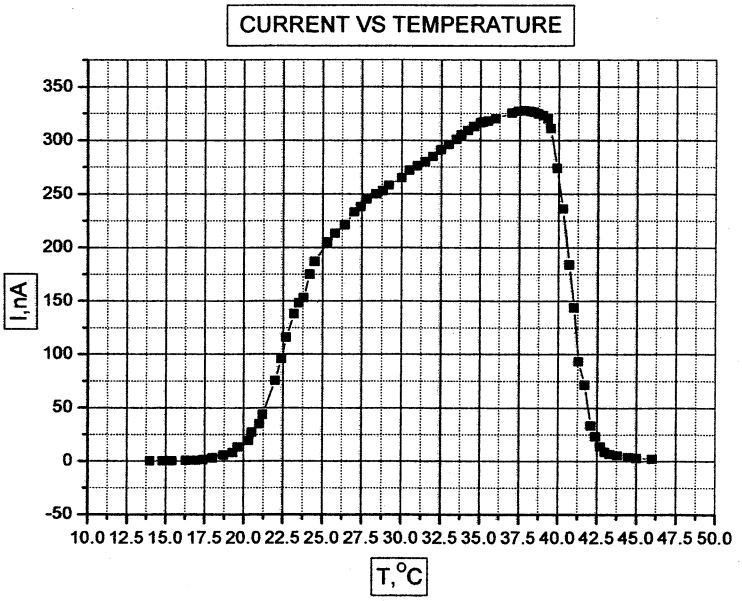

FIGURE 1. Current *vs*. temperature measurement to assess the thermoelectric effect on a single worker larval silk cap. Measurements made within a thermal range of 14–46°C. The current begins to increase with temperature at 17.5°C, its rate of change increases at 20°C, and the current peaks at 37.8°C at a value of 327.4 nA. After that, there commences a sharp drop up to a temperature of 43°C, with the current reverting to its starting level at 46°C.
In these measurements the positive (+) electrode was affixed to the outside of the silk cap.

Voltage. (Spontaneous thermovoltaic effect) A typical first voltage measurement is shown in Figure 2 as a. The voltage was measured under the same conditions as the current (albeit on a different silk cap). Between 15–17.5°C there is hardly any change in the voltage level but between 17.5–18.5°C there is a moderate rise (5.5mV–16mV), which becomes even steeper between 18.5–25°C. At the latter temperature range, the rise in voltage level is in fact by more than one order of magnitude, namely from 16mV to 254mV. Thereafter, between 25–34.5°C, the rate of increase moderates again and the voltage peaks at 347 mV. Between 34.5–40°C there is a sharp drop in the voltage, from 347mV down to 20 mV. This drop tempers off between 40–42°C until it reaches the starting level. To ascertain whether the voltage picture is reproducible within the same silk cap, the active measurement was repeated in the same cap after a 24-hour interval. During the pause between the two recordings, the cap was kept under conditions similar to those in the natural nest, namely, darkness, high RH and a temperature of 29°C. The results of the second measurement are shown in Figure 2 as b.

On the whole, the plots a, b in Figure 2 resemble each other. The differences are as follows: Between 20.5–32.5°C, in the b plot there is a rapid rise in the voltage, but this time the increase is more moderate (from 75mV to 281mV) and the peak is only 281 mV, *vs*. 347mV in the a plot. Subsequently, between 32.5–36°C, the b plot exhibits a sharp drop that tapers off between 36–40°C. In other words, in the repeat recording, the rise in

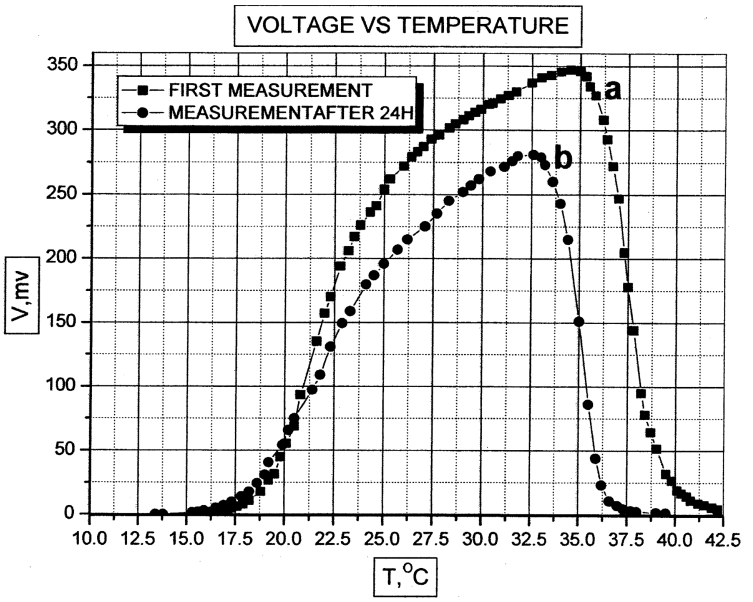

FIGURE 2. Voltage *vs*. temperature measurement to assess the thermovoltaic effect within a thermal range of 15–60°C. In the heating phase of the first cycle (2a), there was rise in the voltage starting from 17.5°C and continuing to a peak of 347 mV at 34.5°C. Thereafter, between 34.5–40°C there was sharp drop in the voltage down to 20 mV, but subsequently, up to 42°C, the voltage decreased slowly down to starting level and remained so up to a temperature of 60°C (not shown in picture). Throughout the measurements, neither the color of the silk nor any other visible feature of it underwent change. Repeat of the measurements on the next day, i.e., after a relaxation period of 24 hours, undertaken at 29°C in the dark at an RH above 90% yields a similar curve (2b) albeit of somewhat smaller values, than the first.

voltage with increase in temperature is smaller by about 20% and also the drop commences earlier (at 32.5°C *vs*. 35°C).

Resistance. Measurements here again as before, and results are shown in Figure 3a: Between 12.5–24°C, in the first measurement (cycle 1) there is a drop in the resistance from 278 MΩ to about 1.25 MΩ, with the lesser value remaining up to a temperature of 31°C. When the temperature reaches 31°C, one observes a rise in the resistance from 2.65 MΩ to 4411 MΩ, meaning an increase by more than three orders of magnitude. At this point (between A and B) and at this temperature the measured specimen was kept for 76 minutes. The main recorded phenomenon (i.e, the large isothermal increase in resistance) was reproducible in first time measurements on other specimens. Moreover, within the temperature range of 12.5–31°C, on the lower branch of the experimental plot, one can temporarily reverse the warming and still get the same reading of resistance *versus* temperature at any given point. After the 76 minutes pause at 31°C, if the silk is then cooled, the resistance at first continues rising moderately up to a maximum of 6818 MΩ. Towards the end of the cooling phase, at about 13°C, the resistance has dropped to 6000 MΩ (Figure 3a cycle 1).

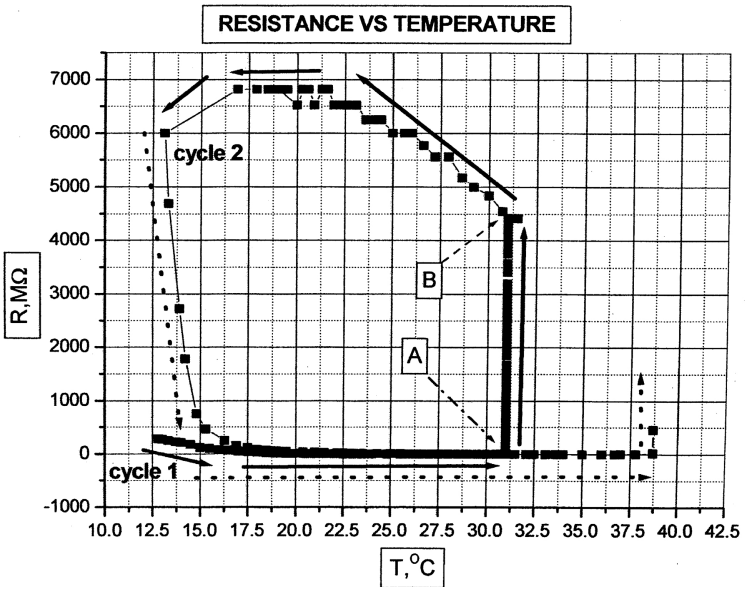

FIGURE 3a. Electrical resistance *vs* temperature measurement. The resistance was found by measuring the current when a voltage of 15V is applied across the thickness of the silk cap (see details in Materials and Methods). One can see that between 13–31°C, the resistance is for the most part low, with an initial dip between 13–15°C. At 31°C in cycle 1 of measurement, the resistance rises sharply, at isothermal conditions from 2.65MΩ to 4411MΩ, which means a difference of more then three orders of magnitude between A-B. Subsequently, during the cooling phase undertaken at the same rate as the heating phase, there was further increase in the resistance which reached 6818MΩ at 21.6°C. Thereafter commenced a slow decrease in resistance down to 6000MΩ at 13°C (3a, cycle 1). At this point, the specimen was heated again and at first the resistance dropped sharply up to a temperature of 15.3°C, where the resistance reached 469 MΩ. This rate of decrease tapered off between 15.3–24°C. At the latter temperature the resistance reached the value of 10 MΩ, and then flattened out to a minimum of 1 MΩ at 38.7°C (which was higher than the top temperature in the first cycle). At 38.7°C there commenced an isothermal rise in the resistance (cycle 2).

At 13°C, another warming phase was started (Figure 3a, cycle 2) and here, between 13–15.3°C there was a sharp drop in the resistance down to 469 MΩ, which tapered off between 15.3–24°C to the value of 10 MΩ, similar to cycle 1. With further increase in temperature, during the warming phase, the resistance flattened out to a minimum of 1MΩ up to 38.7°C, at which temperature there is an acute isothermic rise in the resistance, similar to that recorded in cycle 1 at 31°C.This result appears in Figure 3a, cycle 2. Figure 3b shows the isothermal rise of the resistance at the fixed temperature 31°C. During the first 20 minutes the rise is moderate but its rate increases. After the resistance reaches 400 MΩ, its rate of increase stabilizes, in accordance with the approximate equation R(MΩ) = −625 + 66T(min)

Electrical capacitance. A typical discharge curve is shown in Figure 4. As can be seen, the maximal charge attained 25 V, while the discharge occurred in two distinct stages, to

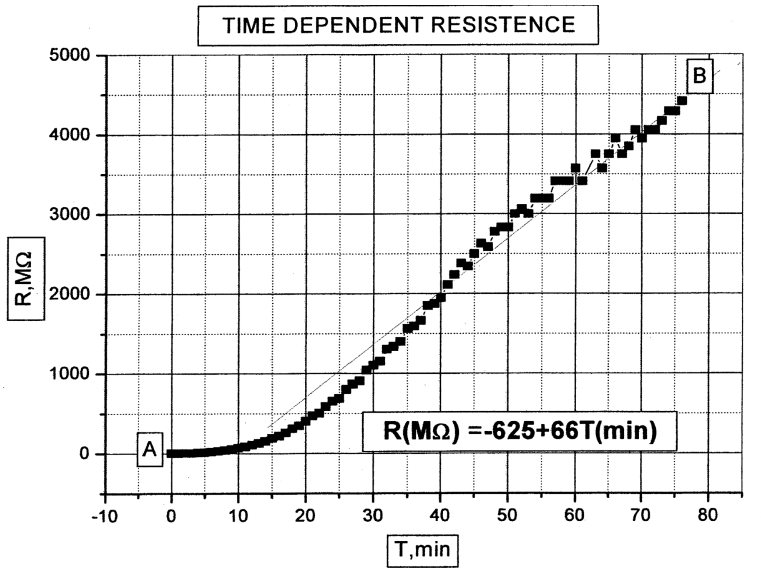

FIGURE 3b. Depiction of the isothermic rise in the resistance between points A-B that was shown in Figure 3a, but this time as resistance *vs*. time. One sees that for the first 20 minutes the resistance rises at a slow but increasing rate, whereas in the next 56 minutes the resistance rises at a more accelerated approximately linear pace, according to the formula R(MΩ) = −625 + 66T(min).

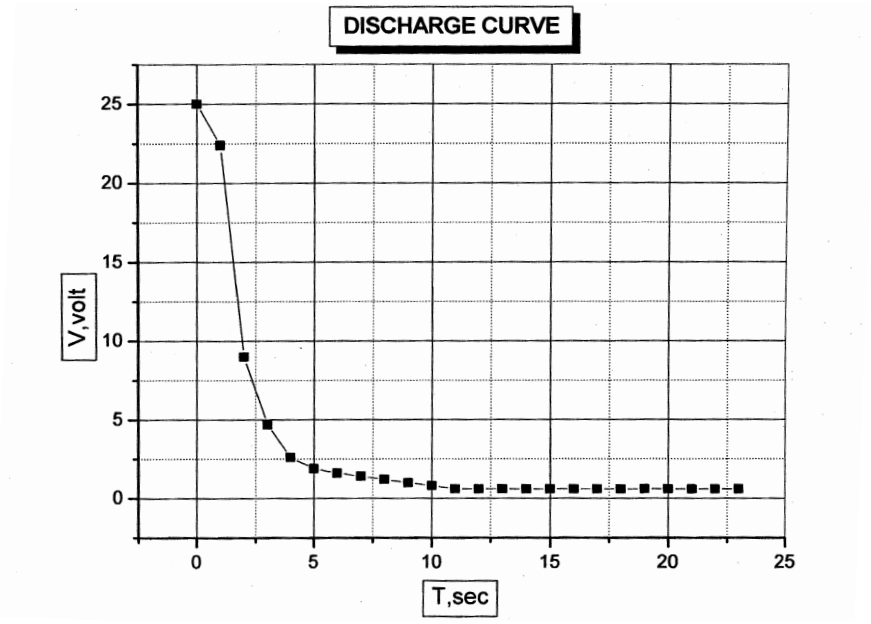

FIGURE 4. Typical instance of voltage discharge following charging of the silk for 10 minutes to a voltage of 25 Volts. Note the rapid discharge during the initial 3 seconds. After that, the curve tapers off and reaches asymptote after about 10 seconds.

wit: 1) rapid discharge to about a level of 5 V, which occurs within the first 3 seconds; and 2) a slow discharge that lasts for a considerable length of time but reaches asymptote after about 10 seconds from the start of the discharge. Using the equation $\tau/R = C$, where $\tau = 2$sec and the static resistance R is 5 MΩ, (measured at the end of the discharge, i.e., after 20 min) we get for the capacitance C = 0.4 μF.

In order to measure the temperature distribution over the comb surface, including the silk caps, we photographed a comb with both filled (silk capped) and unfilled (uncapped) cells at night using an infrared, temperature sensitive camera. From the results of this procedure we gleaned that: a) there are differences between the temperature of the silk and that of the brood comb; b) insofar as the silk cap is concerned, there are differences between various hornet pupae which are probably age dependent; and c) within the same silk cap there is a temperature gradient wherein the center of the cap is the coolest about 25.5°C while at the margins of the cap, at a distance of less than 1cm, the temperature is 27°C, in the walls of a pupa containing comb cell the temperature is about 29°C and in the walls of an empty comb cell within the same comb the temperature reaches up to 31.3°C (see Figure 5).

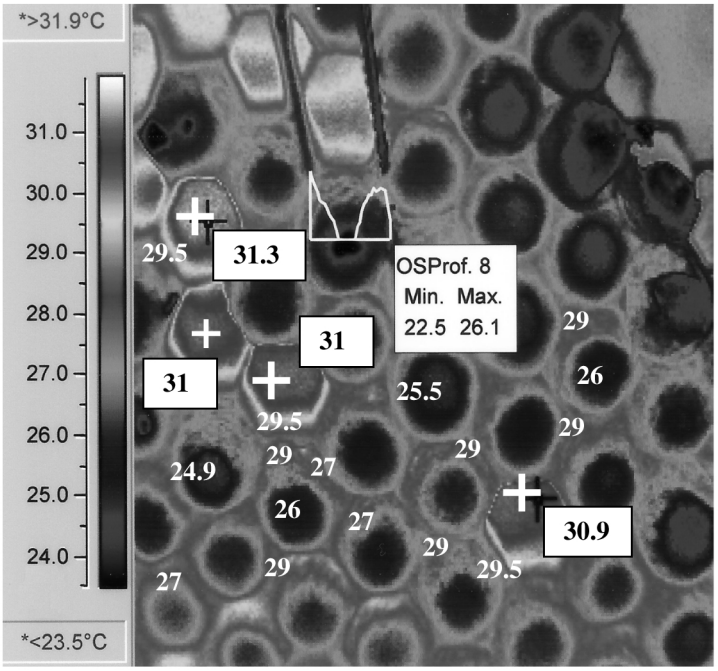

FIGURE 5. Brood comb housing silk-encased pupae as photographed with IR camera. In accord with the temperature scale shown on the left side, we note that there is a temperature gradient over the surface of any silk cap. The center of the cap is coolest, at about 25.5°C, while the margins of the cap, at a distance of less than 1cm, are at 27°C. In the walls of a pupa-containing comb cell the temperature is about 29°C and in the walls of an empty comb cell within the same comb the temperature reaches up to 31.3°C. (after Joseph and Ishay, 2004)

Preliminary results of Raman spectroscopy are presented in Figure 6 from the internal (IN) and the external side (EX). As can be seen a band at 1450cm^{-1} associated with the CH_2 deformation is present, and used as an intensity standard since it is insensitive to the conformation of the protein (Frushour and Koenig, 1974; Yu *et al.*, 1973).

The distinctive peak in 1650cm^{-1} indicate the presence α-helical conformation (Barry *et al.*, 1993; Williams *et al.*, 1994).

Discussion

In the present study assessment was made of the electrical properties of the silk caps produced by pupating hornet larvae just before they undergo metamorphosis. (Figure 7a).

These silk caps are comprised of fibers (1) as well as plaques (2) (Figure 7b). The fibers are laid down in criss-cross fashion in several layers, with lacunae in between to allow for the passage of gases. We propose that the silk cap acts as a structure which filters out both bacteria and dust particles, thus providing a 'clean room', i.e., enabling the metamorphosing larva to create over its body an intact cuticle devoid of any defects that may form by the intrusion of particles or bacteria (Shabtai and Ishay, 1998), much the same as is

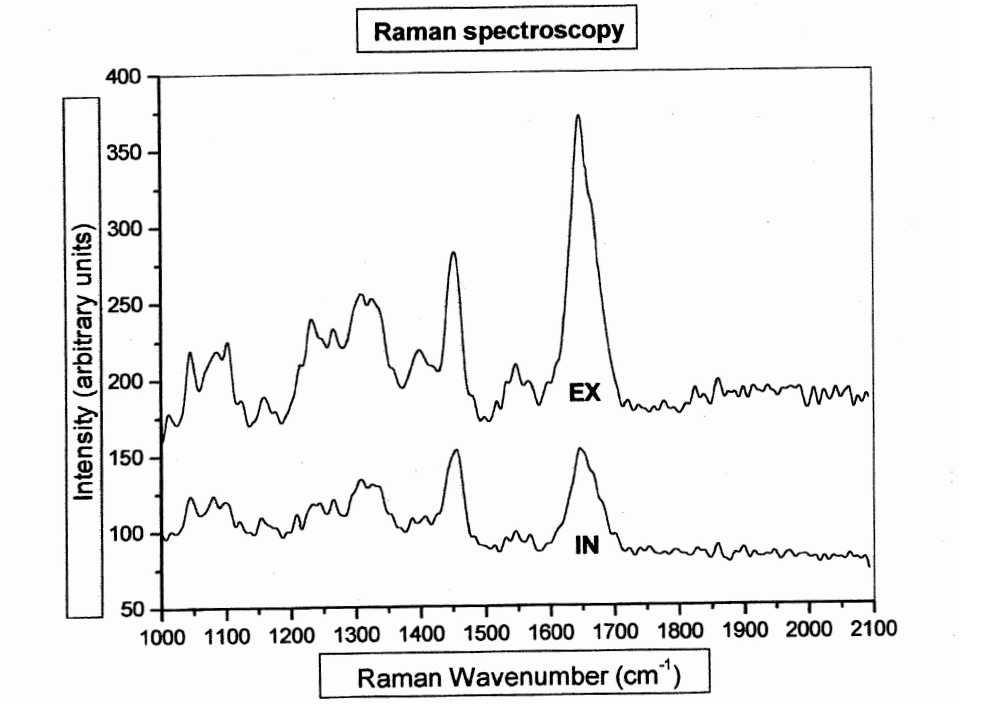

FIGURE 6. Raman spectroscopy of silk of *Vespa orientalis* (IN) silk from the internal side of the cap and *(EX)* external side of the cap. There was no significant difference between the outer and the inner part of the silk cap, which implies that both sides have similar secondary structure.

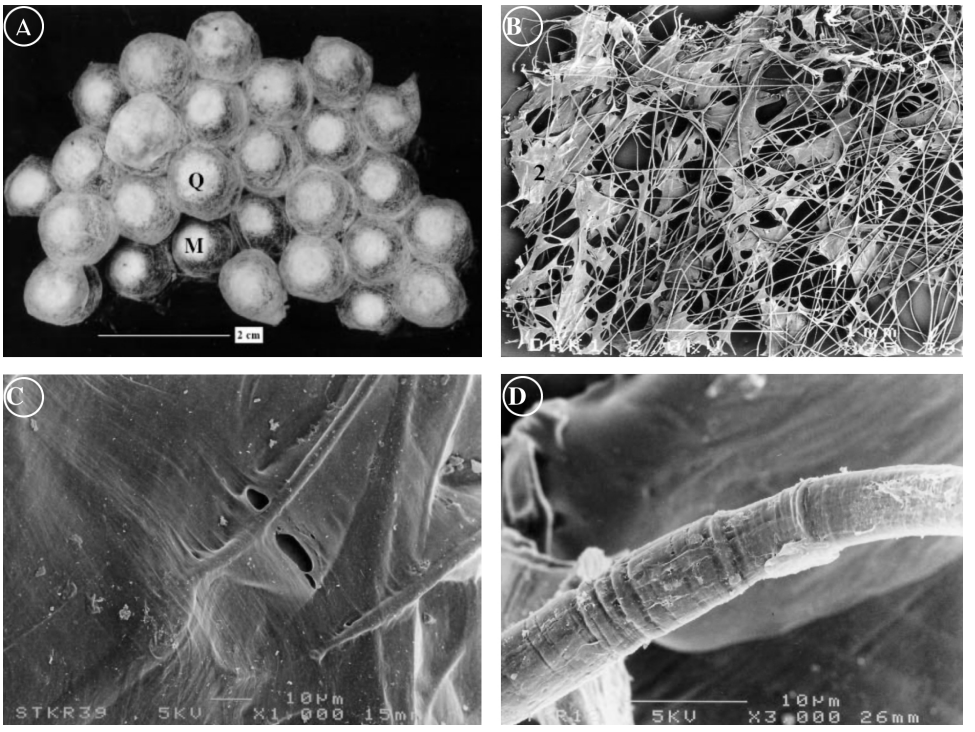

FIGURE 7. **A)** Silk caps from a brood comb in the fall. The big caps are from queen pupae (Q) and the small ones from drone pupae (M). Note the central 'button' in the cap which boasts numerous silk layers as opposed to the sparse amount of silk at the margins of the cap. (after Joseph and Ishay, 2004) Bar = 2cm. **B)** The silk sleeve around the pupating larva. Note the scanty silk fibers and between them the glue — like plaques which fill up all the empty spaces. (after Kirshboim and Ishay, 2000) Bar = 10µm. **C)** Greater magnification of the silk cap of a worker pupa. One can see: 1) silk fibers arranged in several layers; 2) layers of glue material. Between the silk fibers there are gaps that allow for gas flow. (after Shabtai and Ishay, 1998) Bar = 1mm. **D)** A picture of a single silk string, whose diameter is about 7µm. One can see that the sericin coat around the central silk fiber is not smooth or uniform but rather bears striations or grooves whose role is still unclear. (after Joseph and Ishay, 2004) Bar = 10µm.

known and counteracted in the industry of semiconductors (Gutmann *et al.*, 1983). In Figure 7A a bunch of silk caps can be seen. The large ones are of the queen pupae (Q) while the smaller ones are of male pupae (M) We have focused mainly on the structure of the silk cap, but need to remind that apart from the silk cap there is also a silk sleeve that lines the entire length of the walls of the larva's comb cell. This silk sleeve differs structurally from the silk cap, being composed of fewer fibers and between them plaques of silk that are fastened to the cell walls (Figure 7B).

One can see, after greater magnification of the silk cap of a worker pupa, that the silk fibers are arranged in several layers intermittently with glue material. Between the silk fibers there are gaps that allow for gas flow (Figure 7C) .

Turning now to the structure of the silk string produced by the pupating hornet larva, we note that it is composed of two parts, namely, an internal fiber made of the protein fibroin (Ochiai, 1960; Sehnal and Akai, 1990) and an outer coating made of sericin proteins (Michaille *et al*., 1989). We assume that the electric conductivity occurs within the central inner fiber, which is constructed of micro fibrils laid along the silk fiber, whereas the outer coating is an insulator. The latter envelope-like coating is not uniform throughout but may be intermittently grooved, which means that the sericin elements are not of uniform thickness (Figure 7D).

Earlier (unpublished results) it was found that Oriental hornet larvae removed from their cell do not develop or even do not survive without the silk cocoon. We assume that they need something which comes with the silk, most probably the electrical charge.

Electric currents in the silk cap were already measured in previous studies (Ishay and Ben-Shalom, 1992; Ishay and Litinetsky, 1998; Litinetsky *et al*., 1998). In these studies it was found that if one measures spontaneous current within a temperature range of 20–33°C (see Figure 8), cycles of heating-cooling the thermoelectric procedure can be repeated many times, but in each cycle lasting about 40 minutes, it was impossible to obtain a full expression of the properties of the silk. In the present study, a more extensive delineation of the electrical properties of the larval silk was attempted by measuring the current over a wider temperature range (13–46°C), the duration of each cycle was about 90 minutes (twice as long as in the previous studies). Indeed now we obtained a maximal current of 327 nA with a clear cut rise in the current to a maximum at a temperature of

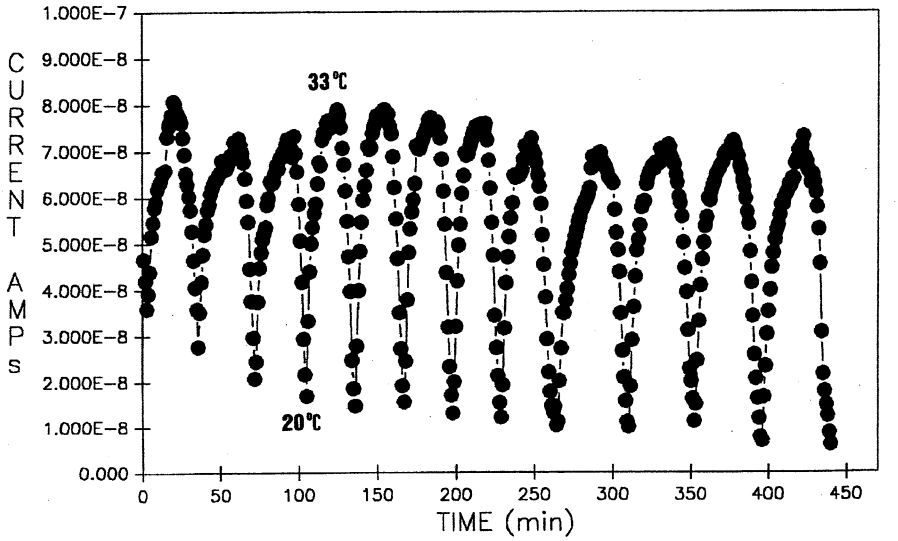

FIGURE 8. Continuous cycles of heating-cooling between 20–33°C. From the presented results it is clear that the thermoelectric effect is reproducible and multiply repeatable, but the cycles seen here are not as complete as in Figure 1, where each cycle is longer and encompasses more extended temperature range. (after Kirshboim and Ishay, 2000)

37.8°C. In measurements on different samples we obtained somewhat different values, both higher and lower, but this is to be expected inasmuch as vespan silk is a natural product and apparently each pupating larva spins a silk of slightly different density, thus its measured values will not be identical. Silk structure depends on various factors such as the food the larva receives from the workers before it begins its silk spinning (Kirshboim and Ishay, 2000) or environmental factors like temperature and humidity which vary somewhat over the different parts of the nest (Ishay and Ruttner, 1971), or because of genetical differences. The thickness of the silk button may differ from nest to nest, so would also the diameter of the silk fibers (Plotkin, unpublished observation) and last but not least — the age of the larva or pupa at the time the silk cap was removed for measuring.

Insofar as the voltage values (Figure 2), the obtained picture is similar to that of the current in Figure 1: The voltage reaches under the same conditions a value of 347mV at 34.5°C, and it, too, shows a clear dependence on temperature (at optimal RH), thus evincing a distinct thermoelectric effect. The voltage measurement was repeated on the sample 24 hours later. We got the same effect but at slightly lower values: The maximum voltage was 281mV, occurring at a temperature of 32.5°C. Conceivably, the silk cap may have undergone some denaturation upon the initial heating above optimal temperature extant in the nest, namely, 29°C (Ishay and Ruttner, 1971) or the silk proteins may have undergone a phase transition. It is also possible that, following the initial heating above normal, more then 24 hours may be needed for recovery.

As for the resistance, our measurement showed that the least resistance occurred at the temperature range of 19–31°C during the first cycle of warming. At 31°C, an interesting phenomenon occurred, the resistance started to rise even while a fixed temperature of 31°C was maintained, that is, *even under isothermal conditions* (Figure 3a, cycle 1). Thus at 31°C the resistance continued to rise during 76 minutes (Figure 3b) up to a value that is 3 orders of magnitude greater than the resistance exhibited by the silk when subject to its spontaneous voltage and current. This is clearly the result of applying an external voltage across the silk cap that is 2 orders of magnitude greater than naturally occurring voltage, and points to a possible phase transition in the silk which is precipitated by the large external voltage. The phenomenon exhibits a clear cut hysteresis. When a second cycle was measured we again observed at 38.7°C the onset of the phenomenon whereby in isothermal fashion the resistance starts rising sharply. In sum, the silk cap behaves in this respect just like the cuticle (Ishay *et al.*, 1987), in that during the warming stage there is a temperature at which, without further rise in temperature, the resistance continues rising sharply and this rise persists even through the cooling phase. Subsequently, during a second heating stage, there is again a minimal resistance. Such hysteretic behavior is a generic property of first order phase transitions. We therefore propose that the silk undergoes some kind of phase change, which is expressed by the sudden rise and fall of the resistance. Subsequently, upon further heating, within biological temperatures, the resistance in cycle 2 was as low as in cycle 1 except that the phase transition occurred at a higher temperature (38.7°C) than in the first cycle (31°C). It is possible that in the wake of the phase transition and the short recovery time, irreversible changes may have occurred in the silk. These will be looked for in future studies.

As for the electrical capacitance, judging from the discharge curve and the fact that the cap resistance was 5 MΩ, the rate of discharge was very slow, with 90% of the charge discharged during the first five seconds. It is highly unlikely that the silk cap really has a

capacity as high as 0.4μF. More likely, in our opinion, is the possibility that the slow relaxation of the voltage is a result of a voltage-dependent first order phase change, which relaxes slowly due to hysteresis, as previously proposed in connection with the thermal response.

Our IR photography reveals that the comb itself, with its component cells, retains an optimal temperature of 29°C. In the comb cells housing silk-encased brood, the temperature is some 2–3°C lower, this phenomenon will be addressed in forthcoming studies.

As can be seen from the preliminary results (Figure 6), Raman spectroscopy can be used as an important tool for understanding the structure of hornet silk. There was no significant difference between the outer and the inner part of the silk cap which implies that both sides have a similar secondary structure. However, further research is needed to precisely describe and explain the differences in relative intensities.

References

Ayub, Z.H., Akai, M. and Hirabayashi, K. (1994) Quantitative structural analysis and physical properties of silk fibroin hydrogels. *Polymer 35(10):* 2197–2200.

Barry, B.W., Williams A.C. and Edwards H.G.M. (1993) Fourier-Transform Raman and IR-spectra of snake skin. *Spectrochimica Acta. 49(5–6):* 801–807.

Edwards, R. (1980) *Social Wasps*. The Rentokil Library. East Grinstead, U.K.

Frushour B.G. and Koenig J.L. (1974) Raman spectroscopy study of tropomyosin denaturation. *Biopolymers. 13(9):* 1809–1819.

Gutmann, F., Keyzer, H., Lyons, L.E. and Somoano, R.B. (1983) *Organic Semiconductors*, Part B. R. E. Krieger Publ. Co., Malabar, Florida.

Imms, A.D. (1960) *Entomology*. London: Methuen & CO LTD.

Ishay, J.S. and Barenholz-Paniry, V. (1995) Thermoelectric effect in hornet silk and thermoregulation in hornet's nest. *J. Insect Physiol. 41(9):* 753–759.

Ishay, J.S. and Ben-Shalom, A. (1992) Electrical properties of hornet silk: the influence of humidity and ether. *Physiol. Chem. Phys. & Med. NMR. 24(4):* 323–238.

Ishay, J.S. and Ganor, E. (1990) Comb cells and puparial silk in the Oriental hornet nest: structure and function. *J. Morphol. 203:* 11–19.

Ishay, J.S. and Litinetsky, L. (1998) Ferroelectric-like properties of hornet structures and constructions. *Physiol. Chem. Phys. & Med. NMR 30(2):* 185–201.

Ishay, J.S. and Ruttner, F. (1971) Die thermoregulation in Hornisennest. *Z. v. Physiol. 72:* 423–434

Ishay, J.S., Peled, N., Tischler, J.R. and Rosenzweig, E. (1987) Photoconductivity in the hornet cuticle: a theoretical approach. *Physiol. Chem. Phys. & Med. NMR 22:* 45–60.

Joseph, Z. and Ishay, J.S. (2004) Silk structure in a hornet cocoon. *J. Electron Micros 53(3):* 293–304.

Kirshboim, S. and Ishay J.S. (2000) Silk produced by hornets: thermophotovoltaic properties. A Review. *Comp. Biochem. Physiol.A, 127(1):* 1–20.

Litinetsky, L., Steinovitz, H., Ishay, J.S. (1998) Thermoelectric properties of hornet silk caps during different stages of pupation. *Physiol. Chem. Physics & Med. NMR 30(2):* 185–201.

Magoshi, J., Mizuide, M., Magoshi, Y., Takahashi, K., Kubo, M. and Nakamura, S. (1979) Physical properties and structure of silk. VI. Conformational changes in silk fibroin induced by immersion in water at 2–130ºC. *J. Polymer Sci. Physics Ed. 17(3):* 515–520.

Matsuura, M., Yamane, S. (1990) *Biology of the Vespine Wasps*. Springer: Berlin.

Michaille, J.J., Couble, P., Prudhome, J.C. and Garel, A. (1989) A single gene produces multiple sericin messenger RNAs in the silk gland of *Bombys mori*. *Biochemie* (Paris) *68:* 1165–1173.

Nation, J.L. (2002) *Insect Physiology and Biochemistry*. London: CRC Press.

Ochiai, S. (1960) Comparative studies on embryology of the bees — *Apis Polistes, Vespula* and *Vespa*, with special reference to the development of the silk gland. *Bull. Fac. Agricul.* Tamagawa Univ. *1:* 13–45.

Prudhome, J.C., Couble, P., Garel, J.P. and Daillie, J. (1985) Silk synthesis. In: *Comprehensive Insect Physiology, Biochemistry and Pharmacology* (G.A. Kerkut and L.J. Gilbert, eds) 17: 571–625.

Rudall, K.M. and Kenchington, W. (1971) Arthropod silks: the problem of fibrous proteins in animal tissues. *Ann. Rev. Entomol. 16:* 73–96.

Sehnal, F. and Akai, H. (1990) Insect silk glands: their types, development and function, and effects of environmental factors and morphogenetic hormones on them. *J. Insect Morph. Embriol. 19(2):* 79–132.

Shabtai, Y. and Ishay, J.S. (1998) Hornet silk caps maintain a clean room environment: a device for filtering out bacteria and dust particles. *Comp. Biochem. Physiol.* Part A *120:* 565–570.

Spradbery, J.P. (1973) *Wasps.* Sidgwick & Jackson, London.

Yu, T-J., Lippert, J.L. and Peticolas, W.L. (1973) Laser Raman studies of conformational variations of poly-L-lysine. *Biopolymers. 12(9):* 2161–2175.

Williams, A.C., Edwards, H.G.M. and Barry, B.W. (1994) Raman-spectra of human keratotic biopolymers — skin, callus, hair and nail. *J. Raman Spectr. 25(1):* 95–98.

Wilson, E.O. (1971) *The Insect Societies.* Belknap, Harvard, Cambridge, Mass.

Received August 10, 2005;
accepted October 18, 2005.

Physiol. Chem. Phys. & Med. NMR (2005) *37*: 85–88

BOOK REVIEW

Bioelectromagnetic Medicine

Edited by Paul J. Rosch, M.D. and Marko S. Markov
Published by Marcel Dekker, Inc., New York.Basel, 2004
851 pages, 90 authors, 50 chapters, hard cover, ISBN: 0-8247-4700-3.

PERMANENT MAGNETS have been used for therapeutic purposes since antiquity; and, both magnetic and electromagnetic devices were used likewise until the late nineteenth and early twentieth centuries. Thereafter, until very recently (in the United States) it was not clever for one in the academic world to speak of such therapies. I had often wondered why? My suspicion as to why was specific, but not satisfactorily founded. While in the process of reviewing Bioelectromagnetic Medicine I, quite by chance, came across a book entitled "The Great Influenza: The Epic Story of the Deadliest Plague in History" by John M. Barry (published by Penguin Books, 2005). In the prologue of Barry's book (p. 7), I read:

> "Not until late — very late — in the nineteenth century, did a virtual handful of leaders of American medical science begin to plan a revolution that transformed American medicine from the most backward in the developed world into one of the best [sic] in the world.
>
> William James, who was a friend of — and whose son would work for — several of these men, wrote that the collecting of a critical mass of men of genius could make a whole civilization 'vibrate and shake.' These men intended to, and would, shake the world."

I suggest that these "men of genius" not only recognized the deplorable state of American medicine during that time period, but also, saw next to no scientific inquiry therein. Neither time nor space allows me to go further into this matter other than to state the obvious: magnet and electromagnetic therapy were causalities of the time. Nevertheless, we should realize that there were essentially no scientific studies evaluating the efficacy of such devices.

Recently, however, we have seen a renewed interest in the use of permanent magnets and electromagnetic devices for therapeutic purposes spurred on by the general public. Indeed, in the more general case, it is now clear that interest in complementary and alternative medicine (in which we find electric and magnetic field therapies) is at a high point defined by cash outlay. As the book under review insures, science is in the process of "catching up." As you well know, emerging fields of scientific inquiry, particularly those

that are outside "orthodoxy," often attract distracters: even those that may be "... charlatans, entrepreneurs, and misguided zealots with worthless devices and unfounded claims..." (see the preface written by Paul Rosch to Bioelectromagnetic Medicine). Rosch further states: "...in this book we have tried to separate the wheat from the chaff by restricting contributions to evidence-based medicine supported by references in peer-reviewed publications and to provide the reader with tools and skills for evaluating the legitimacy of devices and claims." It is my conclusion that the editors have successfully accomplished this goal.

Bioelectromagnetic Medicine contains lessons in history; details of and results from current methodologies; and, a glimpse at the future's vision and hope.

History

Current educational bents would lead most to "brush over" the ancient historical data; laugh at the naiveté of the time; and move on. The time domain covered by this publication is from ancient times to the present with some projection into the future. Beginning in the preface, attention is called to Huang Ti Nei Ching's book *The Yellow Emperor's Canon of Internal Medicine* (our oldest existing medical text dating well before the Greeks) addresses magnetic therapies within its contents. Often there are reflections on the "old" and the "new," as many chapters contain references to historical documentation with direct correlation to current methodologies. In summary, this tome is replete with historical coverage; and, this alone, enhances its value.

Details of and Results from Current Methodologies

In chapter 1, W. Ross Adey — a Giant in the arena of electromagnetics, reviews the potential therapeutic applications of nonthermal electromagnetic fields. (Unfortunately, Dr. Adey died before the book was published — his ever-present contributions will be missed for years to come.) Chapters on the various signal shapes, dosimetry, and image-guided therapy are presented in lucid form — useful for those new to the field and those interested in targeting specific medical problems.

As new research with their methodologies present themselves, they must be tested — some will succeed, some will fail, and some appear to fail, only to be resurrected at a later time. Harold Saxton Burr, known for his theory of "L fields," is one such scholar whose research was inhibited primarily by other preferred paradigms at the time. This historical "tid bit" is discussed (in Chapter 6) along with the methodologies currently being utilized to reinvestigate and expand the further testing of Burr's ideas.

The contributors to *Bioelectromagnetic Medicine* identify concepts and theories that have been put forth to explain the diverse benefits of bioelectromagnetics that have been documented. The works take into consideration how these concepts and theories might relate to ancient concepts as well as subtle energies that are found in the body as well as nature.

A wide spectrum of topics are covered and well documented including issues such as:

- How environmental energies and energies produced internally can produce non-thermal biological effects
- Roles of subtle energies in bioelectromagnetic phenomena
- The possibility of an interface between mind and matter is embraced
- Emerging paradigm of cellular communication at a physical/atomic level
- "Fight or Flight" responses to severe stress
- Current concept of how communication takes place at the chemical and/or molecular level
- Wariness about bioelectromagnetic therapies as they relate to safety concerns
- Standing, walking, and climbing stairs following spinal cord injury, and after neurorehabilitation
- Deep brain stimulation for Parkinson's disease and other disorders of movement
- Biocurrent therapy for macular degeneration
- The use of electrical fields and electromagnetic fields for various orthopaedic problems
- Electroporation therapy
- Electrochemical therapy of tumors
- The effects of static magnetic fields on the microcirculation
- Substitution of magnetic for mechanical force in orthodontic therapy

Attempts may be found in this book to trace the origin and development of therapies such as TENS and vagal nerve stimulation.

Vision and Hope

The field of bioelectromagnetics is an amazing ride with breaking developments frequently occurring. A few "breaking developments" to read about:

- FDA approval for magnetic guidance system to diagnose and treat abnormal cardiac rhythms;
- FDA approval for vagal nerve stimulation for the treatment of epilepsy and potentially certain types of depression and obesity;
- Static magnetic fields for the treatment of epilepsy
- Evaluating the role of water in magnetic fields to provide pain relief
- The phenomenal use of functional electrical stimulation in neurorehabilitation

The use of the scientific method has led to significant progress since the Flexner report — a landmark publication (1910) often cited as leading to the "demise" of electric and magnetic therapy in the United States. When I see how far we've come (and from whence we have come), I'm reminded of "strong words" I read in the book *Scientific Blunders* by Robert Youngson, which reports:

> "There is no known way in which the application of a magnet could have any effect whatsoever on gout, bleeding, headache, toothache or any other disease or symptom. But doctors have always been able, by the display of an authoritative or learned manner, to make their patients believe any sort of nonsense. In addition, even among those members of the lay public with enough knowledge of science to dismiss claims such as this, there will always be

> some with enough latent superstition to give them the feeling that there might be something in it" (Youngson, 1998. page 196).

I cannot help but wonder if those "men of genius" who shaped modern American medicine during the early years of the 20th century in this country, as well Dr. Youngson would have "chirped a different tune" had they had access to *Bioelectromagnetic Medicine*?

In conclusion, if, at this "moment" in time, I could only have one book in my library on the subject of magnetic, electric, and electromagnetic therapeutics, my choice would be *Bioelectromagnetic Medicine* by Paul J. Rosch and Marko S. Markov.

Carlton F. Hazlewood, Ph.D
Research Consultants International
P.O. Box 130282
The Woodlands, Texas 77393-0282

November 6, 2005